Physicochemical and Mineralogical Characterization of Four Spodosols Profiles in Northern Puerto Rico

by

Lyvette Trabal Valentín

A thesis submitted in partial fulfillment of the requirements for the degree of

MASTER OF SCIENCE
in
SOILS

UNIVERSITY OF PUERTO RICO
MAYAGÜEZ CAMPUS
2018

Approved by:

Miguel A. Muñoz, Ph.D. President Graduate Committee	Date
Julia M. O'Hallorans, Ph.D. Member, Graduate Committee	Date
José A. Dumas, Ph.D. Member, Graduate Committee	Date
Ricky Valentín, Ph.D. Representative of Graduate Studies	Date
Roberto Vargas, Ph.D. Chairperson of the Department	Date

ABSTRACT

Spodosols are a soil order with clearly distinct soil profile that have a dark surface horizon of organic origin, a bleached, eluvial E horizon, and a reddish, brownish or blackish B horizon, illuvial in nature enriched with amorphous material and organic matter- the spodic horizon. Spodosols are typical of cold and humid climates, and they form under coniferous forests. Four Spodosols profiles were evaluated in Carmen Regadera Farm, Vega Baja, Puerto Rico. The four profiles were described, and soil samples were collected using the horizon sampling method. Soil field texture was sand, loamy sand, sandy loam, and sandy clay loam and consistent with particle size analysis, which showed that the sand content was greater. Soil Aggregates formed in the deepest horizons and stability ranged from 1.12% to 96.9 %. Soil mineralogy of the clay fraction was determined by X-ray diffraction. All four profiles had similar mineralogy consisting primarily of kaolinite, gibbsite, goethite, hematite, quartz and amorphous material. XRD patterns of the B illuvial horizon shows peaks that correspond to aluminum and iron oxide along with kaolinite and amorphous material, when compared to the eluvial horizon that show a spectra that corresponds to quartz. Mineralogical results are consistent with selective dissolution techniques used to determine the Al^{3+} and Fe^{3+} from the soil using citrate-dithionite-bicarbonate (CBD) method, ammonium oxalate method (AAO) and sodium pyrophosphate method (SP). Using these selective dissolution techniques, we could determine that the Al^{3+} content was always greater than the Fe^{3+} content. The basic cation content was low for three profiles and pH values ranged from 4.16 to 5.19. Profile B showed pH values up to 7.1, possibly due to lateral movement of carbonate enriched water from adjacent areas. The organic matter content determined using the wet oxidation method of Walkley-Black is highest in the surface horizon of the profiles, decreases in the eluvial horizon and accumulates in the B horizon. The fulvic and

humic acid from the spodic horizon was analyzed using Infrared Spectroscopy. The fulvic acid spectrum is less complex when compared to the humic acid spectra this shows that the degree of polymerization for humic acid is always higher than for fulvic acids. The spectra of humic and fulvic acids suggest that chelation occurs between functional groups and oxides and silicate minerals. Strong physical, chemical and mineralogical evidence exist within the four Spodosols profiles studied to show that the pedogenetic process of podzolization is manifested and soil properties are consistent with that of the Spodosols soil order. Differences in physical and chemical properties of the profiles evaluated suggest that these soils belong to the great groups Typic Alorthod and Typic Alaquod.

RESUMEN

Los Spodosols son un orden de suelo con un perfil bien definido, que tiene un horizonte superficial de origen orgánico, un horizonte E eluvial blanqueado y un horizonte B de color rojizo, pardusco o negruzco, de naturaleza iluvial enriquecido con material amorfo y materia orgánica- el horizonte Espódico. Los Spodosols se forman en áreas húmedas de climas fríos bajo vegetación de coníferas. Se evaluaron cuatro perfiles de Spodosols en la Finca Carmen Regadera en Vega Baja, Puerto Rico. Se describieron los cuatro perfiles y se colectaron muestras de suelo utilizando el método de muestreo de horizontes. La textura de campo fue arenosa, arenosa franco, franco arenoso, y franco arcilloso. Estos resultados son consistentes con el análisis de partícula, que mostró que el contenido de arena era mayor. Los agregados de suelo se formaron en los horizontes más profundos y la estabilidad vario de 1.12% a 96.9%. La mineralogía de suelo de la fracción arcilla se determinó mediante difracción de rayos X. Los cuatro perfiles evaluados tenían una mineralogía similar que consistía de caolinita, gibsita, goetita, hematita, cuarzo y material amorfo. Los difractogramas del horizonte iluvial B muestran picos que corresponden a óxidos de hierro y aluminio, junto a caolinita y material amorfo, en comparación con el difractograma del horizonte eluvial que muestra picos que corresponden principalmente a cuarzo. Los resultados de mineralogía son consistentes con las técnicas de disolución selectiva utilizadas para determinar el contenido de Al^{3+} y Fe^{3+} del suelo utilizando el método de citrato-ditionato-bicarbonato (CBD), el método de oxalato de amonio (AAO) y el método de pirofosfato de sodio (SP). Usando estas técnicas de disolución selectiva se determinó que el contenido de Al^{3+} era siempre mayor que el Fe^{3}. El contenido de cationes básicos fue bajo para tres perfiles y los valores de pH variaron de 4.16 a 5.19. El perfil B mostró valores de pH de hasta 7.1, posiblemente debido al movimiento lateral de agua enriquecida con carbonatos

proveniente de zonas adyacentes. El contenido de materia orgánica determinado por el método de oxidación húmeda Walkley-Black es mayor en el horizonte superficial de los perfiles, disminuye en el horizonte eluvial y se acumula en el horizonte B. El ácido fúlvico y el ácido húmico del horizonte Espódico se analizaron mediante espectroscopia de infrarrojo. El espectro de ácido fúlvico es menos complejo cuando se compara con los espectros de ácido húmico, lo que demuestra que el grado de polimerización para el ácido húmico siempre es mayor que para los ácidos fúlvicos. Los espectros de los ácidos húmicos y fúlvicos del horizonte Espódico sugieren que la quelatación se produce entre grupos funcionales y óxidos y minerales de silicato. Las propiedades físicas, químicas, y mineralógicas comprueban que el proceso pedogenético de podzolización se manifiesta y que estas propiedades son consistentes con el orden de suelo Spodosols. Las diferencias en las propiedades químicas y físicas de los perfiles indican que estos suelos pertenecen al gran grupo de suelo *Typic Alorthod* y *Typic Alaquod.*

For,

My family, especially Alynna I., Gabriel A. and Luis Andrés.,

Keep your dreams alive, because success is a combination of hard work, determination and sacrifice.
With all my love!

ACKNOWLEDGEMENTS

Thank you,

To my dearest family, my parents Juan and Ivette, my grandparents Lydia and Heriberto, and my sister, Nohely, thank you for your support. My husband, Luis Andrés, thank you for your unconditional love and support, for encouraging me through the hardest of days. My beloved children, Alynna and most recently Gabriel, you are my inspiration. It's your turn to do great things in life.

Dr. Miguel Muñoz, thank you for your guidance, your support and your friendship. Thank you for this invaluable opportunity, you have truly taught me to love and understand that soils are a marvel in nature.

Dr. Julia M. O'Hallorans and Dr. Jose A. Dumas, members of my graduate committee, your words of wisdom and guidance, helped and encouraged me to complete this research process.

Agro. Robert Bradley, Puerto Rico Land Authority, for your help and coordination to conduct the soil sampling and evaluation at Carmen Regadera Farm.

Agro. Manuel Matos, NRCS State Soil Scientist and personnel form the MLRA Office in Mayagüez, thank you for your help during field observations.

A very special thank you to Eng. Eric Irizarry, and Madelyn Rios, you are role models- academically, professionally and personally. I will be forever grateful.

Yamilis Ocasio, Zidnia Nieto, and Edjomarie Rodriguez, you made instrumental analysis more fun.

Department of Chemistry, UPR-Mayaguez, especially Mrs. Sindia Ramos and Mrs. Aracelis Cardona for allowing the use of the FTIR to characterize humic and fulvic acid fractions.

Department of Geology, UPR-Mayagüez, especially Mr. José Santiago, for their valuable assistance in the XRD analysis of the clay fractions.

The USDA-Tropical Agricultural Research Station, especially Mr. Delvis Pérez, for their countless help in the analysis of iron and aluminum oxide content in the soils by means of ICP.

Faculty, fellow graduate students, and personnel from the Central Analytical Laboratory and the Department of Agro Environmental Science especially Floripe, Evelyn, Norma, H. Pino, Rosario, and Rocío- thank you for all your help along the way. Lynnette, and Joan, you know more of the mishaps along the way, thank you for your unconditional support and words of encouragement.

Thank you, God, for bringing all these people into my life; family, friends and acquaintances, they have shaped who I am today

TABLE OF CONTENTS

LIST OF TABLES

LIST OF FIGURES

LIST OF APPENDICES

INTRODUCTION

Spodosols are acid soils characterized by a subsurface accumulation of humus that is complexed with Al and Fe, with a light colored albic or E horizon overlaying a reddish brown spodic (B_h, B_s, B_{hs}) horizon. The key properties of Spodosols are the accumulation of soil organic C in the upper spodic horizon, the low base saturation, the acid conditions and the accumulation of iron and aluminum in the spodic horizon (Bockheim and Hartemink, 2017). A well-developed Spodosols is a striking example of soil genesis as the horizons are sharply differentiated (McKeague et al., 1983).

The Natural Resources Conservation Service (NRCS) estimates that Spodosols cover approximately 2.56% of the ice-free land area around the world (Soil Survey Staff, 2015). Spodosols develop in sandy to loamy materials that occur in cool, temperate, humid or perhumid regions of the world, however they can also form in hot humid tropical regions of the world, where they occur in areas of quartz-rich sands that have fluctuating ground water (Mckeague et al., 1983; Soil Survey Staff, 1999). The restricted distribution and poor agricultural value of these soils may be the cause why Spodosols have not been studied as much as other soil orders (Horbe et. al., 2004; González-Perez, et. al.2008). In Puerto Rico, three Spodosols series have been established- Algarrobo (Entic Alorthods) (Figure 1), Arecibo (Entic Grossarenic Alorthods), and Corozo (Typic Alorthods) (Muñoz et al., 2018), but the limited information available in the descriptive reports (Mount and Lynn, 2004), stimulates the curiosity to provide more information of the Spodosols found in Puerto Rico.

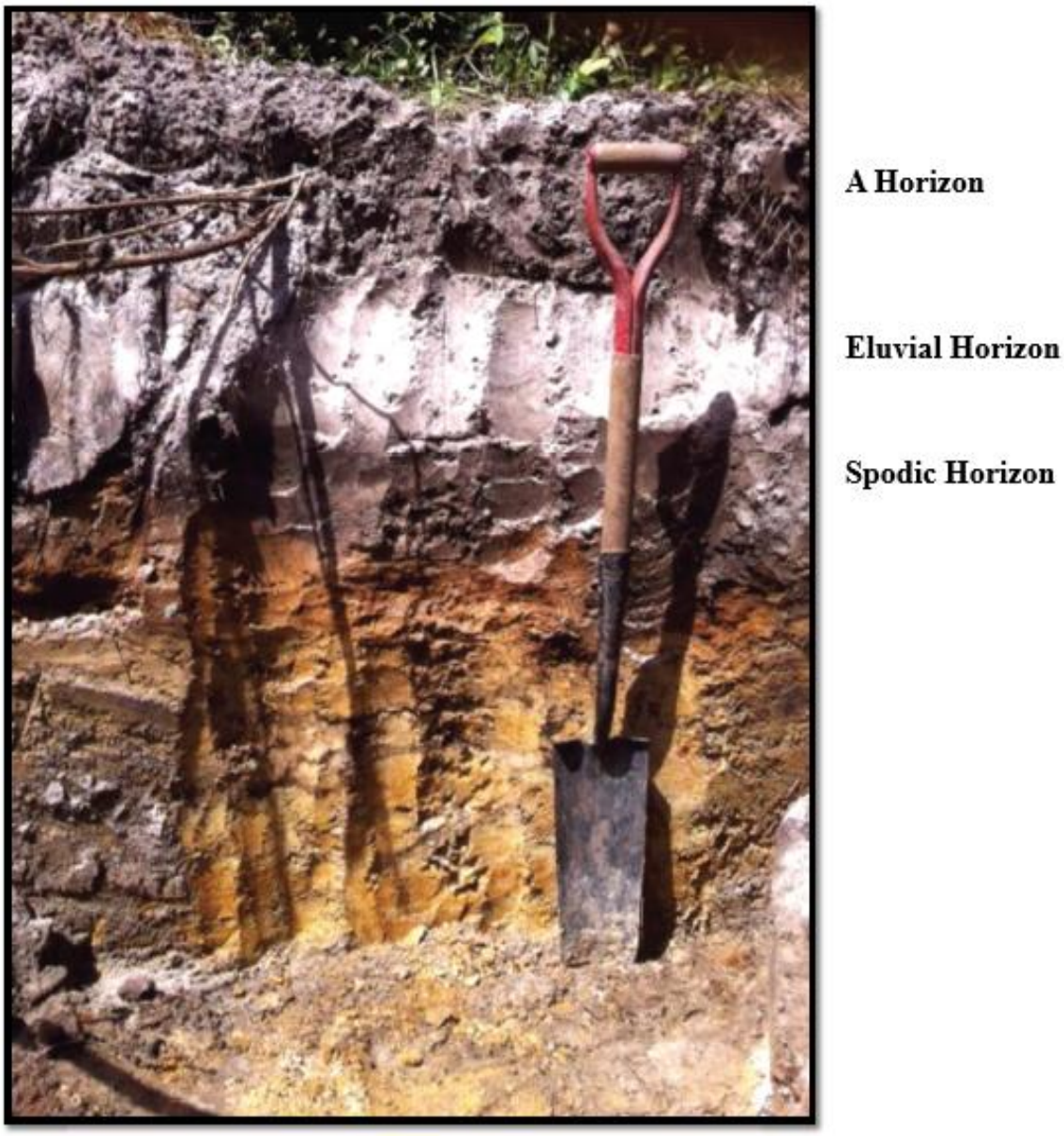

Figure 1. Algarrobo profile (Entic Alorthod) (Muñoz, et. al., 2018)

A detailed characterization of four Spodosols profiles in northern Puerto Rico in comparisons with other Spodosols has been established to provide scientific data to elucidate their process of formation, their physical and chemical properties. The spodic horizon is evaluated in detail using a combination of x-ray diffraction techniques, infrared spectroscopy and selective dissolution to provide information on the nature of the diagnostic horizon.

LITERATURE REVIEW

Spodosols are one of the twelve soil orders of Soil Taxonomy and are acid soils characterized by a subsurface accumulation of humus that is complexed with Al and Fe, with a light colored albic or E horizon overlaying a reddish brown spodic (B_{hs}, $B_{h,}$ B_s) horizon (Bockheim and Hartemink, 2017). Typically, Spodosols consist of an upper layer of decaying organic matter- the O horizon, a gray horizon of varying thickness -the eluvial E horizon, and a black to reddish brown horizon that becomes yellower or less intense in color with depth- the spodic horizon (Figure 2). (Weil and Brady, 2016; Reiger, 1983).

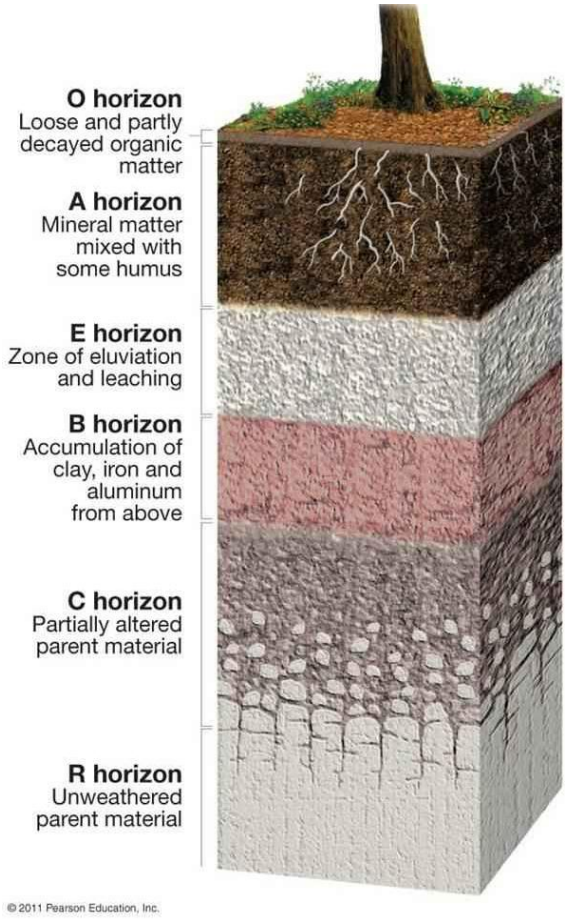

Figure 2. Spodosols profile schematic representation (Weil and Brady, 2016)

The Spodosols name originates from greek *spodos* meaning wood ash (Schaetzl and Anderson, 2005) or possibly from the Russian vernacular *Podzol*, divided into the terms *pod* (beneath) and *zol* (ash) (Buole, 1973; Ponomareva, 1964). Spodosols were described as podzols by Dokuchaev as early as 1879 (McKeague et al, 1983).

Pedogenesis of Spodosols

The formation of soil from raw parent material defines pedogenesis and involves both progressive and regressive processes that act to promote horizonation, preserve it or destroy it. The formation of soils horizons can be described as additions or removals from the soil system as well as transfers and/or transformations within it. Spodosols are formed through a pedogenetic process known as podzolization. The classical view of podzolization is that Al^{3+} and Fe^{3+} are released via weathering in the eluvial E horizon and translocated to the B horizon (Jien et al, 2010). Before discussing podzolization and the different theories that describe it, a brief presentation of individual the mechanisms associated with this pedogenetic process will be reviewed.

Most of the pedogenetic processes involve mobilization, transport and immobilization of constituents. Some materials can be mobilized, transported by water and eventually deposited within the profile (Pedro, 1983). The transfer process is described by eluviation/illuviation couplet. Eluviation is the transfer of material out of a horizon in percolating water; this represents a net loss from a horizon, while illuviation refers to the gain of material by a horizon usually from an overlaying horizon or from a horizon upslope. Commonly observed eluvial/illuvial couplets include those associated with clays, Fe, Al, humus, carbonates, salts, and silica. The effect of the eluvial or illuvial process depends on the strength and duration of the

processes as well as the surface area on the receiving horizon (Anderson, 1982; Farmer, 1982; Schaetzl and Thompson, 2015).

Another process involved in Spodosols genesis are those associated with organic matter. The O horizons form as organic materials such as leaves, grass, seeds, needles and wood accumulate on the soil surface (Bray and Gorham, 1964). As this surface material decomposes it forms intermediate decomposition products, until reaching the most decomposed substance-humus. This humification process is the breakdown and decomposition of litter being fragmented by soil organisms and it is affected by the amount and solubility of organic matter, the decomposer community, the characteristics of the microenvironment that influence the partitioning between the solution and the soil state and decomposer activity.

Soil scientist use chemical fractionation methods based on solubility of organic compounds to separate soil organic matter into humic and fulvic acid. Humic acid, is a larger colloid, with a higher C, lower O concentration, higher molecular weight and more polymerized than fulvic acid (Torn et al., 2009). The humified products of decomposition are mixed with minerals or translocated to mineral horizons below and the more soluble products are eluviated from the surface horizon into the mineral soil. In sandy Spodosols, humus is incorporated into the A horizon more shallowly because the litter will decompose within the O horizon and because of its colloidal size, be translocated into the A horizon by infiltrating water (Schaetzl and Thompson, 2015).

Podzolization

Spodosols tend to develop under climatic, parental material and other conditions that promote the formation of a dark colored surface horizon that serves as a source of downward

migrating organic chelating agents that attack the mineral fabric releasing structural Al and Fe. The classic view of podzolization is that Al and Fe are released via weathering in the eluvial E horizon and translocated further down in the soil profile. Soil formed under this process have three to four mayor horizons, including a dark colored organic surface horizon (O), a bleached eluvial horizon (E), and reddish, brownish or blackish illuvial horizon enriched in amorphous material (B_{hs}), which may be differentiated into an upper B_h (humus enriched) and lower B_s (sesquioxide enriched) horizon (Mckeague et al., 1983). In a well-developed Spodosols profile the horizons express sharply differentiated patterns due to the transport and deposition of Al, Fe and organic matter (Browne, 1995). Models of podzolization must explain the mobilization, translocation, and eventual immobilization of oxidized metal cations and organic compounds (Lundstrom et al., 2000). These theories assume that the parent material has been acidified or exists in such a state that it is conducive to acidification, that the vegetation produces litter rich in low molecular weight organic acids and fulvic acid and that the climate is cool and humid (Lundstrom et al., 2000; Schaetzl and Thompson, 2015).

Theories of Podzolization

Three theories of podzolization are common throughout the studies of pedogenesis of Spodosols (Figure 3), although no single pedogenetic process is consistent with all the morphological expressions of mayor genetic horizons in the soil (De Coninck, 1980; Browne, 1995; Lundstrom et al., 2000; Schaetzl and Thompson, 2015).

The fulvate theory is a two-stage theory, also known as the chelate-complex model (Browne, 1995; Schaetzl and Thompson, 2015). In the first stage organic acids attack the mineral fabric in the E horizon. Soluble Al and Fe chelates form and migrate through the E and humus rich Bhs horizon. The concentrations of organic acids, Al and Fe decreases across the B_{hs} as

selective retention of organic material causes increasing saturation of Al and Fe complexation sites of soluble chelates and a corresponding decrease in the solubility of Al and Fe chelates. At the top of the B_s horizon a critical metal to fulvic acid ratio is reached, causing nearly complete arrest of the migration of the fulvic acid and Al and Fe chelates. In the second stage, microbial decarboxylation of fulvic acids causes the liberation of Al and Fe. Migrating as free metals, they precipitate as trihydroxides in the B_s as pH increases. Imogolite/allophane forms when Si released as a product of weathering in the upper profile combines with the amorphous Al and Fe (Browne, 1995).

The proto-imogolite theory suggests that soluble Al and Si combine in the E horizon to form a positively charged 2:1 Al/Si colloid. After migrating through the E and B_{hs} horizons, the colloid is arrested in the B_s horizon due to decreased solubility with increased pH and the availability of negatively charged sorption sites on mineral surfaces. In the second stage, fulvic acid migrates through the E horizon to form the B_{hs} horizon (Browne, 1995). This inorganic sol model was prompted by the observation that Al can exist in humus poor Spodosols as amorphous inorganic compounds such as imogolite and allophone (Schaetzl and Thompson, 2015). The readily soluble organic acids (formic, oxalic, and citric acids) as well as inorganic acids (nitric acid) promote the release of Al and Fe from primary minerals in the upper horizons (Lundstrom et al, 2000; Schaetzl and Thompson 2015). This model proposes that the metals – Al, and Fe – are translocated first then the organics (Schaetzl and Thompson 2015).

The fulvate bicarbonate theory has two "stages" which may occur sequentially or simultaneously. The first stage involves in situ formation of allophone/imogolite in the B_s horizon by a carbonic acid weathering scheme. High P_{CO2} levels from soil respiration processes promote carbonic acid formation. The carbonic acid attacks mineral surfaces forming an

amorphous Al-rich residue in the B_s. Synthesis of imogolite/allophane results as soluble Si, presumably released elsewhere in the soil profile, combines with Al. The second stage of the theory is similar to the first stage of the "fulvate theory." Fulvic acid forms Al and Fe chelates in the E and B_{hs} horizons. These migrate through the E and B_{hs} horizons and are arrested at the top of the B_s as they interact with amorphous Al-rich residue of the Bs horizon (Browne, 1995).

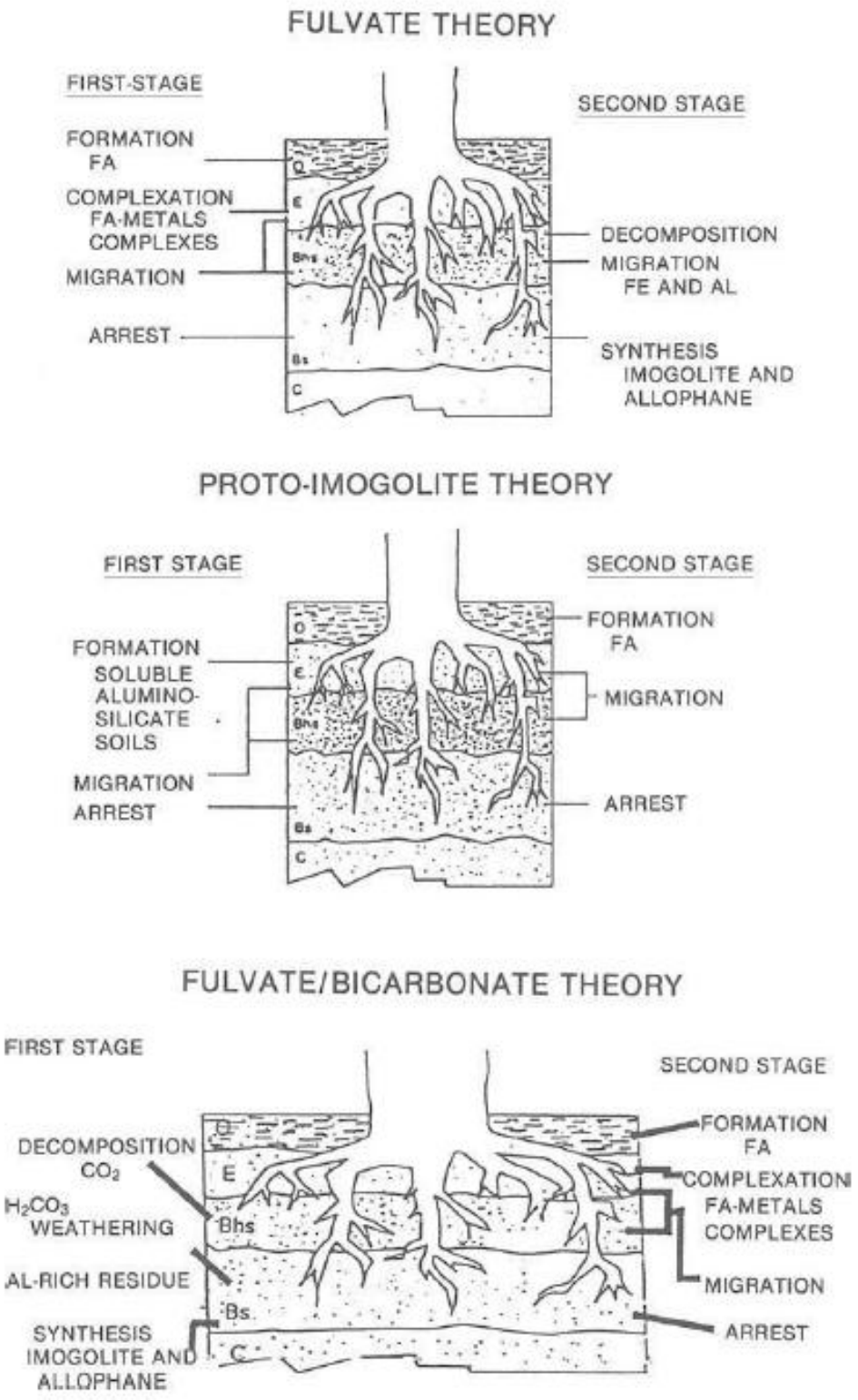

Figure 3. Theories of podzolization (Browne, 1995).

Chemical Expressions of the Podzolization process

The podzolization process is associated to chemical expressions with a significant increase in secondary Al, Fe, and Si weathering products in the illuvial B horizon when compared to the eluvial E horizon. The percentage of Al and Fe, and organically complexed Al and Fe increase along this boundary and is most prominent in the underlying B horizon (Valerio et al., 2016).

Selective dissolution is employed to determine oxide content of Spodosols profiles. Iron and aluminum oxide content is determined using Citrate-Dithionite-Bicarbonate method, the Acid Ammonium Oxalate method and the Sodium Pyrophosphate method. The dithionite extraction yields all free forms of these elements, including crystalline form, the oxalate extraction yields organic and amorphous forms of Fe and Al; and the pyrophosphate extraction yields organic bound forms of iron and aluminum (Jackson, 1965; Bockheim and Hartemink, 2017).

Properties of Spodosols

Although a typical Spodosols soil profile is easily recognized in the field, spodic properties may not be identified from field evidence alone. The Soil Survey Staff (1999, 2015) specifies that Spodosols must have the presence of a spodic horizon, in which amorphous mixture of organic matter and aluminum, with or without iron have accumulated. The spodic horizon must meet chemical criteria in order to be identified as a diagnostic horizon in the classification of Spodosols.

The E Horizon

The E horizon is a mineral horizon in which the main feature is loss of silicate, clay, iron, aluminum, or some combination of these, leaving a concentration of sand and silt particles of quartz and other resistant materials (Wilding et al., 1983). The E horizon is the primary morphological indicator of podzolization. Its coarse texture is due to continued eluviation and chemical weathering of clays and fine silts. Well-developed E horizons in Spodosols qualify as albic horizons (Schaetzl and Thompson, 2015).

The albic horizon originates from intense leaching of clays and Fe oxyhydroxides yielding a bleached horizon with low chroma and values. The color of the albic horizon is determined by the color of primary sand and silt particles rather than by the color of their coatings, this implies that clay and/or free iron oxides have been removed from the materials or that the oxides have been segregated to such an extent that the color of the materials is largely determined by the color of the primary particles (Bockheim, 2014). In Spodosols, this E horizon occurs at or near the mineral surface, with an underlying spodic and other diagnostic horizons such as an argilic, cambic, kandic, or natric horizon (Soil Survey Staff, 2014; Bockheim, 2014). A comparison between properties of the albic horizon and the underlying spodic horizon shows greater amounts of clay, extractable Fe and Al, cation exchange capacity and base saturation in the illuvial than in the albic horizon (Bockheim, 2014).

The Spodic Horizon

The spodic horizon is an illuvial layer with 85% or more spodic materials that contain active (high pH-dependent charge, a large surface area, and high-water retention) amorphous material composed of organic matter and aluminum, with or without iron. The spodic horizon underlies an O, A, A_p or E horizon with >85% spodic materials in a layer 2.5cm thick. Spodic

materials have a pH value (1:1) of 5.9 or less, soil organic carbon 0.6 % or more, strong colors (hues 5YR or 10YR, values 5 or less, chromas 5 or less) cementation of soil organic matter and Al in >50 % of the pedon, Al + ½ Fe percentages (by ammonium oxalate) total 0.5 or more with half that amount or less in the overlaying eluvial horizon (Soil Survey Staff, 1999; Bockheim, 2014).

The spodic horizon is assigned as B_h, B_{hs} and B_s, reflecting the pedogenetic translocation of humus and sesquioxides of Fe and Al (Soil Survey Staff, 1999). This horizon generally occurs in environments with abundant precipitation and cool temperatures and it is most strongly developed under coniferous forest and ericaceous vegetation (Bockheim, 2014).

The spodic horizon forms mostly in sandy materials, from fresh parent material with abundant weatherable minerals or nearly pure quartz sand. A spodic horizon can form in well drained or in soils with fluctuating level of groundwater. If the water table remains within the profile for an extended period, the spodic horizon may contain little or no iron. In warm climates, the spodic horizon occurs under savanna, palm trees, and mixed forest.

Although a typical Spodosols soil profile is easily recognized in the field, Spodic properties may not be identified from field evidence alone. The spodic horizon, has a pH of 5.9 or less, and an organic carbon content of 0.6% or more. In addition, two chemical criteria are used to evaluate spodic materials. The first is the percentage of ammonium-oxalate-extractable aluminum plus one-half of the ammonium-oxalate-extractable iron must total 0.50 or more and must be 2 times or more when compared to the overlaying horizon, and the second is that the optical density of oxalate extract value should be 0.25 or more and at least double eluvial horizon

to the spodic horizon (Soil Survey Staff, 1999). The optical density of the oxalate extract is a measure of the organic C content (Daly, 1982; Mokma, 1993).

Evaluating the Spodic Horizon

Soil organic matter is the organic fraction of the soil that includes plant and animal residues at various stages of decomposition (Brady and Weil, 2004). Soil organic matter influences many soil properties such as capacity to supply N, P and S and trace metals to plants, infiltration and retention of water, degree of aggregation and structure, cation exchange capacity, soil color, adsorption and deactivation of agro chemicals, soil development, and productivity (Van Cleve and Powers, 1995; Nelson and Sommers, 1996).

Soil humus is fully decomposed and stable organic matter and often used as synonyms of organic matter. Two major fractions of soil organic matter are humic and fulvic acids. Stevenson (1982) models of humic acids and fulvic acids (Figure 4.) indicate the presence of a variety of functional groups, including COOH, phenolic OH, enolic OH, quinines, hydroxyquinones, lactose, ethers, and alcoholic OH. These functional groups provide unique chemical behavior (Tan, 2003).

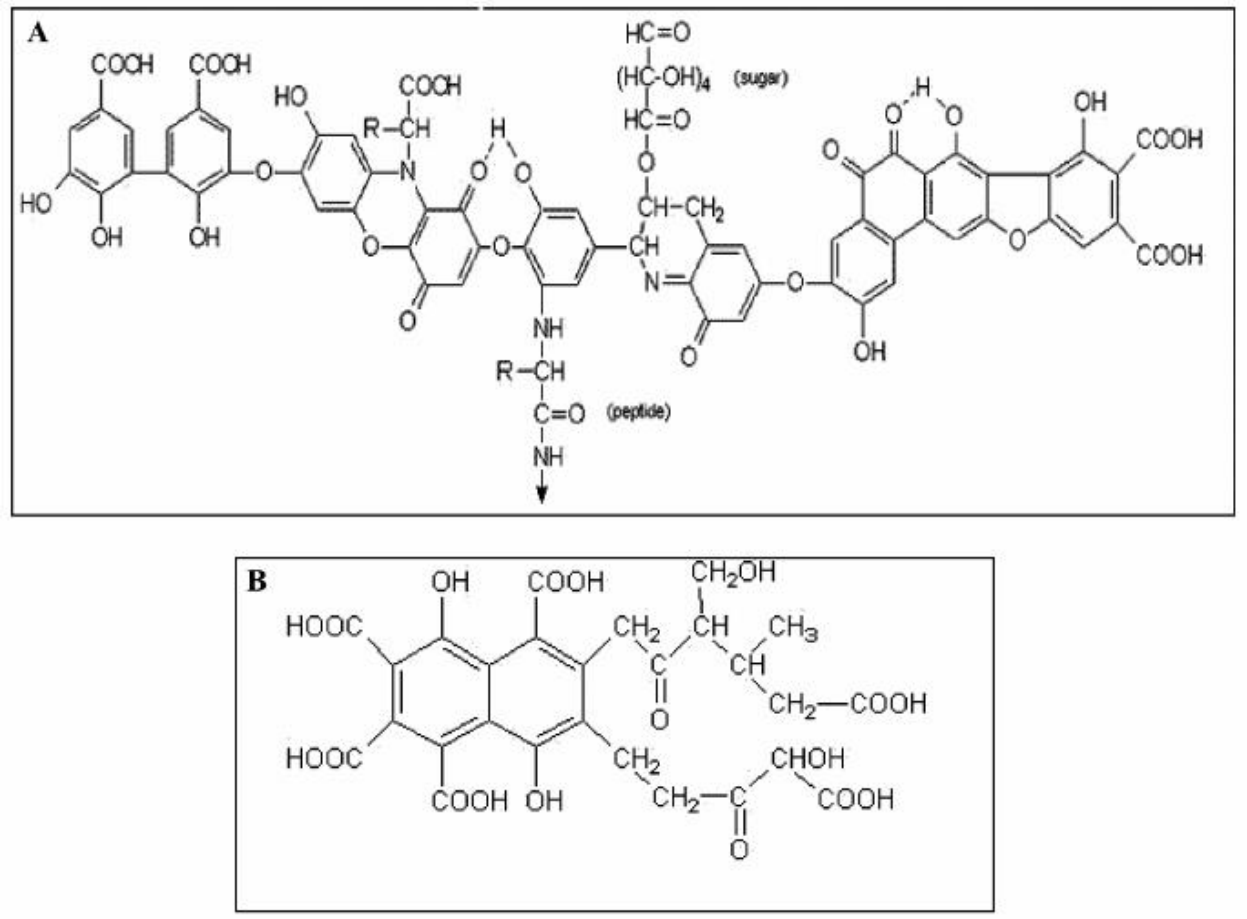

Figure 4. Model Structure of humic (A) and fulvic (B) substances (Stevenson, 1982).

Humic substances arise from the chemical and biological degradation of plant and animal residues and from synthetic activities of microorganisms. The products formed tend to associate into complex chemical structures that are more stable than initial material. An important characteristic of humic substances is their ability to form water-soluble and water-insoluble complexes with metal ions and hydrous oxides and to interact with clay minerals and organic compounds such as alkanes and fatty acids (Schnittzer, 1975). Such properties are fundamental in the eluvial and illuvial processes resulting in the formation of Spodosols. It is the interaction with Al, Fe, and sesquioxides that decrease the solubility of organic acids and the subsequent formation of the spodic horizon.

Infrared Spectroscopy in the Characterization of the Diagnostic Horizon

Spectroscopic measurements provide valuable information about the nature of soil humic substances. The Fourier Transformation Infrared (FT-IR) spectra of humic substances and their derivatives contain a variety of bands that are diagnostic of specific molecular structures because it (1) provides key information regarding the nature, reactivity and structural arrangement of oxygen containing functional groups; (2) the occurrence of protein and carbohydrate constituents can be established; (3) the presence or absence of inorganic impurities (metal ions, clays) in isolated humic fractions can be demonstrated; and (4) the technique is suitable for quantitative analysis (Stevenson, 1982).

The main absorption bands are in the regions of 3300 cm^{-1} (H-bonded OH groups), 2900 cm^{-1} (aliphatic C-H stretching), 1720 cm^{-1} (C=O stretching of COOH and ketonic C=O), 1610 cm^{-1} (aromatic C=O and H-bonded C=O), and 1250 cm^{-1} (C-O stretching and OH deformation of COOH groups). In addition, small bands are often evident at about 1500 cm^{-1} (aromatic C=C), 1460 cm^{-1} (C-H deformation of CH_2 or CH_3 groups), and 1390 cm^{-1} (O-H deformation, CH_3 bending, or C-O stretching) (Stevenson, 1982). Tan, (2003) suggest that the presence of a band near 1000 cm^{-1} is associated to impurities with SiO_2.

Physical Properties of Spodosols

Spodosols are a soil order relatively easy to recognize in the field because of the unique pattern of a grayish E horizon and a dark reddish B horizon that result from the eluviations and illuviation of C compounds, Al, and Fe (Soil Survey Staff, 1999; Mokma and Yli-Halla, 2015). Although field identification is often difficult because the spodic horizon definition includes chemical criteria, color relation between organic C, Al, and Fe contents suggest that Aquods tend

to be yellower than Orthods and that eluviation/illuviation of organo-metallic complexes are the primary determinants of color in Spodosols (Mokma, 1993).

Spodosols form mainly in sandy to coarse loamy acid deposits, and many Spodosols are distributed in areas rich in quartz sands (McKeague et al., 1983). Evidence suggests that sandy materials favor podzolization (Murashkina et al., 2007) They can also be found in chemically richer parent material, such as volcanic sand overlaying liparite tuff and volcanic ash-mantled landscapes (Suharta and Prasetyo, 2009; Valerio et al., 2016). High amounts of gravel disfavor the formation of the spodic horizon (Schaetzl, 1991).

Particle Size data shows that sandy or sandy-skeletal to loamy textures are typical of Spodosols. In addition, particle size class is mostly sandy, sandy-skeletal, coarse-loamy, loamy-skeletal, or coarse-silty, very few have a particle size class of fine loamy (Mckeague et al., 1983; Soil Survey Staff, 1999; Bockheim, 2014;).

Mineralogy of Spodosols

Mineral weathering is a process characterized by chemical and physical breakdown of geologic materials, accompanied by the generation of dissolved solutes plus relatively stable new mineral phases (Cronin, 2018). Figure 4 (Taylor and Eggleton, 2001), summarizes the mineral weathering of silicates. It presents the aluminum and iron sequence weathering, from feldspars and sheet silicates that yield aluminum oxides as the product, also rock forming silicates that release basic cations that result in iron oxides as the product.

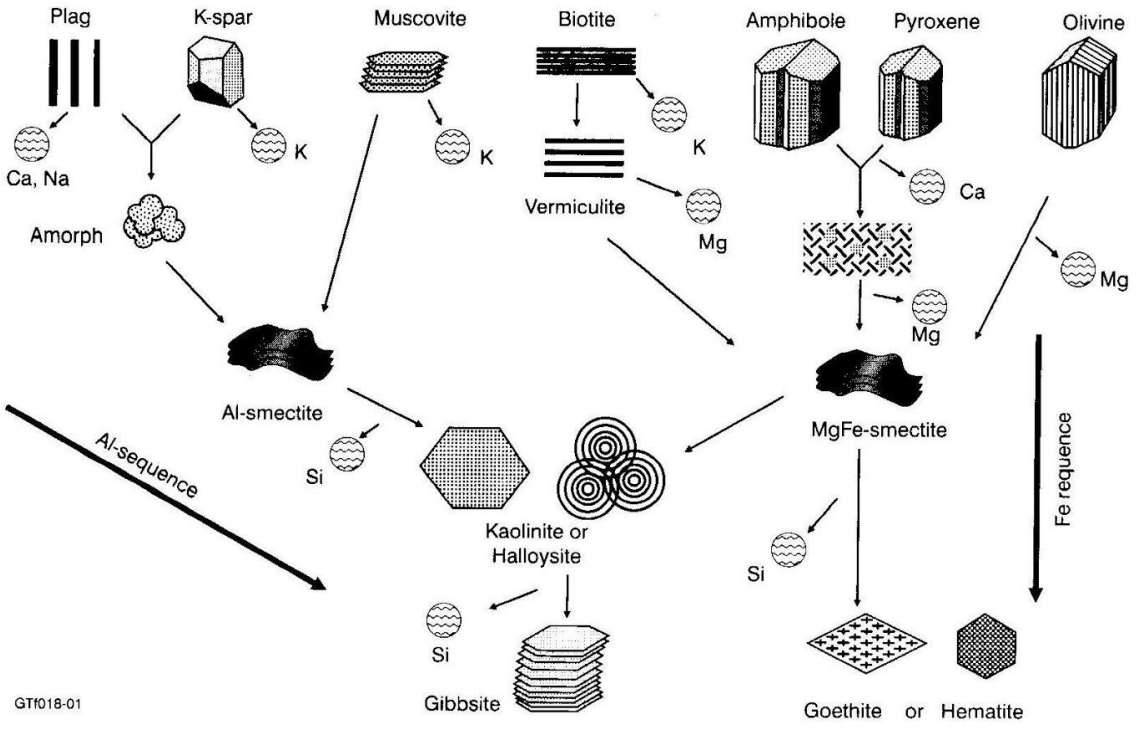

Figure 5. Diagram of silicate mineral weathering (Taylor and Eggleton, 2001).

Spodosols do not have a unique or typical mineralogy (McKeague et al., 1983). Spodosols tend to have a mixed siliceous mineralogy formed in quartzose sands are characterized by the concentrated oxide content in the clay fraction (Coen, 1970; Wilding et al., 1983). Mineralogical differences between the albic and the spodic horizon of Spodosols are often pronounced, the strong acidity and complexing tendency of downward-moving dissolved organic constituents (chelating agents) and the eluviated horizon are zones of strong mineral alterations. Most of the active components of Spodosols consist of poorly crystalline iron and aluminum oxides and Fe-Al organo-mineral complexes that are mostly amorphous to X-Rays. Zelazny and Carlisle (1971) reported that for Spodosols (Orthods) in cooler climates the intergrade minerals, kaolinite and gibbsite increased with depth, leading the authors to conclude that they were less stable than the amorphous components in the acidic upper horizons. Related to transformational

trends, in Aquods, phyllosilicates have a slow transformation process, and the reduction of Fe oxides occurs resulting in net loss of Fe, in Orthods non-expanding and partially expanding 2:1 phyllosilicate transform into smectite and there is a decrease in weatherable minerals in the eluviated horizon (Wilding et al., 1983).

Clay size minerals in Spodosols are analyzed using X-Ray analysis. The mineral transformation shows the dissolution of ferromagnesian minerals near the surface and liberation of Fe, Al, Mg, Si and other associated elements. Spodosols can have few clay sized phyllosilicates (Soil Survey Staff, 1999). Phyllosilicate weathering involves progressive removals and oxidation of Fe.

Mineralogical studies in Spodosols suggest that parent material influences this mineralogy especially that of the clay fraction, in addition, the depth distribution of minerals supports weathering sequences. The sand fraction is dominated by quartz with small amounts of other primary minerals (Haile-Mariam and Mokma, 2015). Quartz is one of the most abundant minerals, found in a variety of rocks and often intergrowing with feldspars, adds a gray or white color to a soil. (Nesse, 1986).

The E horizon is dominated by clean sand grains and organic matters may occur only as roots. In the spodic horizon, the silt and clay fractions occur as coatings on skeletal grains such as Al-, Fe-organic complex material (McKeague et al., 1983).

X-Ray diffraction is a common method used for qualitative and quantitative mineral composition determination in soils but overlapping peaks in X-ray diffraction patterns makes it difficult to carry out the identification and quantitative analysis in multimineral systems such as soils (Brinatti, et al., 2010; Bish, 1994). For example, kaolinite, halloysite, and the less common

dickite and nacrite are 1:1- layer-structured aluminosilicates of the same ideal composition; additionally, they have low surface areas and low cation- and anion-exchange capacity. Of these, kaolinite is the most widespread clay mineral in soil especially those of warm, moist climates. Both kaolinite and halloysite are products of acid weathering. To differentiate these minerals that have the same layer composition, samples may be chemically treated for expansion or contraction of the layers and employ other analytical techniques such as Infrared spectroscopy or nuclear magnetic resonance spectroscopy for a better qualitative analysis (Dixon, 1989).

The poor crystalline aluminosilicates, such as allophone, imogolite and ferrihydrite, lack the long-range crystalline structure when compared to other aluminosilicates. Allophone and imogolite are characterized by having a small particle size, high specific surface area and variable and/or permanent charge. Allophane and imogolite are common in soil derived from volcanic ash, but they have also been identified in soils developed from igneous and sedimentary rock, loess, gneiss and sandstone in a variety of climates and geographic regions throughout the world. The formation of these species may be dependent on time, climate, parent material, vegetation, or the soil solution. For example, halloysite and siliceous Fe oxides can form before or instead of allophone or imogolite. Halloysite formation is favored under conditions of high soluble silica, and kaolinite, more crystalline and stable, forms at a slower rate. Under extensive leaching, silica is depleted to the extent that gibbsite forms after a few thousand years. Halloysite and allophone can coexist with imogolite and gibbsite, alternating seasonal leaching and desiccation patterns can lead to varying concentration of Si, allowing for both halloysite and allophone to form. (Gustafsson, et al, 1995; Harsh, 2005).

The organo-mineral complex

The organo-mineral complex is a term used in broad sense to encompass different kinds of organo-mineral entities in the soil, including the chelate complex- which forms when a metal ion is attached by coordinate links to two or more non-metal atoms in the same molecule or ligand. The mineral components of organo-mineral complexes in soils are generally better known than the organic components, much is known of the structure, surface properties and abundance of clay minerals and oxides in soils (Mckeague et al., 1986). Organo-mineral complexes play a major role in the stabilization of organic matter, because the mineral phase influences not only the proportion but also the nature of the organic compounds present in organo-mineral complexes (De Junet et al., 2013).

Humic substances are a mayor constituent of the organic fraction of most soils, and they are condensed polymers of aromatic and aliphatic compounds produced by the transformation of plant lignin (Stevenson, 1982). The effectiveness of soil organic matter in complexing metal ions will generally depend on the relatively amounts of some ligands present, for this reason substances with phenolic groups, carboxylic acid groups, aliphatic hydroxyl and ketone groups are among the most important ligands in soil development (Mckeague et al., 1986).

In Spodosols two main types of spodic horizons occur based on the occurrence of organo-mineral complex the first is a fulvic acid-Al, Fe complex as the dominant amorphous component and a less common type formed under temporary or prolonged reducing conditions and in some Fe-poor materials has humic acid as the commonly associated with Al as the mayor amorphous component (Mckeague et al., 1986).

Other chemical Properties

Field identification of Spodosols is frequently complicated by the chemical criteria in the definition of the spodic horizon and spodic materials. The criteria that must be met to qualify as spodic material is pH in water $\leq$ 5.9, and organic C $\geq$ 0.6% (Mokma and Yli-Halla, 2015). Spodosols tend to have a high organic C content (1.4-37.7%) and acid soil reaction (pH 3.7-5.3). The base saturation is naturally low (<5%) (Suharta and Prasetyo, 2009), but the cation exchange capacity is large, and it comes from non-silicate clay sources (McKeague et al., 1983). Spodosols are naturally infertile, but they can be highly responsive to good management (Soil Survey Staff, 1999).

A clear chemical distinction in the illuvial horizon is the accumulation of active amorphous organic-sesquioxide material. This material is that which has high cation exchange capacity, large surface area and high water retention which describes the material that accumulates in the Spodic horizon (McKeague et al., 1983).

In Spodosols, the depletion of bases occurs through leaching of soils in humid regions, bacterial decomposition of organic matter is retarded and minerals weather more rapidly releasing Si, Al, Fe and other elements. The water-soluble products of organic matter decomposition move downward, reacting with the mineral surface and complex Al and Fe, but these rates of reaction depend on concentration and nature of organic matter in the soil solution, the pH, the mineral surface susceptible to attack and the nature of minerals. This complex is deposited in soils with available sesquioxides, forming the spodic horizon (McKeague et al., 1983).

Influence of climate, vegetation and time

Spodosols are typically found under coniferous forests where low decomposition rates are promoted by cool climates and short growing seasons and acidic litter that has high contents of slowly degradable compounds such as lignin and waxes (Mckeague, et al., 1983; Lundstrom et al., 2000; Egli, et al., 2004; Mossin et al., 2001; Schaetzl and Thompson, 2015). Spodosols can be found under diverse vegetation including deciduous forest, shrubs and mosses, boreal forest and heath vegetation (Mckeague et al., 1983). Although when vegetation changes, podzolization and related pedogenetic processes change, both in strength and kind (Mossin et al., 2001)

Spodosols are most extensive in areas of cool humid or perhumid climate (Soil Survey Staff, 1999). In typical podzol areas temperature in January varies between -40 and +5 °C, and in July between +10 and +20 °C and precipitation is from 200 to over 1000 mm a^{-1} with a lower evapotranspiration rate (Lundstrom et al., 2000). Podzol development is influenced by increasing snowpack in Spodosols throughout Wisconsin and Michigan, USA. A thick snowpack inhibits frost and allows large fluxes of snowmelt to infiltrate the profile (Schaetzl and Isard, 1996).

Spodosols are also formed in hot, humid tropics and warm, humid regions (Soil Survey Staff, 1999). Most of the Spodosols in tropical or subtropical regions occur on wet sites, where the influence of the water table is central to pedogenesis (Watts and Collins, 2008). These Spodosols are commonly Alaquods, a classification that reflects their wetness and the abundance of Al in the spodic horizon (Stone et al., 1993; Harris and Kollien, 1999).

The formation of the spodic horizon may take from 40 years in a sand pit (Bronick and Mokma, 2005) to hundred years (Boorman et al., 1995; Alexander and Burt, 1996). Other

authors suggest that the formation of the spodic horizon may take up to thousands of years (Barrett and Schaetzl, 1992; Mokma et al., 2004; Sauer et al., 2008)

Classification of Spodosols

In the description of Spodosols suborders, emphasis is divided between soil wetness, soil temperature, spodic horizon dominated by the illuvial accumulation of organic matter and varying amounts of carbon aluminum, and iron in the spodic horizons. Spodosols are classified into five suborders- Aquods, Cryods, Gelods, Humods and Orthods. Aquods are Spodosols that have aquic conditions, a histic epipedon or redoximorphic features in an albic or spodic horizon. Aquods are characterized by a shallow fluctuating water table and the presence of water loving plants. Cryods are Spodosols that have a cryic soil temperature, usually located in high latitudes or high elevations, under coniferous vegetation. Gelods are Spodosols with a gelic temperature regime but lack permafrost. Humods are freely drained Spodosols that have 6.0% or more organic carbon in a layer 10 cm thick or more within the spodic horizon. Orthods are other Spodosols that do not meet the criteria to be classified as previously described. Orthods are freely drained Spodosols that have a moderate accumulation of organic carbon, they are naturally infertile but can be responsive to good management (Soil Survey Staff, 1999; Soil Survey Staff, 2015).

Spodosols in Puerto Rico

In Taxonomic Classification of the Soils of Puerto Rico, 2017 (Muñoz et al., 2018), three Spodosols series are identified. These are Algarrobo (Entic Alorthods), Arecibo (Entic Grossarenic Alorthods), and Corozo (Typic Alorthods). In Puerto Rico, this order is of least extension, occupying about 1,733 ha on the northern coast, throughout the municipalities of Arecibo, Barceloneta, Vega Baja and Vega Alta. A map (Figure 5) of the soil orders of Puerto

Rico, Spodosols are identified in black coloration extend through central north portion of the island (Muñoz et al., 2018).

The three-current series- Algarrobo, Arecibo and Corozo, belong to the Great Group Alorthods (Muñoz et al., 2018). Alorthods are Spodosols that have accumulation of aluminum that occur in relatively high amounts when compared to the accumulation of iron. The low amount of iron accumulation is due to intensive leaching or because parent material has low iron content. These soils form predominantly in sandy deposits and are common in areas of warm climates (Soil Survey Staff, 2015).

Spodosols were likely recognized in Puerto Rico but were not officially included in the classification of the 1975 publication of Taxonomic Classification of the Soils of Puerto Rico (Lugo-López and Rivera, 1975). For these soils, the spodic horizon is an accumulation of Al and organic matter, and they are characterized by a very thick white sandy A_2 horizon that overlies a brittle, slightly cemented spodic horizon with the possibility of classifying as Tropaquods and Tropohumods. The Algarrobo series is described in the Soil Survey of the Arecibo Area-Northern Puerto Rico (Appendix I) (Acevedo, 1982). Algarrobo series had a taxonomic classification coarse-loamy siliceous, isohyperthermic Entic Haplohumods. In general, the Arecibo Area soil survey (Acevedo, 1982), the Algarrobo-Corozo-Arecibo association is described as deep gently sloping to sloping, excessively drained and well drained sandy soils, with low fertility, high acidity, and low available water capacity, with few limitations as a site for buildings and roads and as a good source of road fill. In this soil survey this soil association was identified as being used as a source of sand for industrial purposes.

In the most recent publication of Taxonomic Classification of the Soils of Puerto Rico, 2017 (Muñoz et al., 2018) Algarrobo series has a taxonomic classification of Coarse-loamy over clayey siliceous over mixed, subactive, isohyperthermic Entic Alorthod. This series is described as consisting of deep and excessively drained soils located on coastal plains. These soils form in coarse textured sediments high in quartz and underlain by clayey coastal plain deposits. Algarrobo series areas have been used for silica sand extraction (Muñoz et al., 2018).

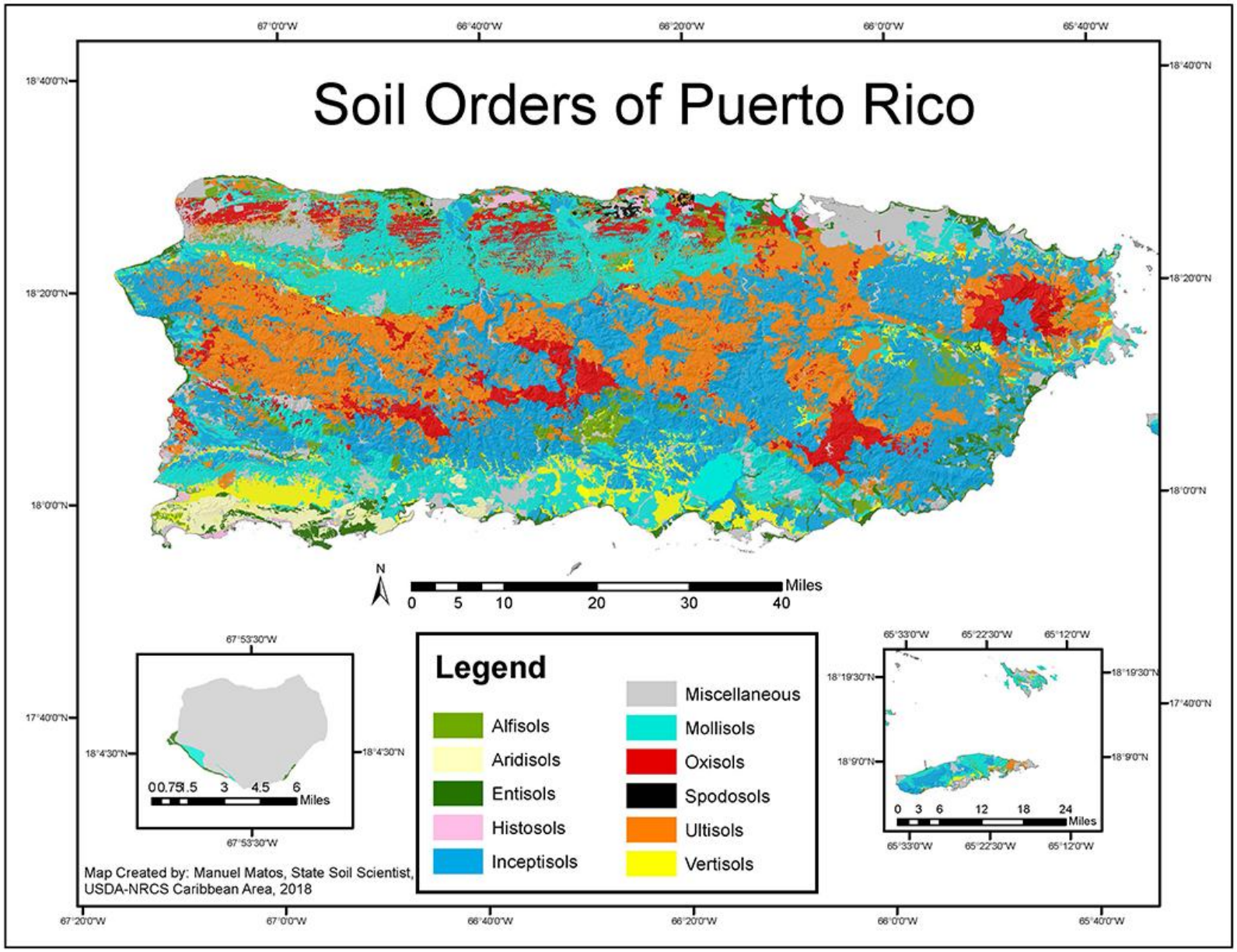

Figure 6. Map of the soil orders of Puerto Rico (Muñoz et al., 2018).

MATERIALS AND METHODS

Site Description

The research was conducted at Carmen Regadera Farm, a property of the Puerto Rico Land Authority, in the municipality of Vega Alta. A soil map of the area of interest is shown on Figure 6. Four sites were selected in an area corresponding to Algarrobo Soil, according to Web Soil Survey (Soil Survey Staff, 2018). A soil pit was dug on each at each site and a description of the profile was conducted. Geomorphologic features, such as hill-slope profile position, were noted. The GPS location of each pit was determined using a Garmin *GPSmap 60C*.

Figure 7. Area map of Carmen Regadera Farm and vicinity with markers indicating Algarrobo profiles location.

Soil Profile Description

The soil profiles were described using *Field Book for Describing and Sampling Soils* (Shoeneberger et al., 2012), and the Pedon description form was used to describe field observations. The soil horizons were identified and described in terms of depth, boundary limits, texture, color and other features. Soil color was described using Munsell Color Charts and soil

texture by the tact method (Thien, 1979). Presence of roots, pores, nodules and other special features was recorded.

Soil Sampling and Analysis

Soil samples from each horizon were collected, air dried, ground and passed through a 2 mm mesh sieve. The samples were analyzed for texture, pH, organic matter content, aggregate stability, surface area, and exchangeable cation content. The mineralogy of the clay fraction was determined using X-Ray Diffraction. The iron and aluminum oxide content of the fine earth fraction were determined by selective dissolution techniques.

Soil Textural Class

The hydrometer method was used to determine soil textural class (Gee and Or, 2002). A 40.00 g sample of soil was weighed and transferred to a bottle with a 200 mL solution of sodium metaphosphate. Each sample was agitated for 5 minutes with a mixer. The suspension was transferred to a 1000 mL sedimentation cylinder and filled to volume with distilled water. The solution was agitated with a plunger for 30 s. The hydrometer was lowered and at 40 seconds after agitation, hydrometer and temperature reading were taken. At two hours after agitation, a second lecture of temperature and hydrometer reading was performed. Hydrometer readings were corrected for temperature using the following formula

$$\text{Corrected lecture} = \left((T^{\circ}) - 67^{\circ}\right) \text{x } 2.2$$

Sand, silt, and clay distribution were calculated using the following formulas

$$\% \text{ Sand} = \frac{DW - R_{1c}}{DW} \text{ x } 100$$

$$\% \text{ Silt} = \frac{R_{1C} - R_{2C}}{DW} \text{ x } 100$$

$$\% \text{ Clay} = \frac{R_{2C}}{DW} \text{ x } 100,$$

were DW is the oven dry weight and R_C is the corrected hydrometer reading, 1 at 40 s and 2 at 2.0 hrs. Textural class for each sample was determined using USDA Soil Texture Triangle.

Particle Size Distribution

Particle size distribution was determined by centrifugation method (Gee and Bauder, 1986). Forty grams of soil were weighed and transferred to a 1000 ml beaker. The sample was moistened with a solution of sodium acetate (NaOAc). If effervescence was noted an additional portion of 5 ml of NaOAc was added. If no effervescence was observed, the sample was treated with 5 ml of H_2O_2 30% and mixed. When the effervescence diminished, the beaker containing the sample was placed in a water bath at 80˚C, another portion of 5 ml H_2O_2 30% was added and the mixing process repeated. Additional 5 ml portions of H_2O_2 30% were added until the effervescence diminished significantly. The process to remove organic matter with H_2O_2 was performed for 3 hours.

The soil from the beaker was transferred to a 250 ml centrifuge bottle using 100 ml of 0.25 M sodium chloride (NaCl). Sample was agitated manually and centrifuged a 1500 rpm. Excess clear liquid was poured out. The soil was transferred to an electric mixer using 150 ml of sodium carbonate solution. The sample was mixed for 15 min, transferred to a clean centrifuge bottle and filled with a sodium carbonate solution. The soil sample was agitated manually, and later centrifuged for 3.5 min at 700 rpm. The supernatant containing the clay was poured into a large beaker. The process was repeated until clay suspension poured into the beaker was clear. The

beaker with suspended clay was covered with paraffin film and after a few days the excess liquid was removed. The clay was saturated with Mg^{2+}, dried at 65° C and ground for XRD analysis.

The silt and sand fractions were separated by sieving using a No. 325 sieve and distilled water. Sand and silt fractions were oven dried for 24 hours at 105˚C. Particle size distribution was calculated as follows:

$$\% \text{ Sand} = \frac{\text{Sand Dry Weight}}{\text{Sample weight}} \text{ x } 100$$

$$\% \text{ Silt} = \frac{\text{Silt Dry Weight}}{\text{Sample Weight}} \text{ x } 100$$

$$\% \text{ Clay} = 100\% - (\%\text{Sand} + \% \text{ Silt})$$

XRD analysis

The Mg-saturated clay was ground in an agate mortar to obtain a fine powder. The X-Ray analysis was performed using powder clay samples. The samples were analyzed using a Siemens Diffractometer D-5000 located at the Geology Department of the University of Puerto Rico. The scans were collected from 4 to 70 degree 2-theta, at a 0.020° step per second.

Surface Area

Specific Surface Area (SSA) was determined as described by Cihacek and Brenmer (1979). Fifty mg of clay and soil sample was placed in a previously weighed vessel and oven dried for 24 hours at 105° C. Samples were left to cool in a desiccator with calcium chloride ($CaCl_2$). The samples were weighed and 1 ml of ethylene glycol monoethyl ether (EGME) solution was added to the sample, allowing a 30 minutes time period to equilibrate. The desiccator was evacuated for

45 minutes using a vacuum pump. Sample weight was recorded daily to monitor weight lost. Once constant weight was attained, SSA was calculated as follows:

$$SSA = \frac{\text{grams of EGME}}{\text{grams of sample}} \text{ x } \frac{1}{2.86 \text{ x } 10^{-4} \text{ g/m}^2}$$

Aggregate Stability

Aggregate stability was determined by the wet sieving method (Nimmo and Perkins, 2002). Air dry soil samples were passed through a No. 4 sieve and collected in a No. 10 sieve. Aggregates retained in the No. 10 sieve were used to determine aggregate stability. Two 30.0 g samples were weighed, one to determine the percent of stable aggregates and the other to determine moisture content of the air-dry soil. This sample was placed in an oven at 105° C for 24 hours.

For the determination of the stable aggregates, the sample was placed on a No. 10 mesh sieve over a No. 20 mesh sieve. The sieves were placed in a recipient and water was added, allowing the samples to absorb capillary water to avoid air slacking. The sample was agitated for 30 min, in an upward and downward motion. The sieves were separated, and placed in an oven at 65˚C oven for 30 min. The aggregates were transferred to a weighing plate and dried at 105˚C overnight. Aggregate stability was calculated as follows:

$$\% \text{ A. S.} = \left(\frac{A+B}{C}\right) \text{ x } 100 \text{ ,}$$

for which A is aggregate weight retained on mesh No. 10, B is aggregate weight retained on mesh No. 20 and C is oven-dry weight of the initial sample.

pH

Soil pH was determined in a 1:1 soil/water ratio. Twenty grams of soil were placed into 120 ml vessels with 20 ml of distilled water. Samples were placed on a mechanical shaker for 30 minutes. The pH was measured using *Thermo Scientific* pH Meter *Orion Star A215.*

Organic Carbon and Organic Matter Content

The soil organic carbon (% OC) and organic matter (% OM) content were determined by the Walkley and Black wet oxidation method (Nelson and Sommers, 1996). A 0.50 g sample of soil was transferred to a 500-ml Erlenmeyer flask and 10-ml of potassium dichromate solution and 20.0- ml of concentrated sulfuric acid were added to each flask. The samples were agitated manually and left to cool for 30-minutes. Afterwards, 200-ml of distilled water were added and 5 drops of ferroin analytical indicator. The samples were titrated with 0.5 N ferrous ammonium sulfate and the organic carbon content was determined as follows,

$$\%\ O.C. = \frac{\text{meq } K_2Cr_2O_7 - \text{meq } Fe(NH_4)_2(SO_4)_2}{\text{Soil weight (g)}} \times \frac{0.003 \text{ g C}}{1 \text{ meq}} \times 100,$$

Organic Matter content was calculated as follows,

$$\%\ O.M. = (\%\ O.C.)\left(1/0.77\right)\left(1/0.58\right)$$

In the formula 0.77 is the % C recovered during the Walkley-Black method, and 0.58 is a conversion factor of carbon to organic matter.

Exchangeable basic cations

Exchangeable basic cations were determined by the Ammonium Acetate Method at pH 7.0 (Sumner and Miller, 1996). Five g of soil were transferred to plastic vessels. Fifty ml of 1 M

ammonium acetate solution was added, and samples were placed in a mechanical shaker for 30 minutes. The solution was filtered using Whatman No. 42. The samples were analyzed using *Thermo Scientific iCap 6000 series* Inductive Couple Plasma Spectrometer.

Exchangeable Aluminum

Exchangeable aluminum was extracted with 1 M KCl (Bertsch and Bloom, 1996). Ten g of soil were transferred to plastic vessels. 100 ml of KCl 1 M solution was added and the samples were placed in a mechanical shaker for 2 hours. The solution was filtered using a Whatman No. 42. The solution was diluted to 10:100 and analyzed using *Thermo Scientific iCap 6000 series* Inductive Couple Plasma Spectrometer.

Iron and Aluminum Oxides

Iron and aluminum oxide content was determined using Citrate-Dithionate-Bicarbonate (CDB) method, the Acid Ammonium Oxalate (AAO) method and the Sodium Pyrophosphate (SP) method. The oxalate extraction yields organic and amorphous forms of Fe and Al; the dithionite extraction yields all free forms of these elements, including crystalline; and pyrophosphate extraction yields organic bound forms of iron and aluminum (Bockheim and Hartemink, 2017). The soil samples used for these analyses were passed through a No. 100 mesh sieve, and the extract was analyzed to determine iron and aluminum content *Thermo Scientific iCap 6000 series* Inductive Couple Plasma Spectrometer.

Acid Ammonium Oxalate Method

Two hundred and fifty mg of soil samples were transferred to 50 ml test tubes. Ten ml of acid ammonium oxalate solution were added to each test tube and the test tubes were covered in aluminum foil to avoid light interference. Test tubes were placed in a mechanical shaker and

agitated for 4 hours, in the dark. The samples were centrifuged at 1,500 rpm for 5 minutes and filtered using a Whatman No. 42. Aluminum and iron content were determined by Inductive Coupled Plasma and expressed as % Al_2O_3 and % Fe_2O_3.

Citrate-Dithionite-Bicarbonate Method

Iron and aluminum oxides were extracted using method described by Mehra and Jackson (1960). Samples of 0.500 g of soil were transferred to 50 ml test tubes. Five ml of citrate bicarbonate solution was added. About 0.2 g of sodium dithionite were added and mixed in. The tubes were placed in a water bath at 75-80˚C and the samples were stirred every 2-3 minutes for 15 minutes. The tubes were removed from the water bath and 1 ml of saturated sodium chloride (NaCl) was added. The samples were centrifuged at 1500 rpm for 5 minutes and filtered using a Whatman No. 42 filter paper into a 100 ml volumetric flask. The extraction procedure was repeated a second time, and the sample was washed twice with a 5 ml portion of citrate-bicarbonate solution and 1 ml of NaCl and the solution was added to the volumetric flask. The samples were brought to volume using distilled water and analyzed by Inductive Coupled Plasma. The iron and aluminum content were expressed as % Al_2O_3 and % Fe_2O_3.

Sodium Pyrophosphate Method

Samples of 0.300 g of soil were transferred to 50 ml centrifuge tubes. A 30 ml solution of 0.1 M sodium pyrophosphate were added to each sample and the centrifuge tubes shaken for 12 hours, using a mechanical shaker. After the shaking period, the samples were centrifuged at 12,000 rpm for 10 minutes and the supernatant filtered using a Whatman No. 42 filter paper into 50 ml tubes for analysis. The iron and aluminum content were expressed as % Al_2O_3 and % Fe_2O_3.

FTIR of the spodic horizon

The extraction of the humic and fulvic acids was performed on the spodic horizon of each profile. The extraction and purification of humic acid and fulvic acid is a modified method as described by Stevenson (1982). Forty grams of soil were place in a suction funnel and washed with two portions of 100 ml of 0.1 N HCl. The soil was transferred to a 250 ml centrifuge bottle and 200 ml of 0.5 N NaOH solution were added. The mixture was shaken for 12 hours and centrifuged at 2,500 rpm for 10 minutes. The dark colored supernatant was decanted into a flask using a glass wool filter. An additional portion of 200 ml of 0.5 N NaOH solution was added to the soil. The mixture was shaken for 1 hour, centrifuged, decanted and the supernatant was added to the previous extract. Two hundred ml of distilled water were added to the soil in the centrifuge bottle, manually shaken to disperse, and centrifuged at 2,500 rpm for 10 minutes. The supernatant was filtered through glass wool and collected with the previous extracts. The pH of the solution was adjusted to 1.0 with concentrated HCl to separate humic (dark precipitate) and fulvic acid fractions (light colored supernatant).

The lighter colored supernatant (fulvic acid) was removed with a siphon, and the dark precipitate was transferred to a centrifuge bottle and centrifuged at 2,500 rpm for 10 minutes to facilitate humic and fulvic acid separation. The humic acid was dissolved with 0.5 N NaOH, pH was adjusted to 1.0 with concentrated HCl and centrifuged again. This procedure was repeated a second time, and the humic acid was washed twice with distilled water. Humic and fulvic acid separated were lyophilized using a Labconco Free Zone freeze dryer.

The fractions were ground to a fine powder and stored until analyzed. FTIR analysis of the powder samples were performed using a Perkin Elmer Spectrum Two FT-IR Spectrometer.

The spectra were obtained in the IR range 4000-485 cm^{-1}. A total of 4 scans per sample were collected, averaged and the spectra recorded in % transmittance (%T).

RESULTS AND DISCUSSION

Four soil profiles were evaluated in Carmen Regadera Farm located in Sector Sabana, in the municipality of Vega Alta, Puerto Rico. A Web Soil Survey map (Soil Survey Staff, 2018) of the farm is shown in Figure 7. The soils of the area are AgC- Algarrobo fine sands (Entic Alorthod), CsC- Corozo fine sands (Typic Alorthod), MmF- Matanzas rock outcrop complex (Lithic Eustrustox), RtF- Rock outcrop Tanamá complex (Lithic Hapluadalf), Vg- Vigía muck (Terric Haplosaprist). An area designated as sand pits (Pt) and water stream (W) are shown in the map. The pits are located are located in a humid coastal plain landscape over a marine terrace. The slope in the area varies from 0-12% (Soil Survey Staff, 2018). The parent material in the area is sandy sediments, sandy sediments underlain by clayey deposits and sand underlain by clayey coastal plain deposits (Soil Survey Staff, 2018).

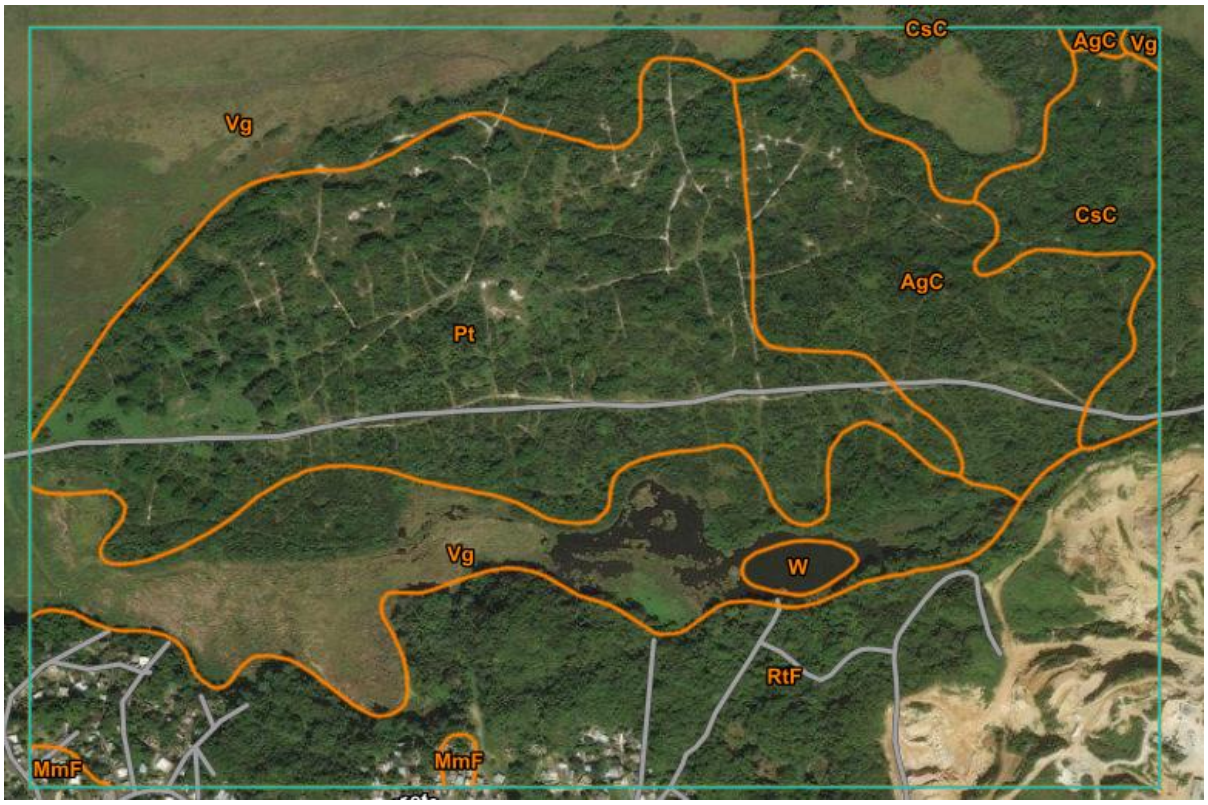

Figure 8. Soil map of Algarrobo series (Soil Survey Staff, 2018).

The farm was not in intensive agricultural use, mostly natural pastures and patches of secondary forest. The presence of horses and cattle was observed. The dominant vegetation in the area are icacos trees (*Chrysobalanus icaco)* and corozo palms (*Attalea cohune)*, with a lesser extent of vegetation that includes confidently identified crotalaria (*Crotalaria sp.)*, tassel flower (*Emilia fosbergii*), nutgrass (*Cyperus sp*.) tick trefoil (*Desmodium s*pp.), *verbe*na (*Stachytarpheta jamaicensis*). Other plants include herbaceous plants that belong to Euphorbiaceae family, plants belonging to the Fabaceaea family (*Senna sp.* and acacias- such as *Vachellia sp*.); plants in the family Convulvulaceae such as *Ipomoea sp.* (Más and Lugo, 2013).

Description of the soil profiles

Algarrobo profile A (Figure 8) is located north of the roadway (18°27'02", -66°20'03"), under dense vegetation composed mainly of Cupey trees (*Clusia rosea)*. Gilgai microtopography is observed various meters NW of the opened pit, and when we observe the soil map, the pit is located near Vigía muck, soils that are described as deep poorly drained soils, formed from the residuum of highly decomposed plant tissues over fine textured sediments, located in depression areas (Soil Survey Staff, 2018). The landscape location of the profile is toe-slope, with an elevation of around 3 m above sea level. This profile shows a morphology described as an egg cup shaped Spodosols. Such morphological trait has been attributed to forest vegetation. Similar Spodosols has been found in New Zealand (Evans and Youngquist, 2004). These authors describe this morphology as a bleached, egg-cup shaped E horizon, beneath roots of old-growth trees, underlain by the spodic horizon.

Figure 9. Image of Algarrobo profile A.

Eight horizons were identified in profile A (Table 1). The distinctness between horizons in most cases is abrupt and the topography between one horizon and the next is smooth in the upper A and E, and turns wavy as we move deeper into the profile. The E horizon is lighter in color, indicative of the eluvial process. The illuvial B horizon shows a darker color that can be attributed to the accumulation of organic compounds and oxides at 30.5 cm deep. A second illuvial is identified at 55.9 cm from the surface; this may have been caused by removal of material and latter deposition event causing burial of the profile. It is possible that the mechanical mixing of sand material occurred as a result of possible sand extraction at this site or nearby, these soils have been used as a source of sand for industrial purposes (Acevedo, 1982). The field texture was sandy, loamy sand and clay, when determined from the surface to the bottom. At the time of evaluation seepage was observed from the profile wall at approximately at 46 cm and 94 cm. Algarrobo profile A has no structural units in the profile, the loose sand that makes up the soil profile describes a structureless soil. Redoximorphic features described as color patterns in a soil caused by depletion or concentration of pigment compared to the matrix color (Schoeneberger et al., 2012), are observed through the 64 – 84 cm horizon. Concretions, possibly iron masses, are observed in both 64 – 84 cm and 114 - 203 cm. The brown/orange coloration of these concretions suggest the occurrence of iron in the form of mottles or soft masses and is used as an indicator of hydric soils and wet Spodosols (Aquods) found in Florida, Alaska, North Carolina, Michigan and Georgia (Tiner, 2016).

Table 1. Horizon designation and description of Algarrobo profile A.

Master Horizon	Depth (cm)	Distinctness	Topography	Color	Texture	Additional observations:
A	0 – 17	Abrupt	Smooth	2.5YR 4/1	Sand	Presence of roots
E_1	17 – 30	Gradual	Smooth	10YR 8/1 10YR 2/1	Sand	Presence of Roots, & Earthworms
B_h	30 – 40	Abrupt	Wavy	10 YR6/1 10YR 3/2	Sand	Mottled- Salt and Pepper
E^1	40 – 54	Abrupt	Wavy	10YR 7/1	Sand	-
B_{hs}	54 – 64	Abrupt	Wavy	10YR 6/4 2.5Y 3/1	Sand	Roots
BC_1	64 – 86	Abrupt	Wavy	2.5Y 5/2	Sand	Few redoximorphic features
BC_2	86 – 114	Abrupt	Wavy	2.5Y 7/4	Loamy Sand	-
2C	114 – 203	Abrupt	Wavy	2.5Y 7/1	Clay	Hard pan, concretions (iron masses)

Algarrobo profile B is shown in Figure 9. This profile is located south of the roadway at 18°27'00", -66°20'02", under dense vegetation dominated by icaco trees (*Crysobalanus icaco)*. The landscape location of the profile is a toe-slope, with an elevation of around 3 m above sea level. In a first evaluation, soil samples were collected to 100 cm deep for chemical analysis, and more detailed evaluation of the profile 10 horizons were identified to a depth of 203 cm (Table 2). Horizon designation is as follows A_1-A_2 –E-B_{hs1}-B_{hs2}-B_{s1}-2BC- $2C_1$-$2C_2$-$2C_3$. A clearly defined E horizon is observed in this profile. The B horizon is found at 33-58 cm depth, with a gradual lose in matrix color as we move deeper into the soil profile. Soil texture was sandy from A to B horizons and changes to sandy loam. Soil structure from the surface to 99 cm is structureless in the form of single grain. The structure transitions to massive at the 99 to 203 cm horizons. Redoximorphic features are observed primarily in the three horizons extending from 75 to 112 cm and are recorded as depletions or areas of decreased pigmentation. The loss of

pigmentation is due to loss of Fe and/or Mn (Schoeneberger, 2012). Tubular pores are observed from the surface to 87 cm deep and are reduced in quantity from the surface to deeper horizons. Krotovinas, or animal burrows are observed in the surface horizons (Figure 11).

Figure 10. Image of Algarrobo profile B.

Table 2. Horizon designation and description of Algarrobo profile B.

Master Horizon	Depth (cm)	Distinctness	Topography	Color	Texture	Additional observations:
A_1	0 – 14	Clear	Wavy	2.5Y 4/1	Sand	Salt and Pepper appearance
A_2	14 – 33	Clear	Smooth	5Y 2.5/1	Sand	Clay pockets and krotovina filled with sand
E	33 – 58	Abrupt	Smooth	2.5Y 7/1	Sand	Krotovina holes; organic splotches; striped sand grains
B_{hs1}	58 – 75	Clear	Smooth	5Y 3/2	Sand	Clay pockets and krotovina, organic horizontal lines; organic tonguing
B_{hs2}	75 – 87	Gradual	Smooth	2.5Y 4/3	Sand	Few redoximorphic features
B_{s1}	97 – 99	Gradual	Smooth	10YR 3/6	Sand	Few redoximorphic features
2BC	99 – 112	Clear	Smooth	10YR 7/1	Sandy Loam	Weakly cemented, Many redoximorphic features; clay bodies
$2C_1$	112 – 148	Clear	Smooth	2.5Y 6/3	Sandy Loam	-
$2C_2$	148 – 167	Clear	Smooth	2.5Y 7/3	Sandy Loam	-
$2C_3$	167 – 203	Clear	Smooth	2.5Y 7/1	Sandy Loam	-

Figure 11. Krotovinas in Algarrobo profile B.

Algarrobo profile C is shown in Figure 12. This profile is located north of the roadway at 18°27’00”, -66°20’02”, in an open area where a vegetation of icaco trees (*Crysobalanus icaco)* predominates. The landscape is a foot-slope, and it is located at an elevation of 9.5 m above sea level.

Figure 12. Image of Spodosols profile C.

Two evaluations were performed in Algarrobo profile C. In a first evaluation soil samples for Algarrobo profile C were collected from four horizons to a depth of 75 cm, because the pit was flooded. In a second evaluation 9 horizons were identified to a depth of 203 cm (Table 3). Horizon designation is as follows A–E-B_{hs1}-B_{hs2}-B_w -B_s-C-C_2-2C_1. A clear distinctness between the eluvial area in the profile around 20 cm deep with the overlaying A horizon and the underlying B horizon around 40 cm is observed. A gradual change in matrix color is also observed as we move deeper into the soil profile. The topography of the surface horizons is wavy and transitions to smooth at 74 cm deep. The distinctness between the eluvial area and the underlying horizon is clear. The presence of roots is observed through the surface horizons and at the 74 – 128 cm horizons, very fine roots were observed in the surface and deeper horizons, and medium roots were observed in the surface A horizon.

A predominant sandy texture is observed throughout Algarrobo profile C, except for the last C horizon at the depth of 188 cm where a clayey texture was observed. In the second evaluation, the soil structure observed was single grain up to 34 cm deep. Soil structure observed in the horizons from 34-87 cm and 129–148 cm deep is weak angular and subangular blocks. The horizons at 87–129 cm and 148–203 had a structureless massive soil structure. Cementation is observed throughout the profile. In the 34-56 cm horizon a weakly cemented observation is noted. In the 56–74 cm horizon a strongly cemented observation is noted and at the 87-129 cm, a very strongly cemented observation was noted. The flooded pit observed initially may be caused by the occurrence of a pan described as a hard and typically impermeable subsurface layer in a soil (Chesworth, 2008) or possibly reduced porosity in sandstone that reduces the permeability (Iscan and Kok, 2009).

Table 3. Horizon designation and description of Algarrobo C profile.

Master Horizon	Depth (cm)	Distinctness	Topography	Color	Texture	Additional observations:
A	0-14	Clear	Smooth	2.5Y 4/1	Sand	Salt and pepper appearance, organic bodies
E	14-34	Abrupt	Wavy	2.5Y 7/1	Sand	Organic splotches
B_{hs1}	34-56	Clear	Wavy	5Y 2.5/2	Sand	Weakly cemented
B_{hs2}	56-74	Clear	Wavy	5Y 3/2	Loamy sand	Strongly cemented, organic stains along root channels,
B_w	74-87	Clear	Smooth	2.5Y 4/3	Loamy sand	Organic stains along root channels
B_s	87-129	Clear	Smooth	10YR 3/6	Sand	Stripped sand grains; Very strongly cemented; clay films
C	129-148	Clear	Smooth	10YR 7/1	Loamy sand	-
C_2	148-188	Clear	smooth	10YR 7/2	Sandy clay loam	-
$2C_1$	188-203	Clear	Smooth	10YR 7/1	Clay	-

Algarrobo profile D is shown in Figure 12. This profile is located at 18°27'06", -66°19'16", north of the roadway in an area where a vegetation of icaco trees (*Crysobalanus icaco*) and corozo palms (*Attalea cohune*) predominates. The profile is located on a footslope with an elevation of around 10 m above sea level, the highest landscape among the observed profiles. Six horizons were identified to a depth of 203 cm (Table 4). Horizon designation is as follows A-E-B_{hs}-B_s- $2C_1$-$2C_2$. An abrupt change in color from light brownish gray (10YR 6/2) in the eluvial horizon to very dark grayish brown and yellowish brown (10YR 3/2 and 10YR 5/6) in the B horizon is observed. Soil texture was sandy throughout the profile structureless single grain

soil structure was determined in the first two horizons. Strong subangular block structure was observed in the 34–45 cm horizon. All horizons deeper than 45 cm had a structureless, very strong massive soil structure. Roots were predominant in the surface horizons.

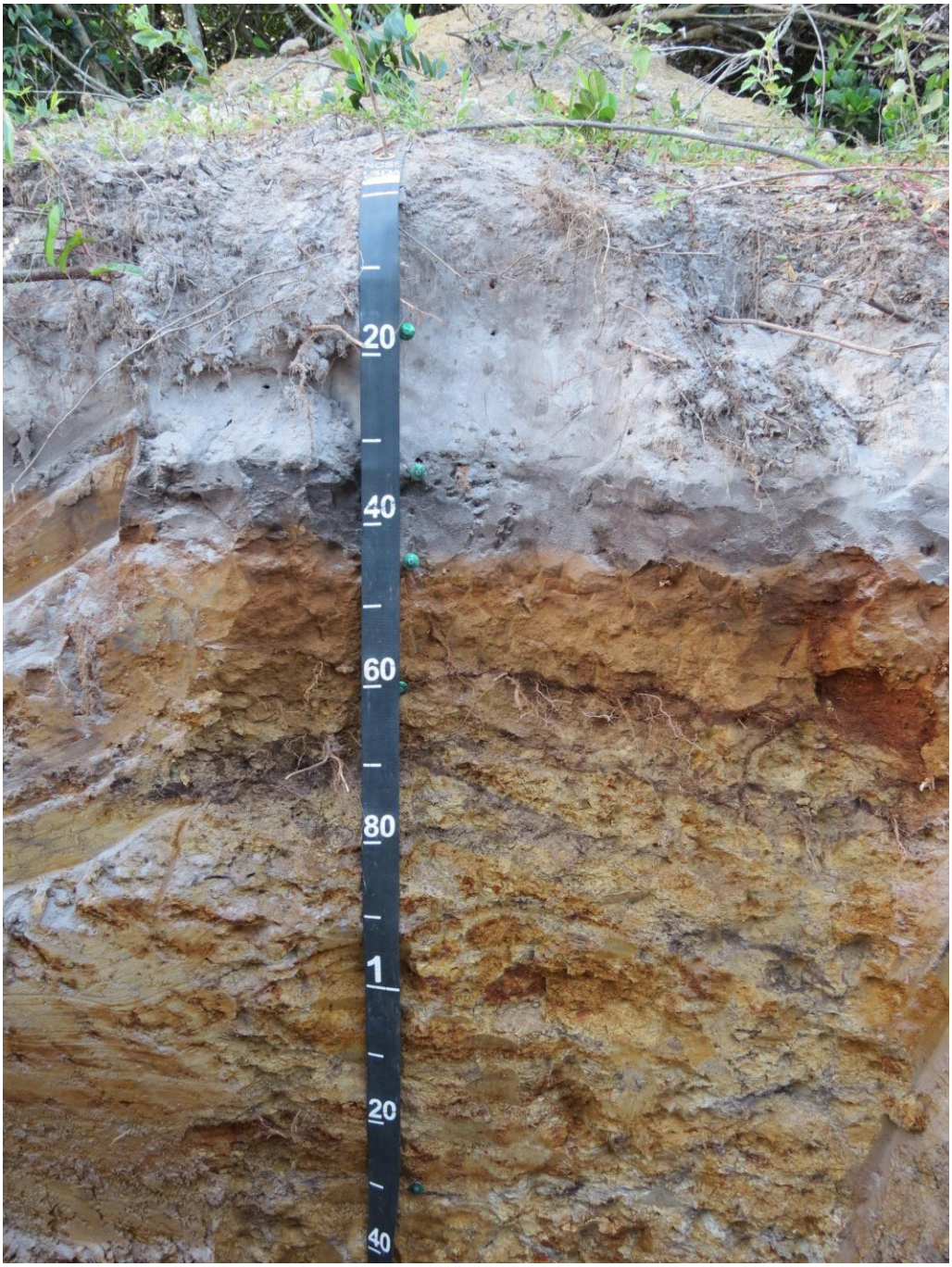

Figure 13. Image of Algarrobo profile D.

Table 4. Horizon designation and description of Algarrobo profile D.

Master Horizon	Depth (cm)	Distinctness	Topography	Color	Texture	Additional Observations
A	0-17	Clear	Wavy	10YR 5/1	Sandy	Presence of roots
E	17-34	Clear	Smooth	10YR 6/2	Sandy	-
B_{hs}	34-45	Abrupt	Smooth	10YR 3/2	Sandy	-
B_s	45-61	Abrupt	Smooth	10YR 5/6	Sandy	-
$2C_1$	61-130	ND	ND	7.5YR 6/6 7.5YR 6/8	ND	Variegated color
$2C_2$	130-203	ND	ND	7.5YR 6/6 7.5YR 6/8	ND	Variegated color

Physical Properties of the soil profiles

Sand is the particle size class that predominates in the four profiles with a range from 66.8% to 98.2%. The sand content was greater in the horizons closest to the surface. When moving vertically downwards through the profile we can observe the increased content of silt and clay separates. This was expected due to larger particle size in the overlaying horizons, which facilitates the transport or illuviation of material from the surface through the profile to deeper areas or horizons, especially accumulation in the B horizon, this particularly occurs in Spodosols soil order that contributes to the formation of the spodic horizon. A sandy texture, characteristic of the Spodosols order predominates in the four profiles. The coarse texture in the A and E horizons, but a finer texture is observed in the spodic, illuvial horizons (B_h, $B_{s,}$ B_{hs}) and C horizons (Table 5). In the four profiles stable aggregates were found in B and C horizons, and their stability range from 1.12% to 96.9%. No aggregates formed in single grain structured and sandy horizons. Nimmo (2005) states that soil aggregates form through the combined action of aggregation and fragmentation process, or the attractive and disruptive forces that act on soil

particles. Soil organic matter, iron and aluminum oxides and carbonate form coatings that bind particles together (Gee and Or, 2002).

Table 5. Particle size, texture and aggregate stability of Algarrobo soil profiles.

Master Horizon	Sand	Silt	Clay	Texture	Aggregate Stability
	----------%----------				%
Algarrobo profile A					
A	92.6	0.7	6.7	Sand	-
E_1	96.9	0.6	2.3	Sand	-
B_h	96.4	1.3	2.3	Sand	-
E^1	87.7	4.7	7.6	Loamy sand	-
B_{hs}	96.0	0.8	3.2	Sand	-
BC_1	95.2	1.4	3.5	Sand	-
BC_2	93.7	1.1	5.2	Sand	-
2C	78.7	2.4	18.9	Sandy loam	1.12
Algarrobo profile B					
A_1	92.5	0.5	7.0	Sand	-
A_2	93.6	1.3	5.1	Sand	-
E	98.2	0.7	1.1	Sand	-
B_{hs1}	86.8	3.3	9.9	Loamy sand	7.0
B_{hs2}	76.9	4.3	18.8	Sandy loam	92.2
B_{s1}	87.4	1.7	10.9	Loamy sand	85.8
2BC	77.4	2.2	20.4	Sandy clay loam	5.4
$2C_1$	ND	ND	ND	Loamy sand	ND
$2C_2$	ND	ND	ND	Sandy clay loam	ND
$2C_3$	ND	ND	ND	Sandy clay loam	ND
Algarrobo profile C					
A	95.7	0.4	3.9	Sand	-
E	98.1	1.4	0.5	Sand	-
B_{hs1}	89.8	2.3	7.9	Sand	-
B_{hss}	84.2	3.4	12.4	Loamy sand	86.63
B_w	73.8	3.0	23.2	Sandy clay loam	ND
B_s	78.8	8.3	12.9	Sandy loam	ND
C	78.7	6.0	15.3	Sandy loam	ND
C_2	87.0	3.9	9.1	Loamy sand	ND
Algarrobo profile D					
A	95.7	0.6	3.7	Sand	-
E	97.0	1.5	1.5	Sand	-
B_{hs}	80.1	6.5	13.4	Sandy loam	13.38
B_s	78.0	9.0	13.0	Sandy loam	96.9
$2C_1$	71.8	10.8	17.4	Sandy loam	91.0
$2C_2$	70.9	11.5	17.6	Sandy loam	47.2

Surface area

Specific surface area is one of the dominant factors that control the fundamental behavior of soils. This value varies greatly between soils because of differences in mineralogy, organic composition and particle size distribution (Cerato and Lutenegger, 2002). It is a physical property that has been used as an indicator of potential reactivity (Goldberg et al., 2001). Specific surface area was determined for the clay fraction. The specific surface area of the clay fraction ranged from 295 m^2 g^{-1} to 5366 m^2 g^{-1}. The presence of amorphous materials and soil organic matter can greatly affect these values. High values of surface areas (>100 m^2 g^{-1}) are expected for amorphous materials, and organic matter (560-800 m^2 g^{-1}) (Sumner, 1999).

Mineralogy of the clay fraction

The X-ray diffraction analysis of the clay fractions indicates that the mineralogy of the horizons varies from the surface to deeper horizons but shows similarities among the four profiles. The major mineral components for all four profiles are quartz, kaolinite, gibbsite and goethite (Table 6, Appendix II). Minor components of the clay fraction identified in the diffractograms include calcite, halloysite, vermiculite, hematite and short-range order aluminosilicates (Dahlgreen and Ugolini, 1991; Jones and Malik, 2004; Johnson Maynard, 2006). The mineralogy of the E horizon in the four profiles contained primarily quartz and kaolinite. Accumulation of aluminosilicates mostly kaolinite and iron and aluminum oxides were observed in the B horizon, indicative of the eluviation from surface to deeper horizons process and podzolization.

Table 6. Mineralogy of the Algarrobo profiles.

Algarrobo profile	Clay Mineralogy 2 Theta
Profile A	Gibbsite (19.9) goethite (20.9), hematite (50), kaolinite (12.2, 25), quartz (26.8)
Profile B	Gibbsite (20.0) goethite (21.0), hematite (50), kaolinite (12.3, 25.2, 60.0), quartz (26.8)
Profile C	Chlorite, vermiculite. Halloysite, montmorillonite, gibbsite (20) goethite (20.9, 35.0, 36.5), hematite (50.2), kaolinite (12.0, 25.0), quartz (26.8)
Profile D	Gibbsite (20) goethite (20.9), hematite (50), kaolinite (12.0, 25.0, 60.0), quartz (26.8)

The distinction of soil horizons in profile A was less pronounced than in the other profiles, and the diversity of minerals was less. Prevalent minerals are gibbsite, goethite, hematite, kaolinite, and quartz. In this profile, the intensity of the quartz peak located at 26.8 2-theta decreases in intensity. Kaolinite (12.2) and oxides such as gibbsite (20.0) and goethite (21.0) peaks increase in intensity. This suggests an increase in these clay minerals as a result of weathering and eluviation from upper horizons.

In Algarrobo profile B, the distinct peaks that correspond to aluminum and iron oxides gibbsite and goethite respectively are more prominent in the illuvial B horizon and indicate the location of the spodic horizon. These sharp peaks may support the idea that podzolization occurs with both vertical and a lateral movement of material from higher areas in the hill-slope facilitated by texture and water flux. The location of Algarrobo profile B in comparison to the other profiles is lowest in the hillslope profile position. This suggests that water flows from the highest elevations to the lowest elevations, carrying material that accumulates in these low areas.

The major mineral components of profile C are gibbsite, goethite, hematite, kaolinite and quartz. The mayor mineral component observed in the eluvial horizon is quartz. In the spodic B

horizon, peaks corresponding to gibbsite, goethite, hematite, kaolinite and quartz were observed. The quartz peak was of lower intensity than in the eluvial E horizon, suggesting the enrichment in oxides as a result of illuviation.

The mineralogy of profile D was similar to that of the other profiles. Gibbsite, goethite, hematite, kaolinite, quartz, are present in horizons throughout the profile. The occurrence of the spodic horizon is observed at lower depth in this profile and although well-defined it is of lesser thickness. This profile is located at higher elevation in the landscape than the other three profiles.

In all the Algarrobo profiles studied, the broadening of bands from 4 to 10 2-theta scale, suggests the presence of amorphous material in the clay mineral fraction. This bands are more prominent in the illuvial B horizon. Halloysite could be present in these profiles because peaks that correspond to halloysite are usually observed around 8-9° 2-theta. When halloysite loses its structural water the peak coincides with those of kaolinite, around 12.2 degrees 2-theta.

Buurman (1986) describes that Spodosols in the humid tropic areas are generally characterized by low content of weatherable minerals. Similar to the mineralogy of the Spodosols studied, Suharta and Prasetyo (2009) describe that clay fraction of Spodosols formed in lowlands in Toba, derived from quartz sand deposits, poor of weatherable minerals and that occur in higher temperatures, quartz is the mineral fraction that dominates the mineralogy, with lesser presence of kaolinite and amorphous minerals. In contrast, Spodosols in highlands that form on chemically richer parent material, with a higher content of weatherable materials and low temperature due to high elevation have a more mixed mineralogy.

Detailed mineralogical assessment of a select Algarrobo profile

Algarrobo profile C shows diffractograms with a very similar mineralogy throughout the profile. The X-ray diffractograms of Algarrobo profile C shows peaks that correspond to the minerals Gb-gibbsite (20.2), Gt-goethite (20.9, 35, 36.5), Hm-hematite (50.2), K-kaolinite (12.2, 25.), and Qz-quartz (26.8).

The diffractogram of the A horizon (Figure 13), shows a very intense peak that corresponds to quartz at 26.8. Kaolinite is detected by the peaks in 12.2, 25.2, and 60. The occurrence of the iron oxide hematite and goethite minerals are shown with peaks in 20.0, 25, 50 and 55 2-theta. In the diffractogram of the E horizon, peaks that corresponds to quartz is the most intense, this is in accordance to the nature of the quartzose material in which these soils form (Acevedo, 1982; Soil Survey Staff, 2018). The intensity of the peaks of the oxide content decreases, and the diagnostic peak of kaolinite around 12.2 disappears. This is evidence of the eluvial nature of the E horizon, and that can be attributed to both chemical and physical weathering (Haile-Mariam and Mokma, 2015) and the dominant sandy texture that occurs.

The diffractogram of B_{hs1} and B_{hs2} are very similar among themselves, and the peaks that correspond to gibbsite, hematite, goethite begin to form, along with kaolinite in the 12.2. This strongly supports the change in soil physical properties, decreasing percent sand content as presented in soil physical analysis in previous section, with an increase in the silt and clay fraction as the texture changes from sand to loamy sand.

The intensity of the kaolinite peak in 12.2 starts to increase as we observe the diffractograms of the B_w and B_s horizons of Algarrobo profile C. This accumulation corresponds to the evident change in soil texture to sandy clay loam, in which the clay content of the

B_w horizon reached 23.2 % and texture in the B_s horizon was a sandy loam with a clay content of 12.9%. The peaks that correspond to the oxide components which includes gibbsite, at 18.9, 20.2, 27.9, 38.2, 40.5, and 53 2-theta, goethite at 21 and 55, hematite in at 20.9, 24.9 and 55 2-theta. These peaks appear with much intensity when compared to the overlaying horizons, indicating the prevailing oxide content of the diagnostic spodic horizons of Spodosols order. The diffractograms that correspond to the C and C_2 horizons shows a sharp peak that corresponds to kaolinite when compared to goethite, gibbsite, and quartz.

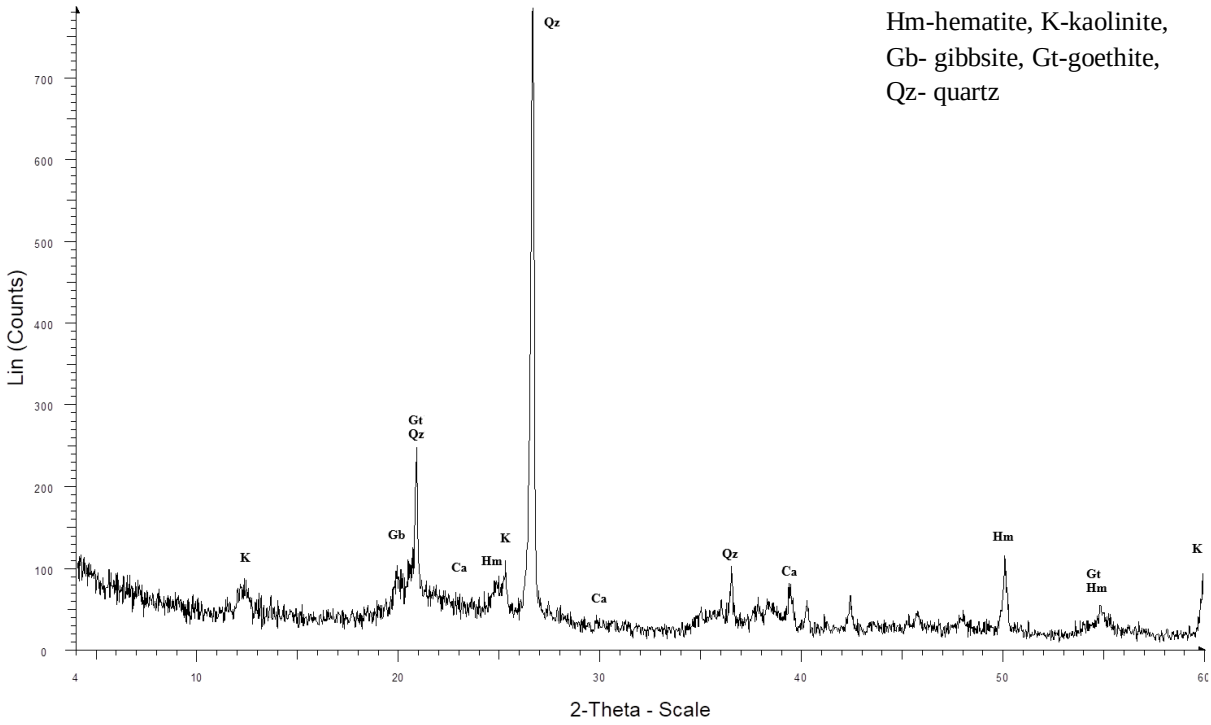

Figure 14. X-ray diffractogram of the A horizon in Algarrobo profile C.

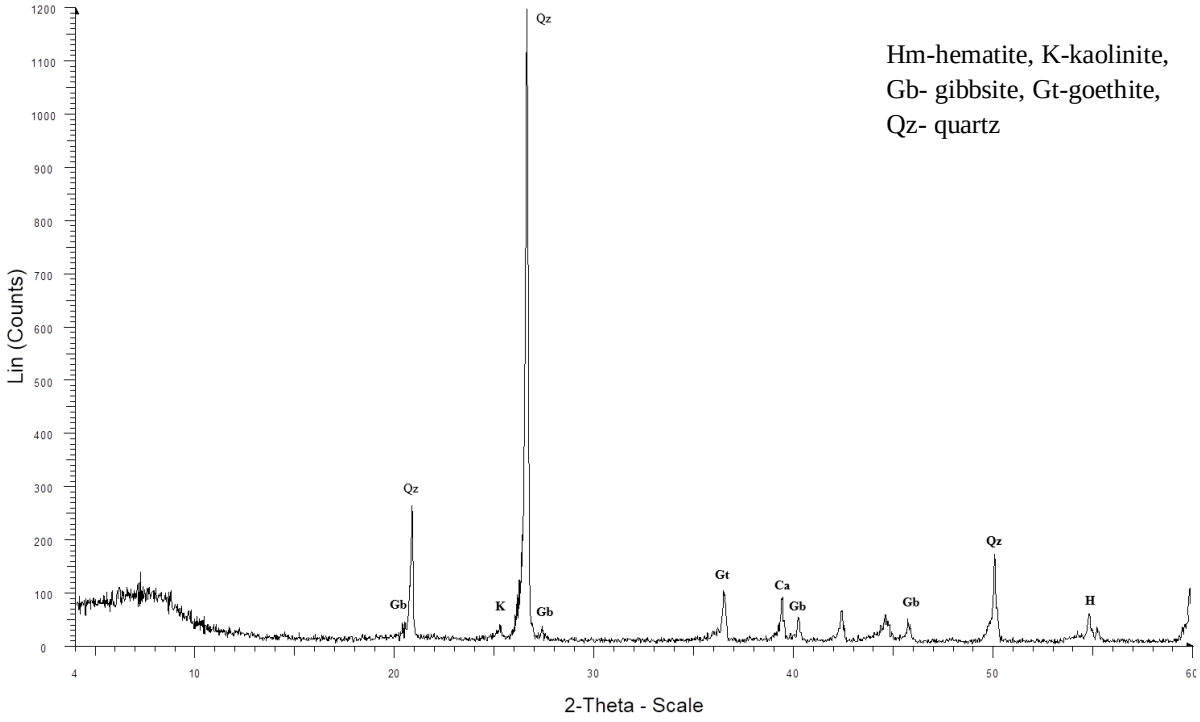

Figure 15. X-ray diffractogram of the E horizon in Algarrobo profile C.

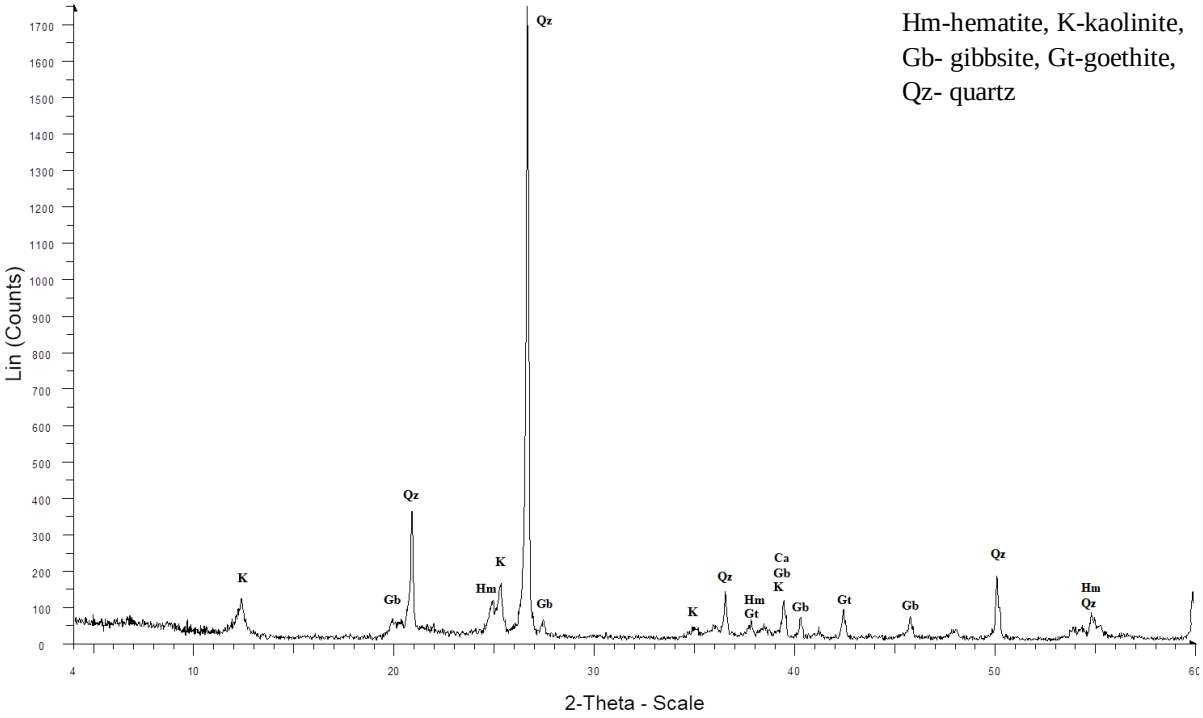

Figure 16. X-ray diffractogram of the B_{hs1} horizon in Algarrobo profile C.

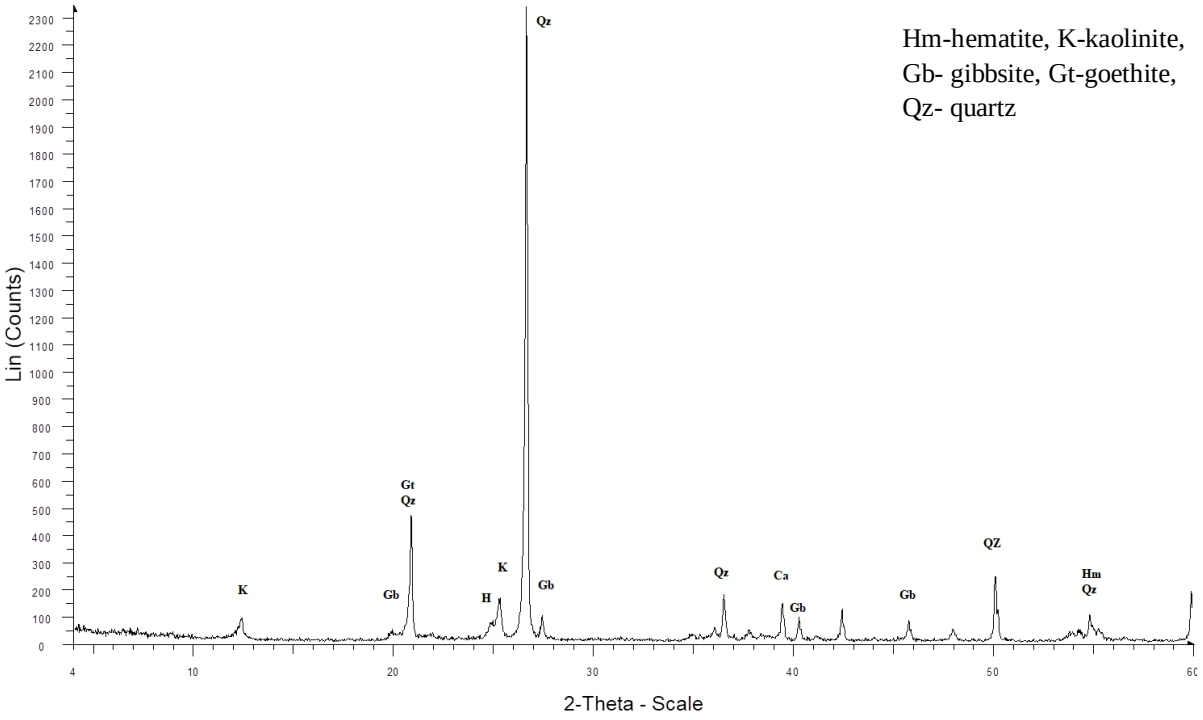

Figure 17. X-ray diffractogram of the B_{hs2} horizon in Algarrobo profile C.

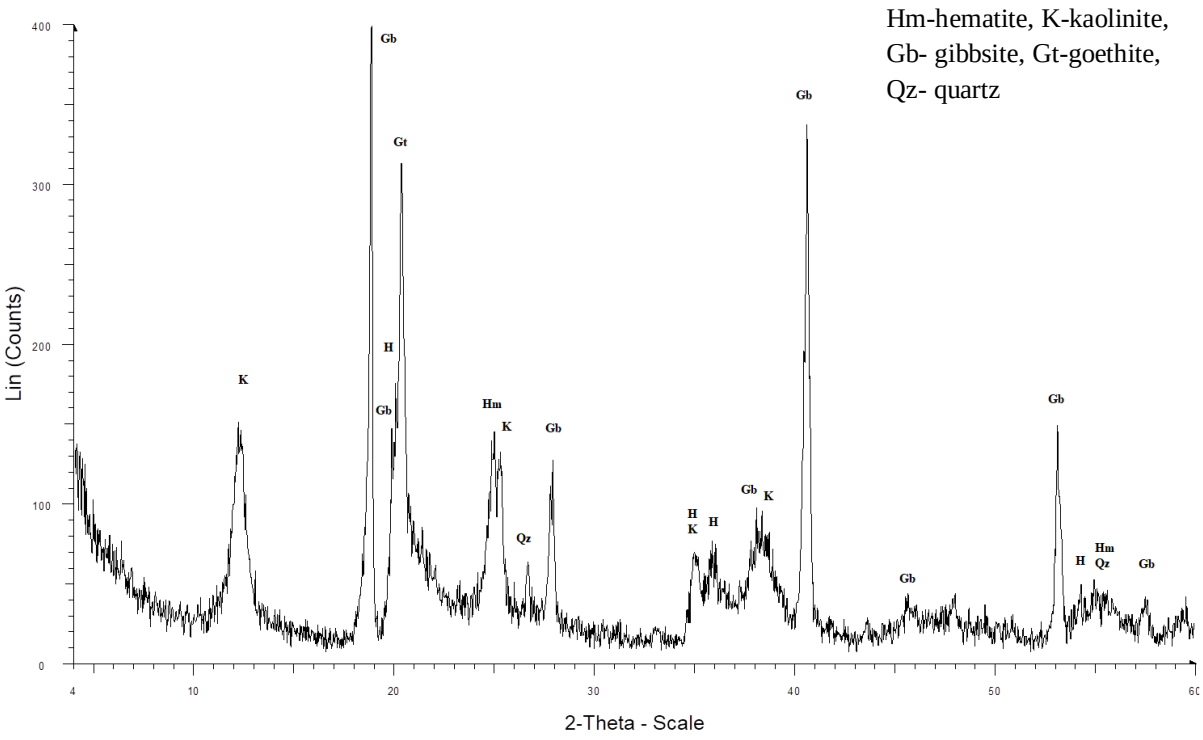

Figure 18. X-ray diffractogram of the B_w horizon in Algarrobo profile C.

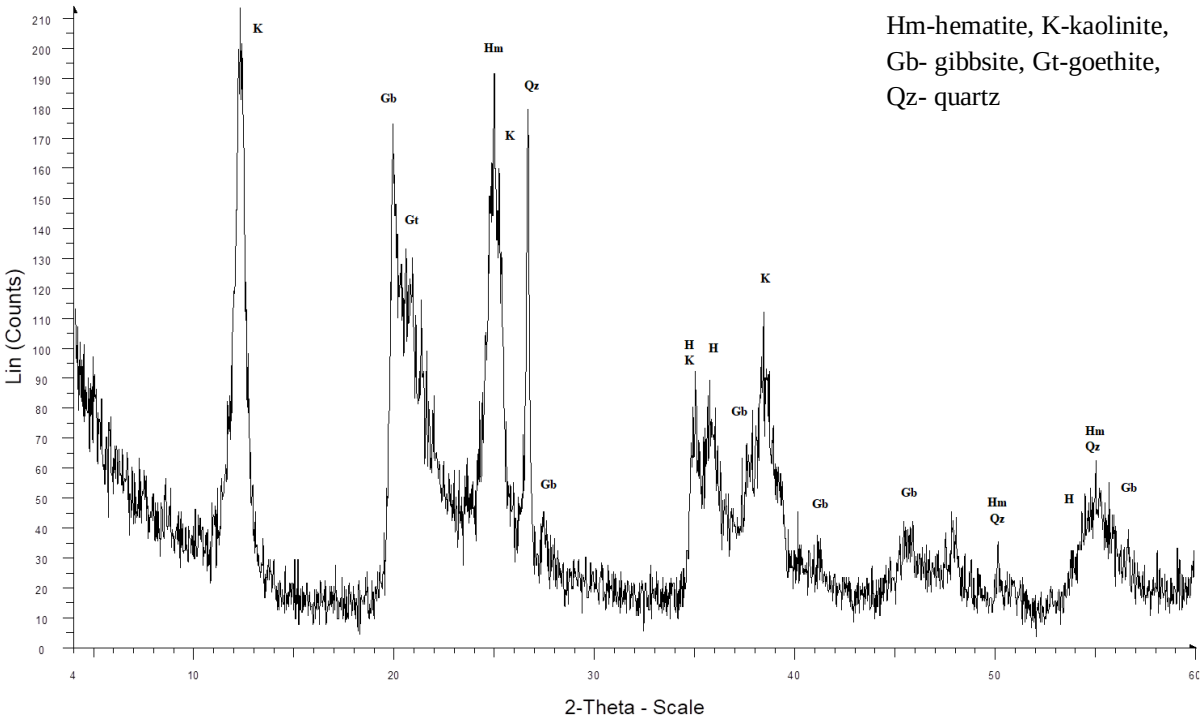

Figure 19. X-ray diffractogram of the B_s horizon in Algarrobo profile C.

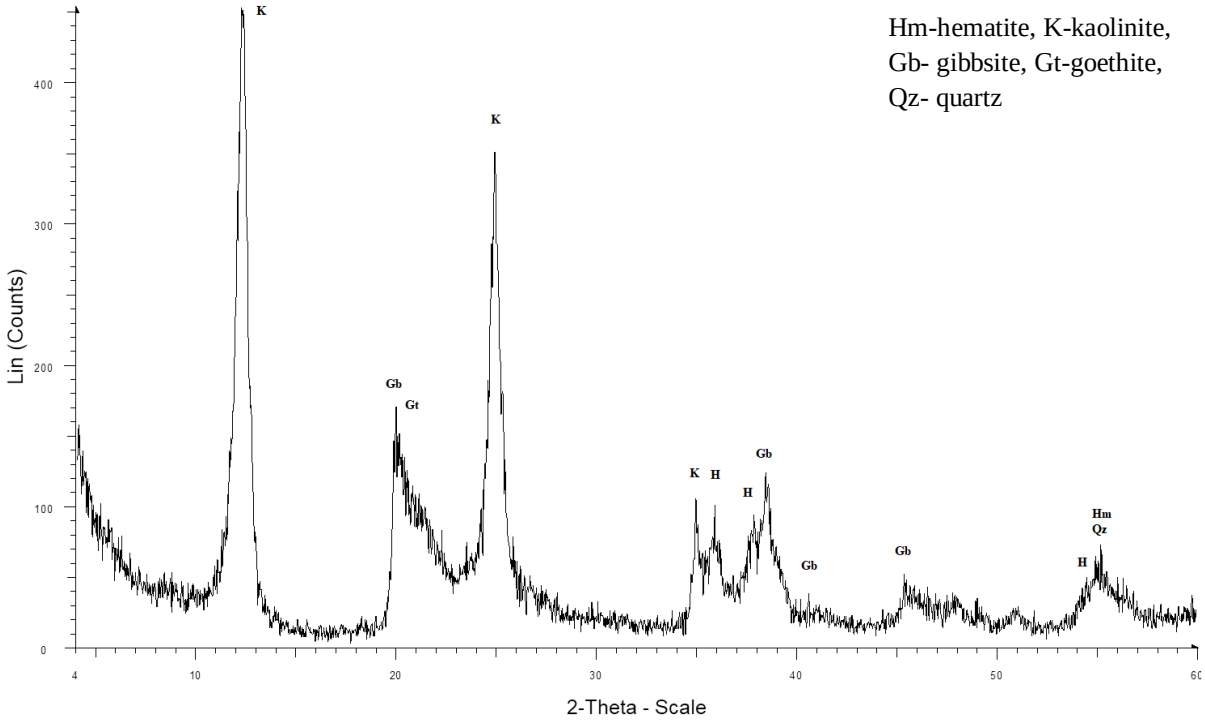

Figure 20. X-ray diffractogram of the C horizon in Algarrobo profile C.

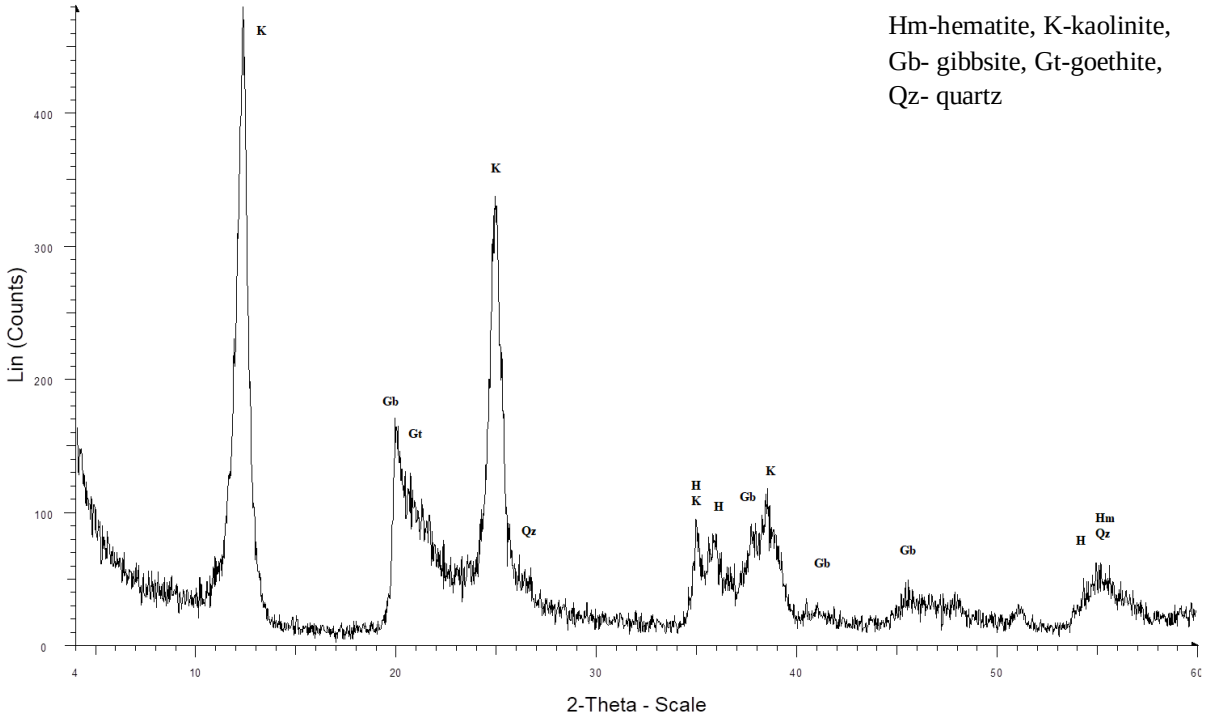

Figure 21. X-ray diffractogram of the C_2 horizon in Algarrobo profile C.

Chemical Properties of the soil profiles

Soil chemical properties were determined using soil samples collected during the first visit to Carmen Regadera Farm. Table 7 shows the results of the chemical properties evaluated-pH, percent organic matter content, and exchangeable basic cations of profiles A, B, C, and D. The soil pH ranged from 4.44 to 7.10. Organic matter content decreased as we move down the profile. Exchangeable Ca^{2+} and Mg^{2+} decreased in subsurface horizons except in profile B where a high concentration of exchangeable Ca^{2+} (108 $cmol_c$ kg^{-1}) was observed. The high amount of Ca^{2+} suggest that we have Ca^{2+} extraction form carbonates in the soil. Although the exchangeable Al^{3+} was higher in deeper horizons within the profile, when comparing the exchangeable Al^{3+} content in the illuvial B horizon to the eluvial zone these values tend to increase from the eluvial horizon to the illuvial horizon, suggesting the location of the diagnostic spodic horizon.

Table 7. Soil chemical properties of Algarrobo Spodosols profiles.

Horizon	pH	% C	% OM	Ca^{2+}	K^{+}	Mg^{2+}	Al^{3+}
				----------$cmol_c\ kg^{-1}$----------			
Algarrobo profile A							
A	4.45	1.76	3.94	3.65	0.61	2.54	3.87
E_1	4.44	0.19	0.43	0.74	0.27	0.55	1.3
B_h	4.68	0.27	0.61	0.67	0.15	0.4	1.07
E^1	4.8	0.83	1.85	1.82	0.09	0.73	6.6
B_{hs}	4.78	0.38	0.85	1.21	0.04	0.49	3.51
BC_1	4.83	0.25	0.56	0.98	0.06	0.49	1.94
BC_2	4.7	0.85	1.91	1.62	0.06	0.59	5.74
2C	4.85	0.30	0.68	2.68	0.34	2.19	14.44
Algarrobo profile B							
A_1	6.29	1.08	2.42	38.43	0.49	2.96	0.06
A_2	6.71	1.18	2.65	34.67	0.08	2.06	0.09
E	6.95	0.11	0.24	3.64	0	0.23	0.03
B_{hs1}	7.1	1.56	3.5	108.3	0.17	2.46	0.08
B_{hs2}	6.61	1.19	2.66	84.25	0.17	1.56	0.18
B_{s1}	5.58	0.60	1.35	14.31	0.12	0.41	4.92
2BC	4.89	0.28	0.62	5.05	0.07	0.62	10.61
Algarrobo profile C							
A	4.58	0.47	1.05	1.04	0.04	0.53	0.39
E	5.02	0.14	0.31	0.86	0	0.22	0
B_{hs1}	4.16	2.14	4.79	0.74	0.07	0.39	13.67
B_{hs2}	4.27	1.21	2.71	1.16	0.19	0.38	16.67
Algarrobo Profile D							
A	5.19	0.42	0.93	2.27	0.34	1.36	2.88
E	4.97	0.20	0.44	0.77	0.09	0.25	0.24
B_{hs}	4.69	0.64	1.43	0.8	0.18	0.39	11.22
B_s	4.91	1.86	4.17	0.33	0.21	0.26	11.02
$2C_1$	4.88	1.14	2.55	0.28	0.18	0.32	13.56
$2C_2$	4.96	0.92	2.05	1.18	0.36	1.48	25.0

Soil pH

The soil pH was acid, except in the eluvial B horizon of Algarrobo profile B that had a pH value of 7.1. Bloom et al. (2005) states that the pH value is the single most important chemical characteristic of a soil and knowledge of it is needed to understand important chemical processes, such as ion mobility, metal ion equilibrium and the rate of precipitation and dissolution reactions. For acid soils, the cation exchange capacity includes the pH-dependent charges in pH-dependent charge components like soil organic matter, kaolinite and oxides and hydroxides of Al and Fe that are created by neutralizing weak acid sites. In soils, many processes produce acidity, and acidification is a natural process in which leaching occurs (Bloom et al., 2005). Soil acidification occurs when there is a net donation of protons to the soil components with a loss of bases by leaching or removal by plant uptake. At a wide range of pH values, aluminosilicate clay edges and the surfaces of oxides and hydroxides of Al and Fe provide reversible charge sites for the adsorption and desorption protons, such that an increase in pH results in a more negative net charge and a decrease in pH in a more positive net charge, these surfaces are amphoteric and can be both acidic or basic depending on pH. The most important reversible charged surfaces in soils are Al- and Fe- oxides and hydroxides, kaolinite and short range ordered Al-silicates such as allophane, imogolite and protoimogolite (Bloom et al., 2005).

The pH values are acidic, and these values are consistent with the classification criteria for Spodosols and the Spodic horizon in Keys to Soil Taxonomy that is pH value must be 5.9 or less (Soil Survey Staff, 2014). The more neutral pH values observed in Algarrobo profile B can be attributed to lateral movement of water enriched with carbonates from the nearby rock outcrops. This profile is the lowest in elevation, and seepage was observed from the backside of the profile during the field evaluation (Appendix I). Classical podzolization studies assume

vertical percolation; however lateral translocation of material, especially organic matter complexed with Al and Fe from surrounding hillslopes was responsible for the observed morphology. Soil scientists tend to focus on pedon scale studies of pedogenesis and the classification system of Spodosols rely on the assumption of vertical development (Egli, et al., 2007; Bourgault, et al., 2015; Buurman and Vidal Torrado, 2015). In a study of 99 podzols in Hubbard Brook Experimental Forest in New Hampshire, USA, hillslope-scale lateral podzolization occurs where lateral subsurface water flux predominates. The hydropedologic study of these soils concluded that laterally developed spodic horizons were twice as thick as vertically developed spodic horizons, and that laterally developed spodic horizons could form via lateral translocation of solutes or physical transport and deposition of colloidal amorphous organometallic complexes with unsaturated or saturated flow (Bourgault, et al., 2015). More evidence that podzolization occurs laterally along hillslopes is presented by Sommer, et al (2001). The authors describe that podzol morphology in the Black Forest of Germany varied with landscape position, thick E horizons with thin spodic B horizons were found upslope, while thin E horizons with thick spodic B horizons were found downslope. In these soils podzolization occurred because of the translocation of material with lateral flow. In this study, thick B horizons were observed in Algarrobo profiles B and C, in comparison to A and D profiles.

Soil Organic Carbon and Organic Matter

Soil organic matter had the tendency to decrease in the eluvial E horizon and increase in the illuvial B horizon. The mathematical relationship between organic carbon and organic matter through the Walkley-Black wet oxidation procedure shows that the range of organic carbon content ranged from 0.107 to 0.197 % and corresponding organic matter content was 0.24 to 0.44

% in the eluvial E horizon. In the illuvial spodic B horizon, the organic matter percent content ranged from 0.61 to 4.79 %. The corresponding range of organic carbon is 0.272 to 2.13 %.

In Soil Taxonomy (Soil Survey Staff, 2014), the classification criteria of the spodic horizon indicates that the organic carbon content must be equal to 0.6 percent or more. Algarrobo profile A does not meet these classification criteria, although the field appearance of this profile seems like a Spodosols profile, chemical and mineralogical properties suggest a weaker pattern of podzolization. The other three profiles meet this classification criterion and these values point to the horizon that corresponds to the diagnostic spodic horizon.

The formation of the spodic horizon is influenced by the type of vegetation and surface litter. The Soil Survey Staff (2014) indicates that in warm climates the spodic horizon occurs under savanna, palm trees, and mixed forest. Algarrobo profile A was under a canopy of cupey trees, a vegetative cover very different from the rest of the Spodosols profiles studied, in which icaco tress, and corozo palms are the predominant vegetation. In this profile A, the organic carbon and organic matter were highest in the surface horizon when compared to the B, C and D profiles, showing that organic carbon and organic matter are accumulating in the surface rather than eluviating through the profile. This difference may cause the weak appearance and weak spodic and chemical properties of the B horizon of Algarrobo profile A.

Exchangeable basic cations

The exchangeable Ca^{2+} and Mg^{2+} decreased when compared to surface horizon, although for Algarrobo profile B there was a considerable amount of exchangeable Ca^{2+} (up to 108.3 cmol kg^{-1}) and a less acidic pH values that may be caused by the lateral movement of carbonate enriched water from surrounding outcrop formations, and supported by the observation of water

seepage from profile walls at time of field analysis and sampling. Exchangeable Al^{3+} was higher in deeper horizons within the profile when compared to the eluvial zone above, suggesting the location of the B horizon and the location of the Spodic horizon. The exchangeable Na^{+} content was evaluated, but in none of the profiles this cation was detected.

Podzolization and base cation leaching are dominant soil-forming processes that occur in Spodosols. Base cation leaching is the opposite of biological enrichment of base cations and involves the eluviation of Ca^{2+}, Mg^{2+}, K^{+} and Na^{+} from the solum (Bockheim and Hartemink, 2017). Vertical nutrient distributions are dominated by plant cycling relative to leaching, weathering dissolution, and atmospheric deposition. In a study of more than 10,000 different soil profiles, the authors suggest that nutrients strongly cycled by plants, such as P and K, were most concentrated in the top soil (Jobbagy and Jackson, 2001). This is the case of the Algarrobo profiles under study. The surface horizon had more basic cation content than the underlying horizons. In the E horizon, results showed the least amount of basic cation content. These results are consistent with the eluvial nature of the E horizon. This E horizon forms when percolating waters eluviate fine clays, organic matter, free iron oxides, and aluminum, leaving a lighter colored horizon when compared to the A or B horizons (Assmus, 1993). The B horizon, illuvial in nature, shows areas of accumulation of material eluviated from the horizons above.

Exchangeable aluminum

Aluminum is among the most important and commonly analyzed constituents in the soil, because it is a ubiquitous element in the soil and geological systems and because Al^{3+} can be toxic to plants and other organisms (Bertsch and Bloom, 1996). The exchangeable aluminum content in the four Algarrobo soil profiles ranged from 0 to 1.3 $cmol_c\ kg^{-1}$ in the eluvial E horizon and had the tendency to increase with depth, reaching up to 25.0 $cmol_c\ kg^{-1}$.

Minerals that contain significant quantities of Al^{3+} are aluminosilicates which include feldspar, micas, kaolins, smectites, and other phyllosilicate minerals. It is also a primary component of other non-silicate minerals such as gibbsite [$Al(OH)_3$]. Chemically active soil Al^{3+} can have a variety of forms that are controlled by the pH and the mineralogical composition of the system. For example, Al^{3+} can be bound to negatively charged clay surfaces by electrostatic forces and can be freely exchangeable with other cations such as Ca^{2+}, Mg^{2+}, or K^{+}, or it can be bound to carboxylate and phenolic groups on organic matter and only be partially exchangeable (Bertsch and Bloom, 1996).

Aluminum and iron oxide content

Aluminum and iron oxide content was determined in the soil fine fraction using the Acid Ammonium Oxalate (AAO) method, Citrate-Dithionite-Bicarbonate (CDB) method, and the Sodium Pyrophosphate (SP) method. The oxalate extraction yields organic and amorphous forms of Fe^{3+} and Al^{3+}; the dithionite extraction yields all free forms of these elements, including crystalline forms; and the pyrophosphate extraction yields organic bound forms of iron and aluminum, (Bockheim and Hartemink, 2017).

The Al^{3+} content is greater than the Fe^{3+} content in all extractions. The amount of Al^{3+} and Fe^{3+} extracted by pyrophosphate was higher than the other extraction methods, except in Profile B, in which oxalate extractable content was higher. The least amount of extractable material was obtained with the citrate-bicarbonate-dithionite method. In some samples no Fe^{3+} was extracted by ammonium oxalate. The eluvial horizon in each profile had the least amount of extractable Al^{3+} and Fe^{3+} oxides. In the illuvial horizon a significant increase was observed, denoting the presence and location of the diagnostic spodic horizon.

Table 8. Extractable aluminum and iron content in Algarrobo profile A.

	CBD				AAO				SPY			
	Fe	Fe_2O_3	Al	Al_2O_3	Fe	Fe_2O_3	Al	Al_2O_3	Fe	Fe_2O_3	Al	Al_2O_3
	----------%----------				----------%----------				----------%----------			
A	0.012	0.018	0.019	0.035	0.017	0.024	0.023	0.043	0.034	0.049	0.036	0.067
E_1	0.006	0.008	0.007	0.014	ND	ND	0.018	0.033	0.008	0.011	0.023	0.044
B_h	0.007	0.010	0.010	0.019	ND	ND	0.018	0.035	0.007	0.010	0.028	0.052
E^1	0.015	0.021	0.059	0.111	0.016	0.023	0.062	0.118	0.026	0.037	0.072	0.135
B_{hs}	0.005	0.007	0.047	0.089	ND	ND	0.054	0.101	0.010	0.015	0.078	0.148
BC_1	0.002	0.002	0.028	0.052	ND	ND	0.029	0.054	0.008	0.011	0.054	0.102
BC_2	0.006	0.009	0.097	0.183	ND	ND	0.074	0.140	0.010	0.014	0.092	0.174
2C	0.009	0.012	0.030	0.057	0.002	0.002	0.051	0.096	0.013	0.018	0.063	0.119

Table 9. Extractable aluminum and iron content in Algarrobo profile B.

	CBD				AAO				SPY			
	Fe	Fe_2O_3	Al	Al_2O_3	Fe	Fe_2O_3	Al	Al_2O_3	Fe	Fe_2O_3	Al	Al_2O_3
	----------%----------				----------%----------				----------%----------			
A_1	0.109	0.156	0.039	0.074	0.055	0.079	0.049	0.092	0.057	0.081	0.050	0.095
A_2	0.053	0.076	0.047	0.089	0.040	0.058	0.062	0.116	0.041	0.058	0.062	0.118
E	0.004	0.006	ND	ND	ND	ND	0.014	0.026	0.006	0.009	0.008	0.015
B_{hs1}	0.011	0.016	0.313	0.592	ND	ND	0.419	0.792	0.015	0.021	0.394	0.745
B_{hs2}	0.066	0.095	0.533	1.007	0.005	0.006	0.684	1.292	0.056	0.080	0.607	1.147
B_{s1}	0.042	0.060	0.331	0.626	0.030	0.043	0.562	1.063	0.106	0.152	0.426	0.805
2BC	0.097	0.138	0.105	0.198	0.042	0.059	0.131	0.248	0.052	0.074	0.188	0.355

Table 10. Extractable aluminum and iron content in Algarrobo profile C.

	CBD				AAO				SPY			
	Fe	Fe_2O_3	Al	Al_2O_3	Fe	Fe_2O_3	Al	Al_2O_3	Fe	Fe_2O_3	Al	Al_2O_3
	----------%----------				----------%----------				----------%----------			
A	0.011	0.016	0.007	0.014	ND	ND	0.017	0.032	0.011	0.015	0.025	0.047
E	0.004	0.005	ND	ND	ND	ND	0.009	0.018	0.002	0.003	0.002	0.005
B_{hs1}	0.006	0.008	0.131	0.248	ND	ND	0.112	0.212	0.006	0.008	0.167	0.315
B_{hs2}	0.007	0.010	0.185	0.350	ND	ND	0.168	0.317	0.007	0.010	0.248	0.468
B_w	0.009	0.013	0.142	0.267	ND	ND	0.152	0.287	0.014	0.019	0.312	0.589
B_s	0.021	0.030	0.502	0.949	ND	ND	0.528	0.997	0.013	0.019	0.532	1.004
C_1	0.005	0.007	0.046	0.086	ND	ND	0.085	0.160	0.006	0.009	0.096	0.181
C_2	0.005	0.007	0.031	0.059	ND	ND	0.051	0.096	0.005	0.007	0.050	0.094

Table 11. Extractable aluminum and iron content in Algarrobo profile D.

	CBD				AAO				SPY			
	Fe	Fe_2O_3	Al	Al_2O_3	Fe	Fe_2O_3	Al	Al_2O_3	Fe	Fe_2O_3	Al	Al_2O_3
	----------%----------				----------%----------				----------%----------			
A	0.018	0.025	0.030	0.056	ND	ND	0.035	0.066	0.013	0.019	0.059	0.112
E	0.006	0.009	0.003	0.005	ND	ND	0.013	0.025	0.004	0.006	0.011	0.020
B_{hs}	0.032	0.046	0.091	0.172	0.003	0.005	0.097	0.183	0.024	0.034	0.136	0.256
B_s	0.446	0.637	0.950	1.794	0.122	0.175	0.728	1.375	0.186	0.265	1.023	1.933
$2C_1$	0.507	0.725	0.867	1.639	0.139	0.198	1.121	2.118	0.309	0.442	1.345	2.541
$2C_2$	1.231	1.760	0.518	0.979	0.512	0.732	0.802	1.516	0.519	0.742	0.608	1.149

FTIR of the Humic and Fulvic Fractions in the Spodic Horizon

The FTIR spectrum can be divided into 4 regions 900-700 cm^{-1} (aromatic substitution), 1800-1000 cm^{-1} (O-containing groups), 3000-2800 cm^{-1} (aliphatic structure) and 3700-3000 cm^{-1} (hydrogen bond regions) (Wang et. al, 2017). The FTIR spectra obtained from fulvic acid (FA) and humic acid (HA) of the spodic horizon of the four pits is observed in Figure 22 to Figure 28.

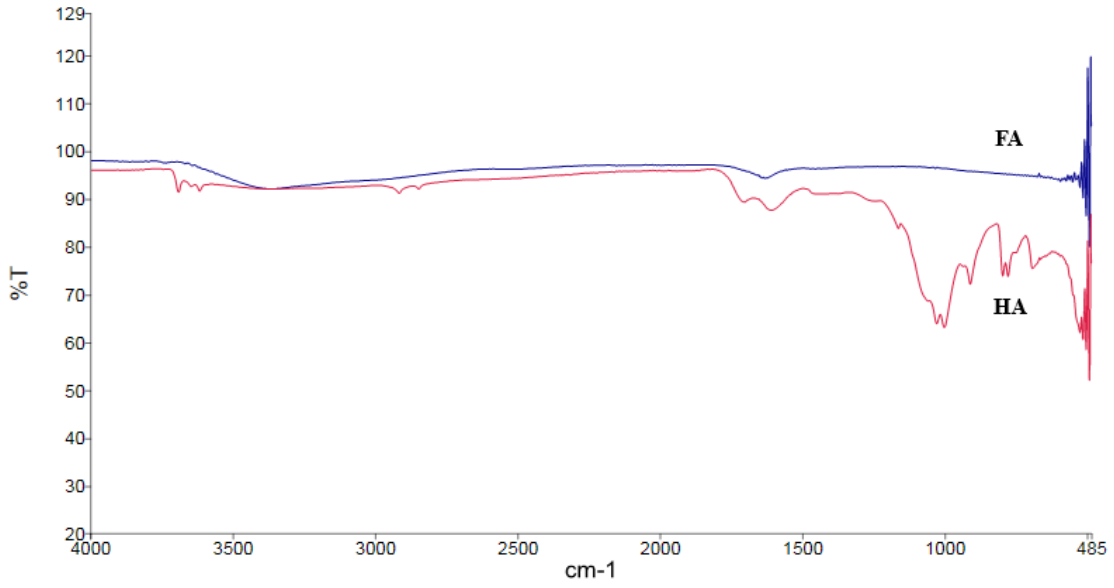

Figure 22. FTIR analysis of fulvic acid (FA) and humic acid HA) of the B_h spodic horizon of Spodosols pit A.

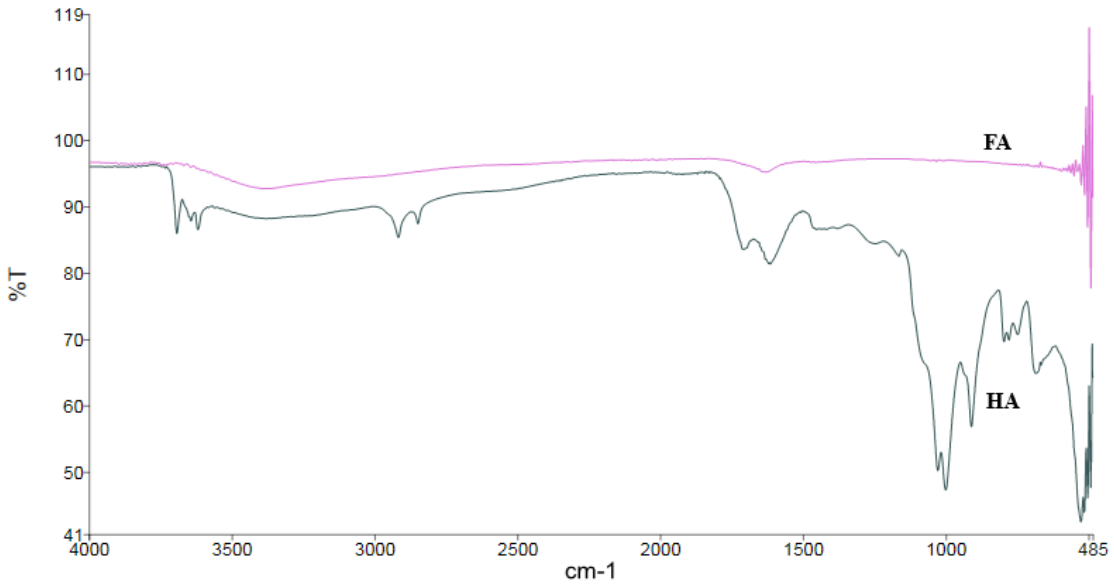

Figure 23. FTIR analysis of fulvic acid (FA) and humic acid HA) of the B_{hs} spodic horizon of Spodosols pit A.

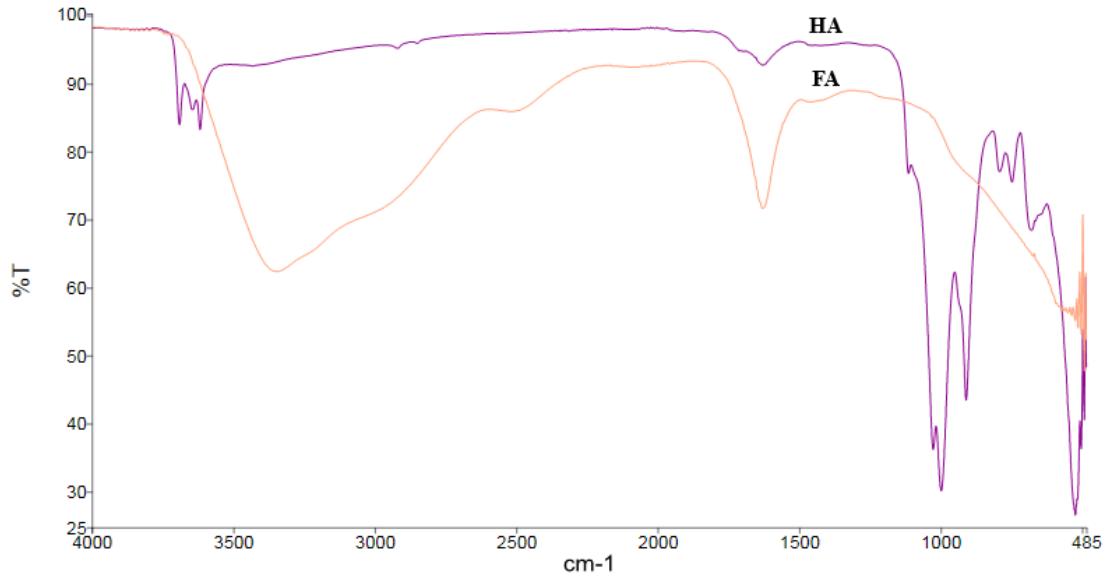

Figure 24. FTIR analysis of fulvic acid (FA) and humic acid HA) of B_{hs1} horizon (58-75 cm) of Spodosols pit B.

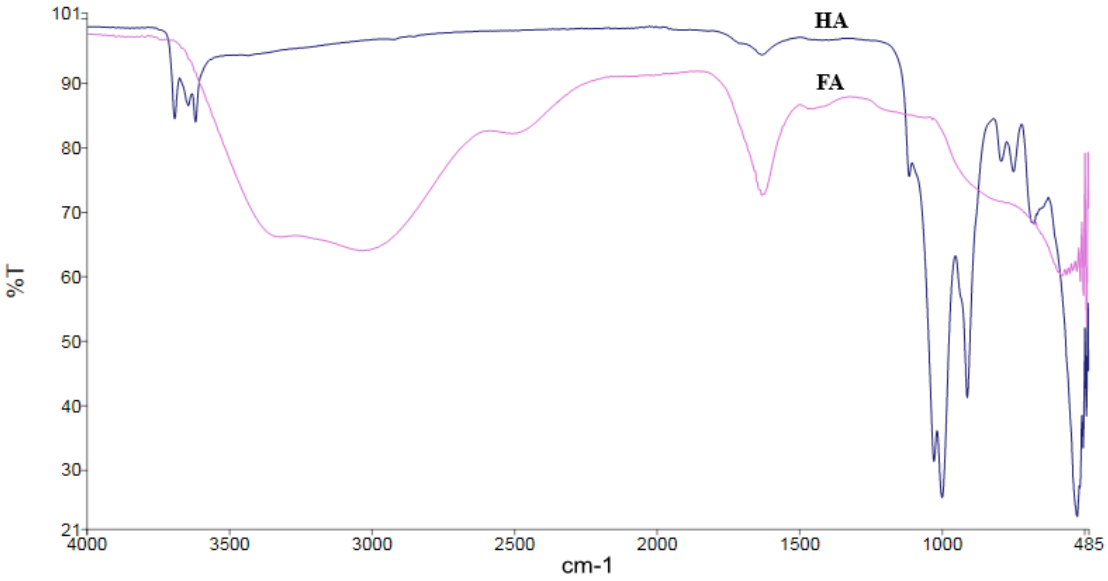

Figure 25. FTIR analysis of fulvic acid (FA) and humic acid HA) of B_{hs2} horizon (75-87 cm) of Spodosols pit B.

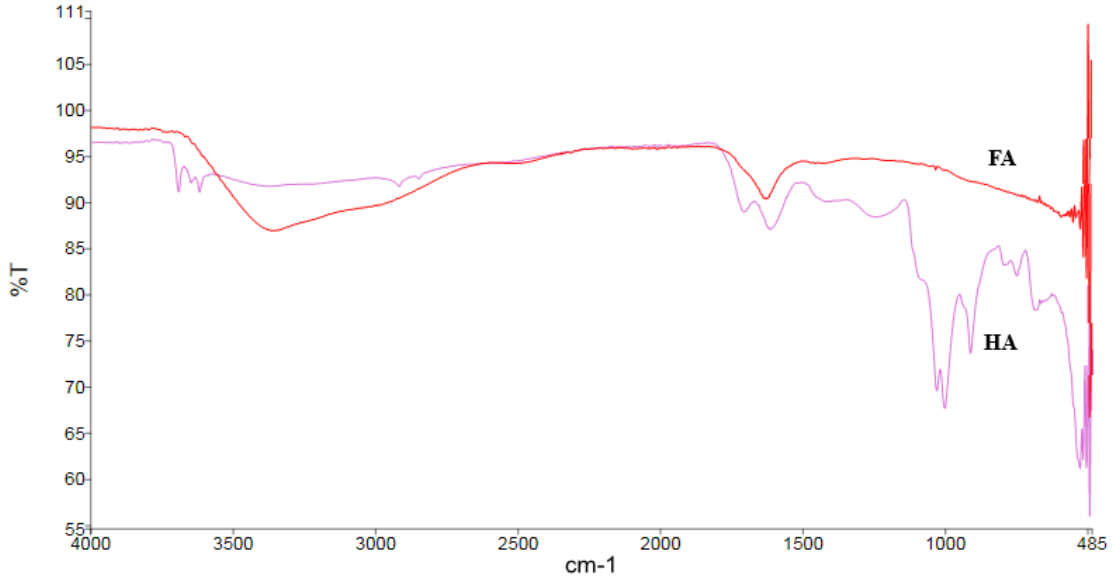

Figure 26. FTIR analysis of fulvic acid (FA) and humic acid HA) of B_{hs1} horizon (34-56 cm) of Spodosols pit C.

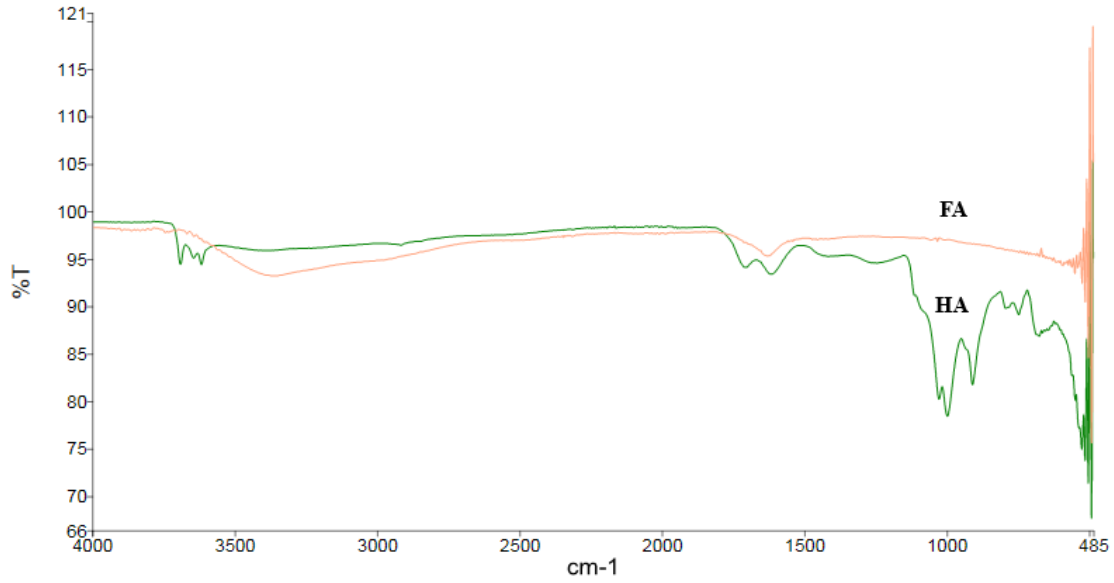

Figure 27. FTIR analysis of fulvic acid (FA) and humic acid HA) of the B_{hs2} horizon (56-74 cm) of Spodosols pit C.

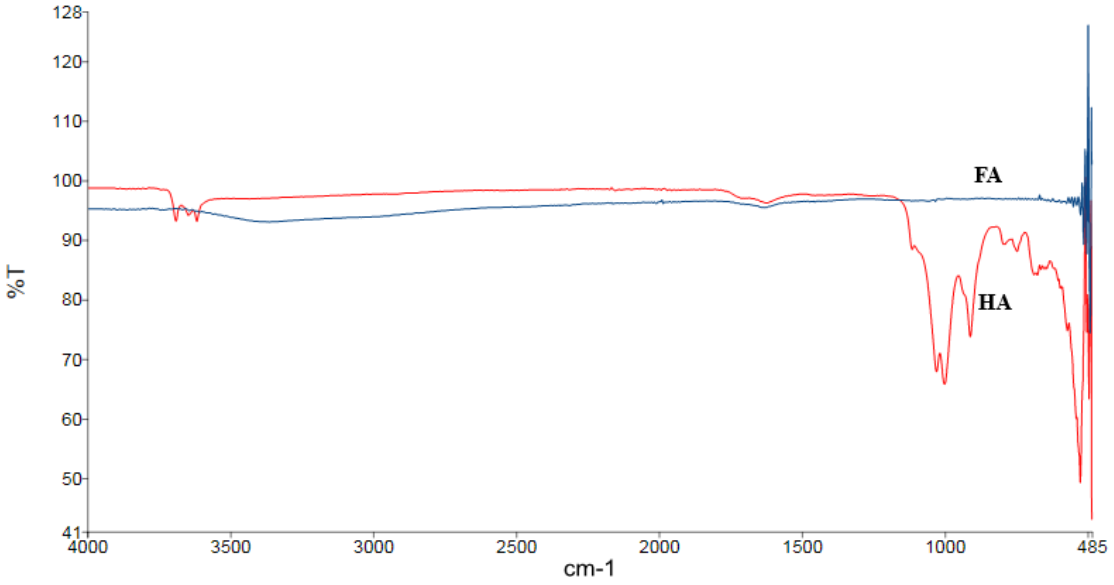

Figure 28. FA FTIR analysis of fulvic acid (FA) and humic acid HA) of the B_{hs} (34-45 cm) horizon of Spodosols pit D

The fulvic acid spectra are less complex when compared to the humic acid spectra. FA spectra is characterized by bands in the 490 to 520 cm^{-1} regions, that may correspond to main absorption bands possibly correspond to C-C skeletal vibration of alkyl groups, branched and/or straight chain alkanes (490 cm^{-1} to 600 cm^{-1}). The 1640 cm^{-1} signal corresponds to C=O

stretching of amide groups, quinone C=O, and or C=O of H-bonded conjugated ketones, in addition that the band corresponding to the 1640 cm^{-1} is characteristic of low-molecular weight fulvic acids. The signals in the 3300 cm^{-1} region suggests O-H stretching and/or N-H stretching, although Stevenson (1982) argues that this broad band might be caused by moisture adsorption. The fulvic acid fraction in Spodosols due to recent formation should be of low molecular weight. Low degree of polymerization should favor water adsorption contributing to the broad band between 2,000 and 3,700 cm^{-1}.

The corresponding humic acid fraction of the profiles is more complex, with distinct peaks in the 490-520 cm^{-1} that may correspond to C-C skeletal vibration of alkyl groups, branched and/or straight chain alkanes (490 cm^{-1} to 600 cm^{-1}). A peak at or near 777 cm^{-1} corresponds to ethyl polysaccharide. The peaks at 100 cm^{-1} and 1040 cm^{-1} may correspond to primary alcohol and aliphatic ether. In addition, the peak or shoulder near 1068 cm^{-1} corresponds to Si-O stretching. The signals generated near 1233 correspond to C-O stretching of phenols, carboxylic acid ethers and COOH groups. The broad band near 1400 corresponds to aliphatic C-H deformation. At the 1625 cm^{-1} Vinkler et al., (1976) suggests that Al^{3+} ions complex with humic acids, producing this signal. The band near 2900 cm^{-1} corresponds to aliphatic C-H, stretching.

The sharp peaks that form between 3600 cm^{-1} and 3700 cm^{-1} suggest the presence of mineral impurities present (Stevenson, 1982). Saika and Parthasarathy (2010) indicate that the mineral impurity corresponds to kaolinite. Kaolinite is an abundant aluminosilicate mineral that has the capacity to adsorb organic molecules. An description of the FTIR of kaolinite suggests that the band in 3670-3656 cm^{-1} corresponds to Al-OH stretching; 3645 cm^{-1} corresponds to -OH stretching and crystalline hydroxyl; 1620 cm^{-1} is assigned to H-O-H bending of absorbed water;

918-909 (range from 918 to 893 cm^{-1}) is attributed to -OH deformation linked to –Al. In the area of 1080 to 900 cm^{-1}, sharp peaks can correspond to metal-oxygen vibrations; 1035 cm^{-1} corresponds to Si-O stretching present in clay minerals; 542-535 cm^{-1} correspond to Fe-O, Fe_2O_3 and/or Si-O-Al stretching; and 475-468 cm^{-1} is assigned to Si-O-Si bending. In addition, a band in 1031-1038 cm^{-1} (1027 cm^{-1}) can be attributed possibly to a quartz interference.

The degree of polymerization of humic acids is always higher than for fulvic acid. There is the possibility that during the ageing process of humic acids, a strong interaction, such as chelation/metal bonding, occurs between functional groups of the humic acid and the oxides and silicate minerals. Such interaction may be the cause of the –OH stretching bands observed around 3,600 $cm^{-1}$and the low frequency bands that correspond to Si-O, Al-O, and Fe-O bonds.

Remarks on profile classification

Algarrobo profile A presented weak Spodosols profile, when compared to the rest of the profiles. The soil chemistry and mineralogy coincide with the classification of a Spodosols. The designation of master horizons in the field should be evaluated as the E^1 horizon shows more illuvial than eluvial properties and could possibly be a weak spodic horizon identified through chemical evaluation. The evidence presented with this evaluation suggests that this profile could belong to the Spodosols classification Typic Alorthod.

Algarrobo profile B did not meet the chemical criteria of pH value for confirmation of spodic horizon classification in the laboratory; nonetheless, field evaluation yields a profile that is consistent with a Spodosols soil. This profile shows evidence that the eluviation/illuviation couplet of podzolization is occurring, evident with the formation of a soil horizon enriched with organic carbon and complementing soil mineralogy, but the basic cation content is too high and

alters the soil pH. In addition, the boundary line between the bleached eluvial E horizon and the spodic horizon is smooth, when compared to the rest of the profiles. This may be caused by a fluctuating water table that reaches that specific area in the profile, creating that clear distinction and the appearance of a smooth boundary between these horizons. Redoximorphic features were observed within the mineral soil profile. This profile has more characteristics that coincide with the Spodosols Great Group Alaquods. Aquods are wet Spodosols, with a white or nearly white albic horizon over reddish brown spodic horizon. In comparison with the Myakka series (Soil Survey Staff, 2015), a smooth boundary between soil horizons E and B occurs very similar to boundary topography observed between horizon E and B in profile B.

Profile C has an acid soil profile, with evidence of translocation of organic carbon from the surface to deeper horizons and mineralogical evidence of accumulation of sesquioxides are key to classify as a true Spodosols. This profile classification should also correspond to a Typic Alaquod, because of the flooded condition during the first evaluation of the profile and the ammonium oxalate extraction did not detect Fe^{3+} in the soil profile. The classification of Profile D is consistent with properties of a Typic Alorthod, acid by nature with accumulation of organic carbon in the profile and mineralogical evidence to support eluviation and illuviation of material.

Geomorphologic properties surrounding the soil profiles such as position in the landscape and slope distinguish Spodosols profile A from profile C, and profile B from profile C. Although the four Spodosols prfolies studied are similar in chemical properties, profile A and C should be classified as Typic Alorthods and profiles B and C as Typic Alaquods. The data presented shows that the profiles B and C are different from the Alorthods identified in Puerto Rico and may be necessary to classify them as a new series.

CONCLUSIONS

- The four soil profiles analyzed showed clearly distinct soil horizons: a dark organic surface horizon, a bleached eluvial horizon and a dark reddish spodic horizon.

- The four profiles had a dominant sand content and increasing clay content with depth. The texture was sand, sandy loam, loamy sand, sandy clay loam, a physical property that facilitates the eluviation of material from the horizons above and an increasing clay content which promotes the accumulation of material. The soil mineralogy consisted of kaolinite, quartz, gibbsite, goethite, hematite and amorphous material. Although the poor crystallinity of the amorphous material, showed a broad band in the lower end of the diffractograms this shows that organic material is complexed with mineral components. A high value of specific surface area shows that organic material and amorphous material influence this soil property. The amorphous fractions may favor the formation of multiple layers of EGME, which results in the extremely high surface area values observed.

- The basic cation content is low, a soil property of Spodosols order that shows the depletion of material from the soil profile. Soil pH was acid in three of the four soil profiles. Profile B presented a high pH (7.1) that is due to a high content of carbonates. The accumulation of basic cation content is favored by the position of the profile in the landscape. This site occupies the lowest elevation and water enriched with carbonates from the surrounding areas flows into the depression area, altering the soil pH. The organic carbon content was high in the surface horizon and decreases in the eluvial E horizon. Organic carbon content increases in the B horizon, showing the

position of the diagnostic spodic horizon. Soil mineralogy of this horizon shows that amorphous material is detected with a broad and low intesity band at the lower end of the XRD diffractogram.

- The highest Al^{3+}content was found in the deepest horizons, supporting evidence that metal cations eluviate from the soil profile and can bind to organic matter exchangeable sites and acidify the soil profile.

- The fulvic acid spectrum is less complex when compared to the polymerized humic acid spectra. This is shown with the presence of less peaks and broader bands in the fulvic acid spectra. Sharp bands between 1000-900 cm^{-1} can be attributed to complexation of Al^{3+} with humic acid, due to metal-oxygen vibrations, evidencing the formation of the organo-metallic complex. Mineral impurities in the humic acid fraction are present in the spodic horizons analyzed.

- Soil data shows that Profiles A and D belong to the classification Typic Alorthods and Profiles B and C, Typic Alaquods. It is possible that differences in the hill-slope location may result in the establishment of new Spodosols series in Puerto Rico, if the area is large enough according to Soil Taxonomy Standards.

LITERATURE CITED

Acevedo, G., 1982. Soil Survey of Arecibo Area, Northern Puerto Rico. USDA Soil Conservation Service in Cooperation with the University of Puerto Rico, 268-941/29. College of Agricultural Sciences, U.S. Government Printing Office, Washington, DC.

Alexander, E.B. and R. Burt. 1996. Soil development on moraines of Mendenhall Glacier, southeast Alaska 1: The moraines and soil morphology. Geoderma. 72(1-2): 1-17.

Anderson, H. A., M. L. Berrow, V. C. Farmer, A. Hepburn, J. D. Russell, and A.D. Walker. 1982. A reassessment of Podzol formation processes. Journal of Soil Science. 33(1): 125–136.

Assmus, R.J. 1993. Genesis of the E horizon in the soils of Massie Lagoon in Clay County, Nebraska. Ph.D. Diss. University of Nebraska, Lincoln.

Barrett, L.R., and R.J. Schaetzl. 1993. Soil development and spatial variability on geomorphic surfaces of different age. Physical Geography. 14(1): 39-55.

Bertsch, P. M., and P. R. Bloom 1996. Aluminum. p. 517-550. In D.L. Sparks, A.L. Page, P.A. Helmke, R.H. Loeppert (ed.). Methods of Soil Analysis Part 3: Chemical Methods. SSSA Book Ser. 5.3. SSSA, ASA, Madison, WI.

Bish D.L. 1994. Quatitative X-Ray diffraction analysis of soils. p. 267-295. In J.E. Amonette and L.W. Zelazny (ed.). Quantitative Methods in Soil Mineralogy. Soil Science Society of America. Madison, Wisconsin.

Bloom, P. R., U. L. Skyllberg, and M. E. Sumner 2005. Soil Acidity. p. 411-459. In M.A. Tabatabai, and D.L. Sparks (ed.). Chemical Processes in Soils. SSSA Book Ser. 8. SSSA, Madison, WI.

Bockhiem, J.G. 2014. Albic Horizon. p. 79 – 87. In J.G. Bockheim (ed.). Soil Geography of the USA: A Diagnostic-Horizon Approach. Springer International, Switzerland.

Bockheim, J.G., and A.E. Hartemink. 2017. Spodosols. p. 149 – 166. In J.G. Bockheim and A.E. Hartemink (ed.). The Soils of Wisconsin. Springer. Cham, Switzerland.

Boorman, D.B., J.M. Hollis, and A. Lilly. 1995. Hydrology of soil types: a hydrologically based classification of the soils of the United Kingdom. Institution of Hydrology. Oxfordshire, UK.

Bourgault, R., D. Savage Ross, and S.W. Bailey. 2015. Chemical and Morphological Distinctions between Vertical and Lateral Podzolization at Hubbard Brook. Soil Science Society of America Journal. 79(2):428 – 439.

Brady, N.C., and R.R. Weil. 2004. Elements of the Nature and Properties of Soils (2nd ed.) Pearson. New York, USA.

Bray, J.R., and E. Gorham. 1964. Litter Production in Forests of the World. Advances in Ecological Research. 2: 101 – 157.

Brinatti, A.M., Y. Primerano Mascarenhas, V. Paulo Pereira, C. S. de Moya Partiti, and A. Macedo. 2010. Mineralogical characterization of highly weathered soils. Sci. Agric. (Piracicaba, Braz.) 67(4): 454-464

Bronick, C. J., and D. L. Mokma. 2005. Podzolization in a Sand Pit in Northern Michigan. Soil Science Society of American Journal. 69:1757-1760.

Browne, R.H. 1995. Toward a New Theory of Podzolization. p. 253-273. In W.W. McFee and J.M. Kelly (ed.). Carbon Forms and Functions in Forest Soils. Soil Science Society of America. Madison, Wisconsin.

Buol, S.W., R.J. McCracken, and F.D. Hole. 1973. Soil Genesis and Classification (2nd ed). Iowa State University Press. Ames, Iowa.

Buurman, P., and P. Vidal-Torrado. 2015. A Comment on "Chemical and Morphological Distinctions between Vertical and Lateral Podzolization at Hubbard Brook" by Bourgault et al. Soil Science Society of America Journal. 79(6): 1815 – 1817.

Buurman, P. 1986. pH-dependant character of complexation in Podzols. p. 181 – 186. In D. Righi and A. Chauvel (ed.). Podzol et Podzolisation: comptes redus de la table ronde internationale, Poitiers. INRA, Paris.

Cerato, A. and A. Lutenegger,. 2002. Determination of Surface Area of Fine-Grained Soils by the Ethylene Glycol Monoethyl Ether (EGME) Method. *Geotechnical Testing Journal*, 25(2): 315-321.

Chesworth, W. 2008. Encyclopedia of Soil Science. Springer. Netherlands. pp 504.

Cihacek, L.J. and J.M. Bremner. 1979. A simplified ethylene glycol monoethyl ether procedure for assessment of soil surface area. Soil Sci. Soc. Am. J. 43:831:822.

Coen, G.M., and R.W. Arnold. 1972. Clay mineral genesis of some New York Spodosols. Soil Sci. Soc. Am. Proc., 36:342-350.

Cronin, D. 2018. Handbook of Soil Fertility.

Dahlgren, R.A., and F. Ugolini. 1991. Distribution and characterization of short-range-order minerals in Spodosols from the Washington Cascades. Geoderma. 48(3-4): 391 – 413.

Daly, B.K. 1982. Identification of podzols and podzolized soils in New Zealand by relative absorbance of oxalate extracts of A and B horizons. Goderma. 28(1): 29 – 38.

De Coninck, F. 1980. Major mechanisms in formation of spodic horizons. Geoderma. 24(2): 101 – 128.

De Junet A., Basile-Doelsch I., Borschneck D., Masion A., Legros S., Marol C., Balesdent J., Templier J., Derenne S.. 2013. Characterization of organic matter from organo-mineral complexes in an andosol from Reunion Island. Journal of Analytical and Applied Pyrolysis, 99: 92-100.

Dixon, J.B. 1989. Kaoline and Serpentine group minerals. In J.B. Dixon, S.B. Weed (ed). Minerals in Soil Environments. SSSA Book Series 1. SSSA, Madison, Wisconsin.

Egli, M., A. Mirabella, and G. Sartori. 2004. Weathering of soils in Alpine areas as influenced by climate and parent material. Clays and Clay Minerals. 52: 287 – 303.

Egli, M., A. Mirabella, G. Sartori, and P. Fitze. 2003. Weathering rates as a function of climate: results from climosequence of the Val Genova (Trentino Italian Alps). Geoderma. 111: 99-121.

Egli, M., A. Mirabella, G. Sartori, D. Giaccai, R. Zanelli, and M. Plötze. 2007. Effect of slope aspecto on transformation of clay minerals in Alpine soils. Clay Minerals. 42: 373 – 398.

Evans, J. and J.A. Younquist. Spodosols. p. 1216 In. Encyclopedia of Forest Sciences. Academic Press.

Farmer, V.C. 1982. Significance of the presence of allophane and imogolite in Podzol Bs horizons for podzolization mechanisms: A review. Soil Science and Plant Nutrition. 28(4): 571 – 578.

Gee, G. W. and J. W. Bauder 1986. Particle-size Analysis1. p. 383-411. In A. Klute (ed.). Methods of Soil Analysis: Part 1—Physical and Mineralogical Methods. SSSA, ASA, Madison, WI.

Gee, G.W. and D. Or. 2002. Particle Size Analysis. p. 255-293. In J. H. Dane and C.G. Topp (ed) Methods of Soil Analysis: Part 4: Physical Methods, SSSA Soil Book Series No. 5. Madison, Wisconsin.

Goldberg, S., I. Lebron, D. L. Suarez, and Z. R. Hinedi. 2001. Surface Characterization of Amorphous Aluminum Oxides Contribution from the U.S. Salinity Lab. Soil Sci. Soc. Am. J. 65:78-86.

González-Pérez, M., P. Vidal Torrado, L.A. Colnago, L. Martin-Neto, X.L. Otero, D.M.B.P. Milori, and F. Haenel Gomes. 2008 ^{13}C NMR and FTIR spectroscopy characterization of humic acids in spodosols under tropical rain forest in southeastern Brazil. Geoderma. 146(3-4): 425-433.

Gustafsson, J.P., P. Battacharya, D.C. Bain, A.R. Fraser, and W.J. McHardy. 1995. Podzolization mechanisms and the synthesis of imogolite in northern Scandinavia. Geoderma. 66(3-4): 167 – 184.

Haile-Mariam, S., and D. L. Mokma. 1996. Mineralogy of Two Fine-Loamy Hydrosequences in South-Central Michigan. Soil Horizons 37:65-74.

Harris, W. G., and K. A. Kollien. 1999. Changes in quantity and composition of crystalline clay across EBh boundaries of Alaquods. Soil Sci. 164:602-608.

Harsh, J. 2005. Amorphous materials. p. 64-71. In D. Hillel. Encyclopedia of Soils in Environment. Elsevier.

Horbe, A.M.C., M.A. Horbe, and K. Sugio. 2004. Tropical Spodosols in northeastern Amazonas State, Brazil. Geoderma. 119(1-2): 55-68.

Iscan, A.G., and M.V. Kok. 2009. Porosity and Permeability Determinations in Sandstone and Limestone Rocks Using Thin Section Analysis Approach. Energy Source, Part A: Recovery, Utilization and Environmental Effects. 31(7): 568 – 575.

Jackson, M.L. 1965. Clay transformations in soil genesis during the Quaternary. Soil Scince. 99: 15-22.

Jien, S.H., S.P. Wu, Z.S. Chen, T.H. Chen, and C.Y. Chiu. 2010. Characteristics and pedogenesis of podzolic forest soils along a toposequence near a subalpine lake in northern Taiwan. Botanical Studies. 51: 223 – 236.

Jobbagy, E.G., and R.B. Jackson. 2001. The distribution of soil nutrients with depth: Global patterns and the imprint of plants. Biogeochemistry. 53: 51-77.

Johnson-Maynard, J.L. 2006. Allophanes. p. 72 – 74. In R. Lal. Encyclopedia of Soil Science (2nd ed.). CRC Press, Taylor and Francis Group. Boca Raton, Florida.

Jones, R. C., and H. U. Malik 1994. Analysis of Minerals in Oxide-Rich Soils by X-Ray Diffraction. p. 296-329. In J. E. Amonette and L. W. Zelazny (ed.). Quantitative Methods in Soil Mineralogy, SSSA, Madison, WI.

Lugo-López, M.A., and L.H. Rivera. 1975. Taxonomic Classification of the Soils of Puerto Rico, 1975. University of Puerto Rico, Rio Piedras, P.R. 245:4 – 32.

Lundström, U.S., N. van Breemen, and D.C. Bain. 2000. The podzolization process: A review. Geoderma. 94(2-4): 91-107.

Más, E. G. & M. de L. Lugo-Torres. 2013. Malezas Comunes en Puerto Rico & Islas Vírgenes Americanas/Common Weeds in Puerto Rico & U.S. Virgin Islands. Universidad de Puerto Rico, University of Puerto Rico, Recinto Universitario de Mayagüez/Mayagüez Campus. USDA Servicio de Conservación de Recursos Naturales. Natural Resources Conservation Service. Área del Caribe/Caribbean Area

McKeague, J.A., F. DeConinck, and D.P. Franzmeier. 1983. Spodosols. p. 217-252. In L.P. Wilding, N.E. Smech and G.F. Hall (1st ed.). Pedogenesis and Soil Taxonomy II: The Soil Orders. Elsevier, Netherlands.

McKeague, J. A., M. V. Cheshire, F. Andreux, and J. Berthelin. 1986. Organo-Mineral Complexes in Relation to Pedogenesis1. p. 549-592. In P. M. Huang, M. Schnitzer (ed.). Interactions of Soil Minerals with Natural Organics and Microbes. Soil Science Society of America. Madison, WI.

Mehra, O.P. and M.L. Jackson. 1960. Iron oxide removal from soils and clays by a dithionate-citrate system buffered with sodium bicarbonate. p. 317-327. 7th Natl. Conf. Clays and Clay Minerals.

Mokma, D.L. 1993. Color and amorphous materials in Spodosols from Michigan. Soil Science Society of America Journal. 57: 125 – 138.

Mokma, D.L., and M. Yli-Halla. 2003. Problems with Spodosol Classification in the Field. Soil Survey Horizons 44: 117-122.

Mokma, D.L., M. Yli-Halla, and K. Lindqvist. 2004. Podzol formation in sandy soils of Finland. Geoderma. 120(3): 259 – 272.

Mossin, L., B. T. Jensen, and P. Nørnberg. 2001. Altered Podzolization Resulting from Replacing Heather with Sitka Spruce. Soil Science Society of America. 65: 1455-1462.

Mount H.R., and W.C. Lynn. 2004. Soil survey laboratory data and soil descriptions for Puerto Rico and the U.S. Virgin Islands. United States Department of Agriculture, Natural Resources Conservation Service, National Soil Survey Center, Soil Survey Investigations Report No. 49.

Muñoz, M.A., W. Lugo, C. Santiago, M. Matos, S. Ríos, and J. Lugo. 2018. Taxonomic Classification of the Soils of Puerto Rico, 2017. University of Puerto Rico, Rio Piedras, PR. 313: 1-73.

Murashkina, M.A., R.J. Southard and G.S. Pettygrove. 2007. Potassium fixation in San Joaquin Valley soils derived from granitic and nongranitic alluvium. Soil Science Society of America Journal. 71: 125-132

Nelson, D. W., and L. E. Sommers. 1996. Total Carbon, Organic Carbon, and Organic Matter. p. 961-1010. In D.L. Sparks, A.L. Page, P.A. Helmke, and R.H. Loeppert (ed.). Methods of Soil Analysis Part 3: Chemical Methods. Soil Science Society of America. Madison, WI.

Nesse, W.D. 1986. Introduction to optical mineralogy. Oxfor University Press, New York.

Nimmo, J.R. 2005. Aggregates. p. 22-35 In D. Hillel Encyclopedia of Soils in the Environment. Elsevier.

Nimmo, J.R. and Perkins KS. 2002. Aggregate stability and size distribution. Soil Sci. Soc. Am. J. 5: 317-328

Pedro, G. 1983. Structuring of some basic pedological processes. Geoderma. 31(4): 289 – 299.

Ponomareva, V.V. 1964. Theory of Podzolization 1969. Israel Program for Scientific Translation, Jerusalem. 309 pp.

Reiger, S. 1983. Spodosols. 71-103. In S. Rieger (ed.). The genesis and classification of cold soils. Academic Press. New York, New York, USA.

Saikia B. and G. Parthasarath. 2010. Fourier Transform Infrared Spectroscopic Characterization of Kaolinite from Assam and Meghalaya, Northeastern India. *Journal of Modern Physics*,1 (4) 206-210

Sauer, D., I. Sshulli-Maurer, R. Sperstad, R. Sorenson, and K. Stahr. 2008. Podzol development with time in sandy beach deposits. J. Soil Sci. Plant Nutr. 171:483-497

Schaetzl, R.J., and S. Anderson. 2005. Soils Genesis and Geomorphology. Cambridge University Press. New York, NY.

Schaetzl, R.J., and S.A. Isard. 1996. Regional-scale relationships between climate and strength of podzolization in the Great Lakes Regions, North America. Catena. 28: 47 – 69.

Schaetzl R.J., and M.L. Thompson. 2015. Soils Genesis and Geomorphology (2nd ed.). Cambridge University Press, NY.

Schnitzer, M. 1975. Chemical, spectroscopic, and thermal methods for the classification and characterization of humic substances. p. 293-310. In D. Povoledo and H. L. Golterman (ed.). Humic substances: Their structure and function in the biosphere. Center for Agricultural Publishing and Documentation, Wageningen.

Schoeneberger, P.J., D.A. Wysocki, E.C. Benham, and Soil Survey Staff. 2012. Field book for describing and sampling soils, Version 3.0. Natural Resources Conservation Service, National Soil Survey Center, Lincoln, NE.

Soil Survey Staff. 2015. Illustrated guide to soil taxonomy. U.S. Department of Agriculture, Natural Resources Conservation Service, National Soil Survey Center, Lincoln, Nebraska.

Soil Survey Staff. 2014. Keys to Soil Taxonomy (12th ed.). USDA-Natural Resources Conservation Service, Washington, DC.

Soil Survey Staff. 1999. Soil Taxonomy: A basic system of classification for making and interpreting soil surveys (2nd ed.). U.S. Department of Agriculture, Natural Resources Conservation Service, National Soil Survey Center, Lincoln, Nebraska.

Soil Survey Staff, Natural Resources Conservation Service, United States Department of Agriculture. Web Soil Survey. Available online at the following link: https://websoilsurvey.sc.egov.usda.gov/. Accessed [08/2018].

Sommer, M., D. Halm, C. Geisinger, I. Andruschkewitsch, M. Zarei, and K. Stahr. 2001. Lateral podzolization in sandstone catchment. Geoderma. 103: 231 – 247.

Stevenson, F.J. 1982. Humus Chemistry. Genesis, Composition, Reaction. John Wiley & Sons, New York, NY.

Stone, E.L., Harris, W.G., Brown, R.B., and Kuehl, R.J. 1993. Carbon storage in Florida Spodosols. Soil Science Society of America Journal. 57: 179–182

Suharta, N., and B.H. Prasetyo. 2009. Mineralogical and chemical characteristics of Spodosols in Toba Highland, North Sumatra. Indonesian Journal of Agricultural Science. 10 (2): 54-64.

Sumner, M.E. 1999. Handbook of Soil Science. CRC Press LLC, Florida.

Sumner, M.E. and W.P. Miller. 1996. Cation exchange capacity and exchange coefficients. p. 1201-1229. *In* D.L. Sparks et al. (ed.) Methods of Soil Analysis. Part 3. Chemical Methods. SSSA Book Ser. no 5. SSSA and ASA, Madison, WI.

Tan, K.H., 2003. Humic Matter in Soil and the Environment. Marcel Dekker, New York.

Taylor G., and R.A. Eggleton. 2001. Regolith Geology and Geomorphology. John Wiley and Sons. England.

Thien, S.J. 1979. A flow diagram for teaching texture by feel analysis. Journal of Agronomic Eduucation. 8: 54-55

Tiner, R.W. 2016. Wetland Indicators: A guide to wetland formation, identification, delineation, classification, and mapping. CRC Press, Taylor & Francis Group. Boca Raton, Florida.

Torn, M.S., C.W. Swanston, C. Castanha, and S.E. Trumbore. 2009. Storage and turnover of organic matter in soils. 215 – 268. In N. Senisi, N. Xing and P.M. Huag (ed.). Biophysico-Chemical Processes Involving Natural Nonliving Organic Matter in Environmental Systems. John Wiley & Sons, Inc. Hoboken, NJ.

Valerio, M.W., P.A. McDaniel, and P.E. Gessler. 2016. Distribution and Properties of Podzolized Soils in the Northern Rocky Mountains. Soil Sci. Soc. Am. J. 80:1308-1316.

Van Cleve, K., and R. F. Powers 1995. Soil Carbon, Soil Formation, and Ecosystem Development. p. 155-200. In W. W. McFee, J. M. Kelly (ed.). Carbon Forms and Functions in Forest Soils. Soil Science Society of America. Madison, WI.

Vinkler, P., B. Lakatos, and J. Meisel. 1976. Infrared spectroscopic investigations of humic substances and their metal complexes. Geoderma 15: 53-67.

Wang, C., R. Long, Q. Wang, W. Liu, Z. Jing, and L. Zhang, Fertilization and litter effects on the functional group biomass, species diversity of plants, microbial biomass, and enzyme activity of two alpine meadow communities. Plant Soil 331: 377–389.

Watts, F. C., and M. E. Collins. 2008. Soils of Florida. Soil Science Society of America. Madison, WI.

Weil, R.R., and N.C. Brady. 2016. The Nature and Properties of Soils (15th ed.). Pearson. New York, USA.

Wilding, L.P., N.E. Smeck, and G.F. Hall. 1983. Pedogenesis and Soil Taxonomy II: The Soil orders. Elsevier. New York, NY.

Zelazny, L.W., and V.W. Carlisle. 1971. Mineralogy of Florida Aeric Haplaquods. Proc. Soil Crop. Sci. Soc. Fla. 31:160-165.

APPENDICES

Appendix A. Algarrobo Soil Profile Description

Soil Survey of the Arecibo Area, Northern Puerto Rico (Acevedo, 1982).

Soil Description

AgC—Algarrobo fine sand, 2 to 12 percent slopes. This soil is deep, gently sloping to sloping, and excessively drained. It is on coastal plains. Slopes range from about 100 to 400 feet long. The areas of the soil range from 20 to 200 acres.

Typically, the surface layer is gray, loose fine sand about 11 inches thick. The subsurface layer is light gray, very friable fine sand 21 inches thick. The subsoil is 5 inches of black and brown, very friable sandy loam. The next 31 inches is extremely firm, gray and brown clay. The underlying layer is very firm sandy clay loam to a depth of 80 inches.

Included with this soil in mapping are areas of Corozo and Arecibo soils and soils from which the surface layer has been removed for industrial purposes. Included soils make up 10 to 15 percent of the unit.

The permeability of this Algarrobo soil is rapid in the upper part and slow in the lower part. The available water capacity is low. Runoff is slow, and tilth is good. Reaction in the surface layer and subsoil is extremely acid to strongly acid.

This soil is well suited for coconuts and for such pasture plants as pangolagrass and merkergrass. The major limitations are the low available water capacity, the acidity, and a low fertility level. Establishing and maintaining a mixture of pangolagrass and legumes, preventing overgrazing, using proper stocking rates and deferred grazing, controlling weeds, and liming and fertilizing are the main pasture management concerns.

This soil has few limitations for most types of nonfarm use.

The capability subclass is VIIs.

Algarrobo series

The soils of the Algarrobo series are coarse-loamy, siliceous, isohyperthermic Entic Haplohumods. They are deep and excessively drained and are on coastal plains. They formed in coarse textured sediments with a high content of quartz and are over coastal plain clays. The Algarrobo soils are in pangolagrass, native pasture, coconuts, and brush. Slopes range from 2 to 12 percent.

Algarrobo soils are associated with Corozo, Jobos, Guerrero, Arecibo, and Carrizales soils. The Corozo soils have less organic matter than the Algarrobo soils, and the Jobos and Guerrero soils have no organic matter but have plinthite. The Arecibo soils do not have organic matter within a depth of 50 inches, and the Carrizales soils are not as gray as the Algarrobo soils and have no organic matter.

Typical pedon of Algarrobo fine sand, 2 to 12 percent slopes, 3 meters northeast of Highway 668, 200 meters from kilometer 42.9 of Highway 2, in a palm tree field:

A1—0 to 11 inches, gray (10YR 5/1) fine sand; single grain; loose, very friable, nonsticky, nonplastic; many fine and medium roots; 15 percent black (10YR 2/1) rounded and elongated friable organic matter accumulations 1/4 inch thick; extremely acid; abrupt smooth boundary.

A2—11 to 32 inches, light gray (10YR 7/1) fine sand; single grain; very friable, nonsticky, nonplastic; common medium roots; extremely acid; clear wavy boundary.

Bh1—32 to 37 inches, black (10YR 2/1), dark brown (10YR 3/3), and very dark brown (10YR 2/2) stratified sandy loam; single grain; very friable, nonsticky, nonplastic; few medium roots; extremely acid; abrupt wavy boundary.

IIB2—37 to 50 inches, mixed light gray (10YR 7/1), brown (7.5YR 5/2), and strong brown (7.5YR 5/8) clay; weak coarse subangular blocky structure; extremely firm, slightly sticky, plastic; very dark gray (10YR 3/1) along root channels; very strongly acid; clear wavy boundary.

IIC1—50 to 68 inches, mixed gray (10YR 7/1) and brown (7.5YR 5/2) clay; massive; extremely firm, slightly sticky, plastic; very strongly acid; clear wavy boundary.

IIC2—68 to 80 inches, light gray (10YR 7/1) sandy clay loam; massive; very firm, slightly sticky, plastic; very strongly acid.

The depth to the accumulation of illuvial organic matter ranges from 30 to 50 inches. Reaction ranges from strongly acid to extremely acid throughout.

The A1 horizon has hue of 10YR, value of 5 or 6, and chroma of 1.

The A2 horizon has hue of 10YR, value of 7 or 8, and chroma of 1.

The Bh horizon has hue of 10YR, value of 2 or 3, and chroma of 1 or 2. It ranges from sandy loam to loamy sand.

The B2 horizon has hue of 10YR and 7.5YR, value of 5 to 7, and chroma of 1 to 8. It ranges from sandy clay to clay. Structure is weak moderate or weak coarse subangular blocky.

Appendix B. X-ray Diffractograms of Algarrobo Soil Profiles

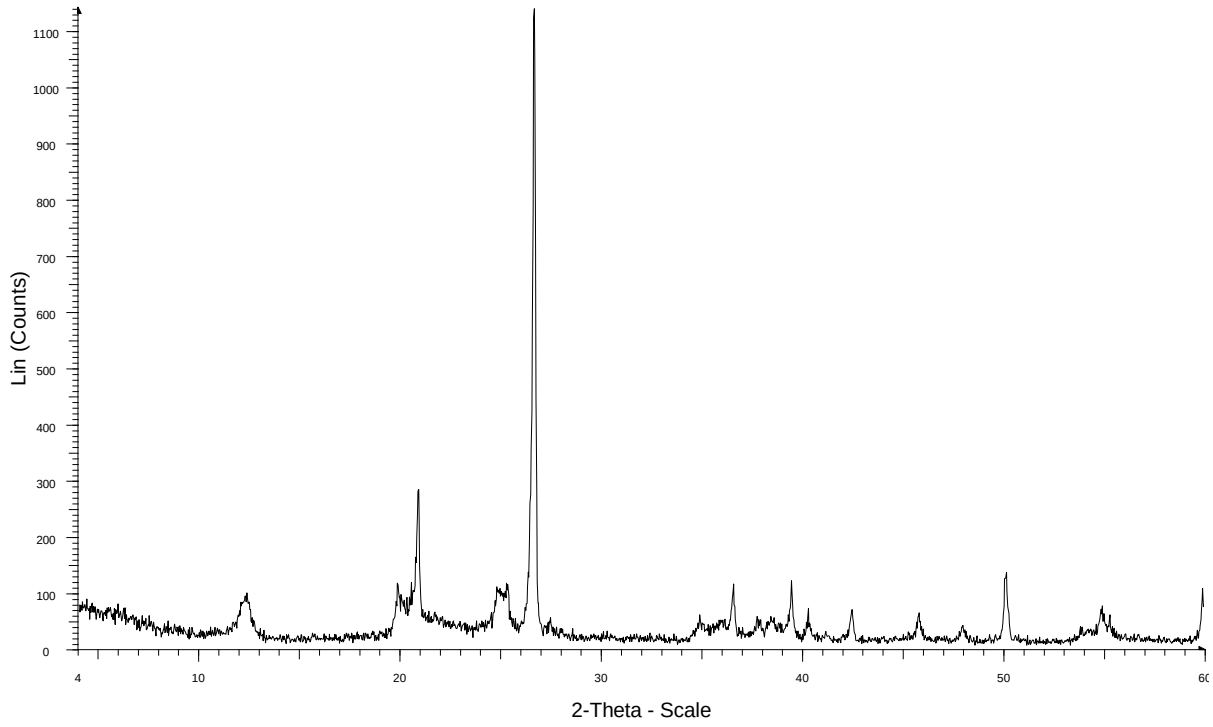

Figure B 1. X-ray diffractogram of the A horizon in Algarrobo profile A.

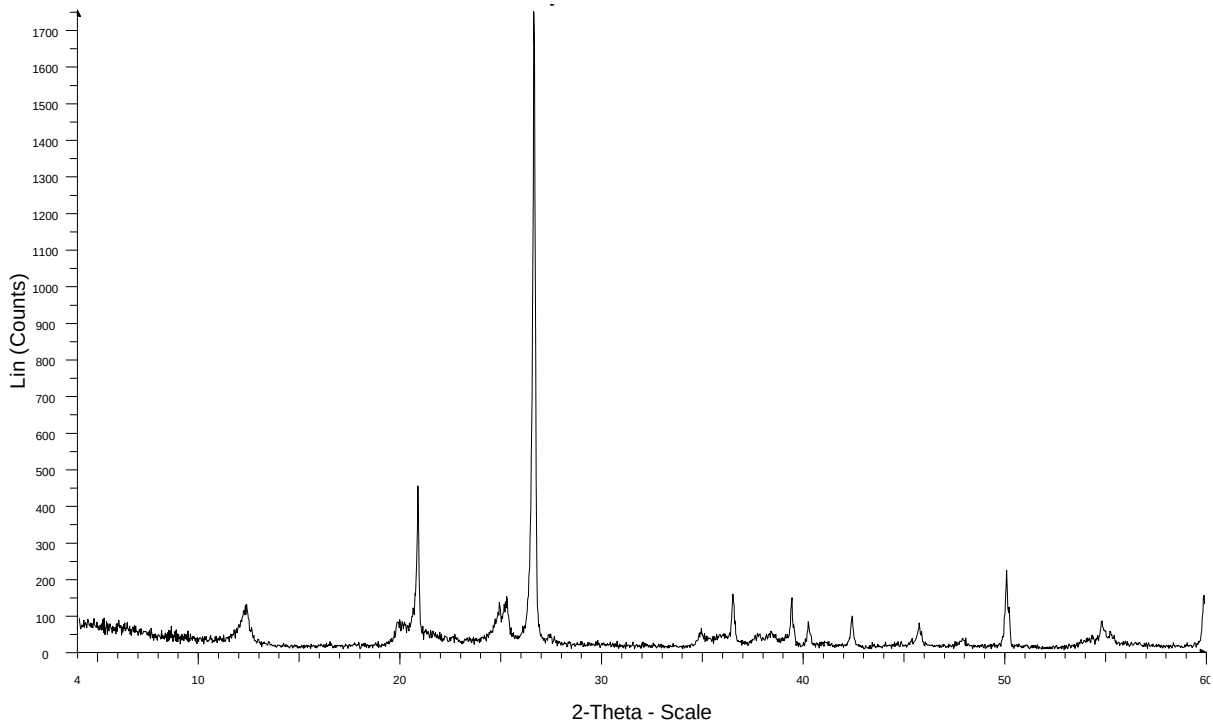

Figure B 2. X-ray diffractogram of the E_1 horizon in Algarrobo profile A.

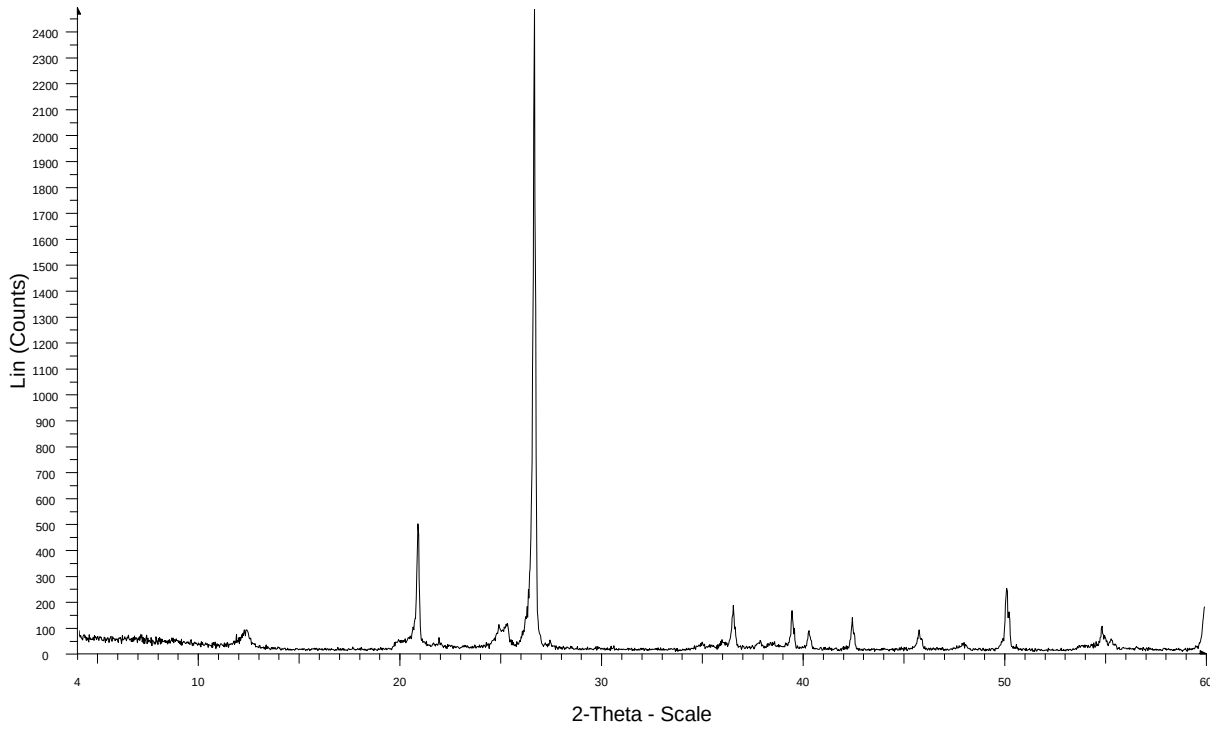

Figure B 3. X-ray diffractogram of the B_h horizon in Algarrobo profile

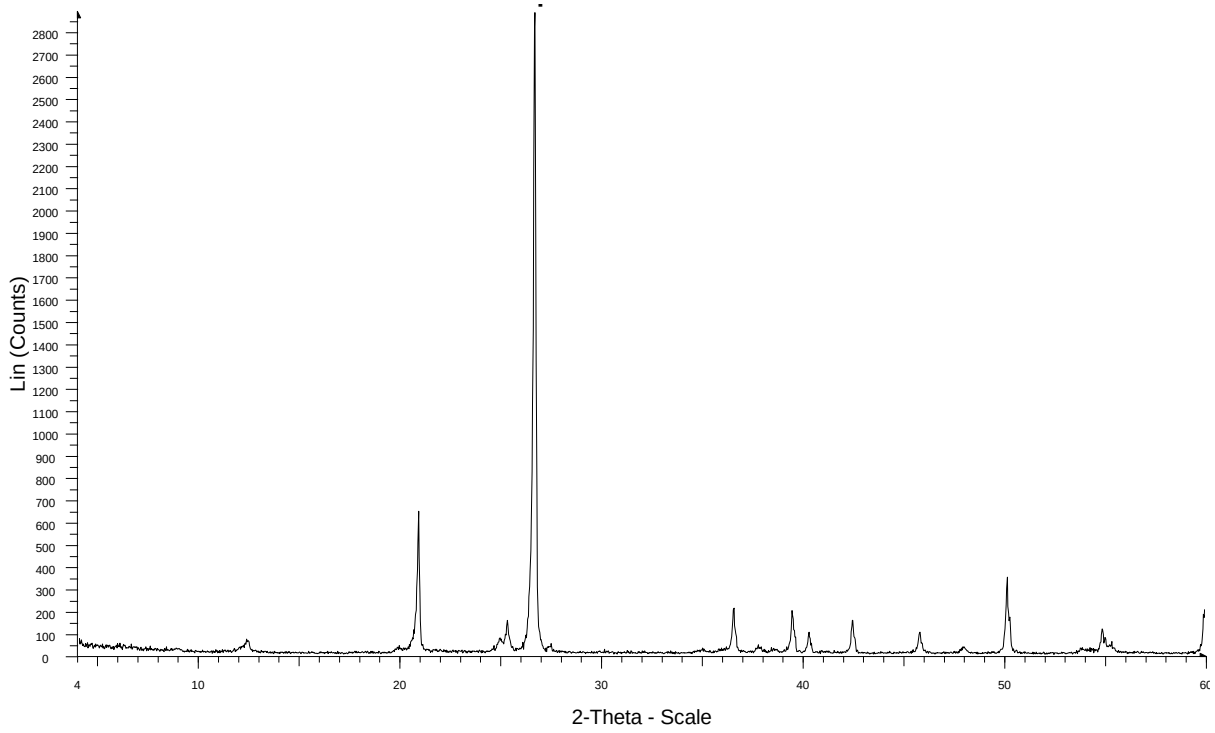

Figure B 4. X-ray diffractogram of the E^1 horizon in Algarrobo profile A.

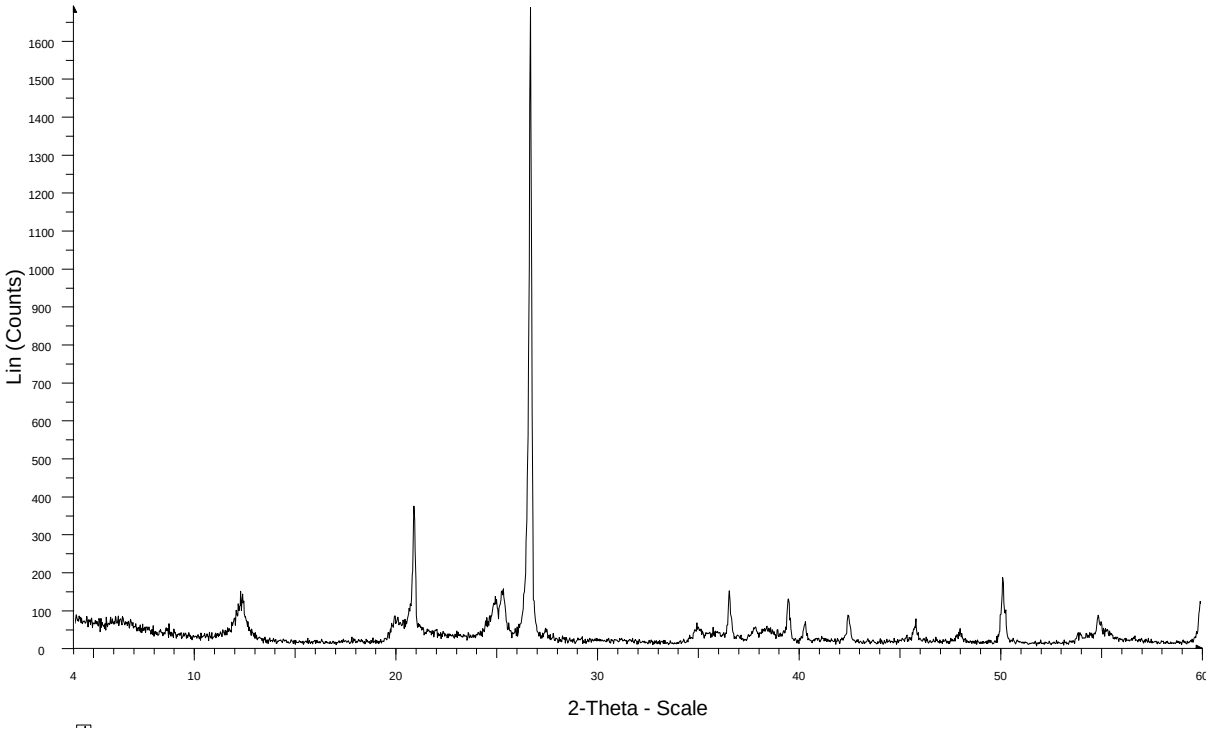

Figure B 5. X-ray diffractogram of the B_{hs} horizon in Algarrobo profile

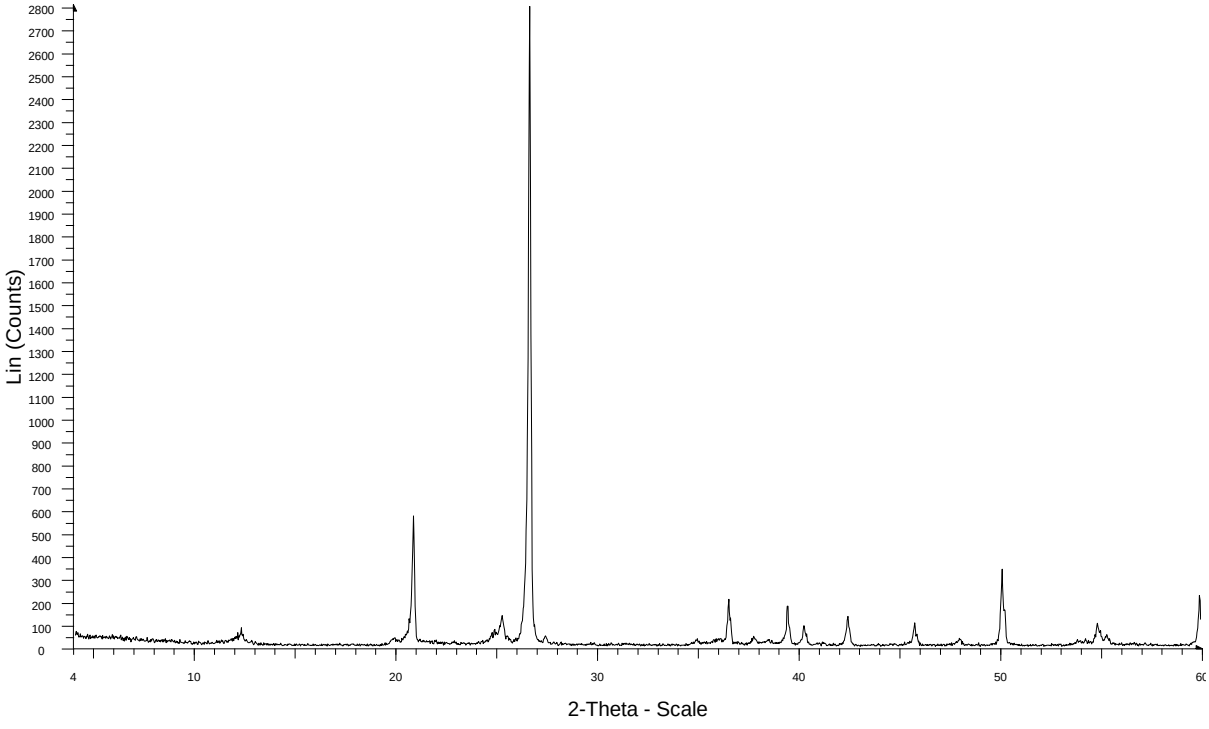

Figure B 6. X-ray diffractogram of the BC_1 horizon in Algarrobo profile A.

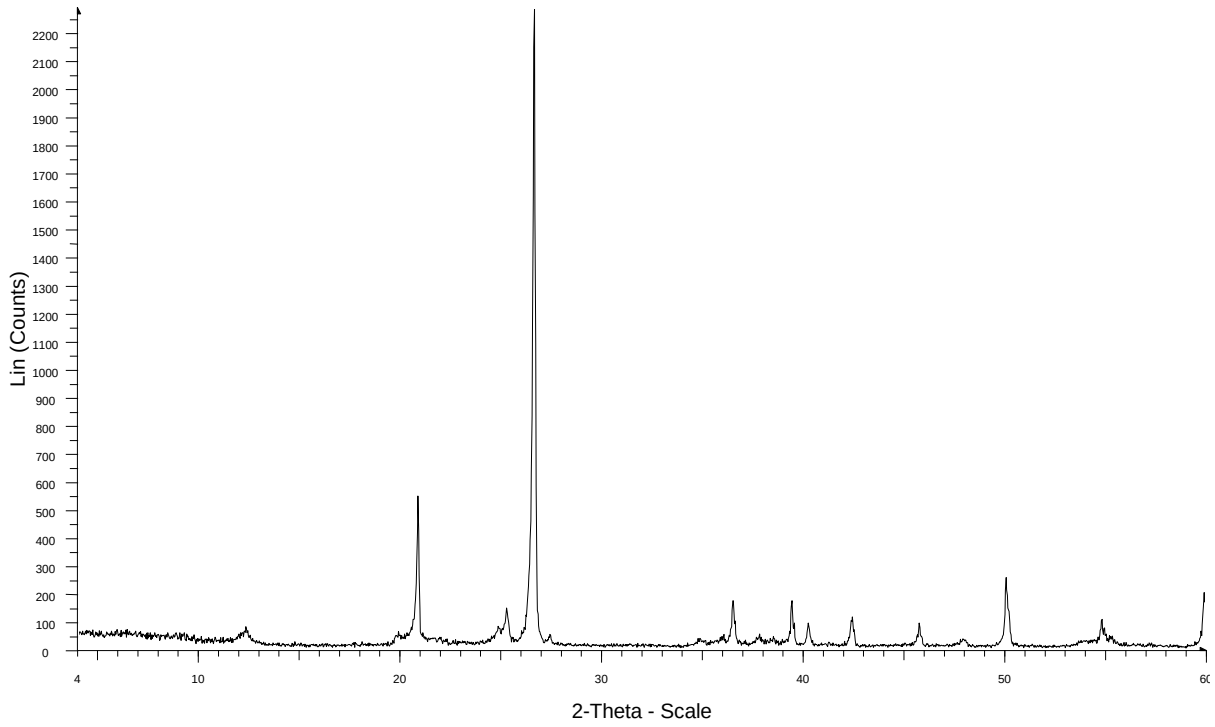

Figure B 7. X-ray diffractogram of the BC_2 horizon in Algarrobo profile A.

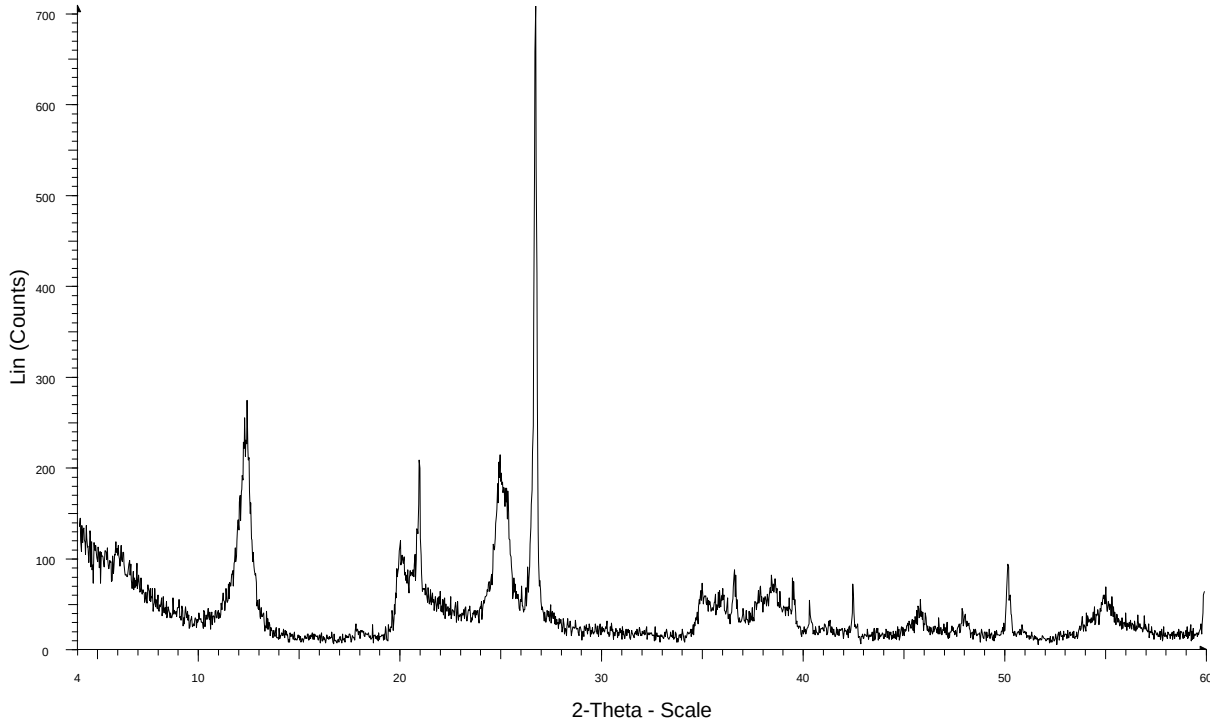

Figure B 8. X-ray diffractogram of the 2C horizon in Algarrobo profile A.

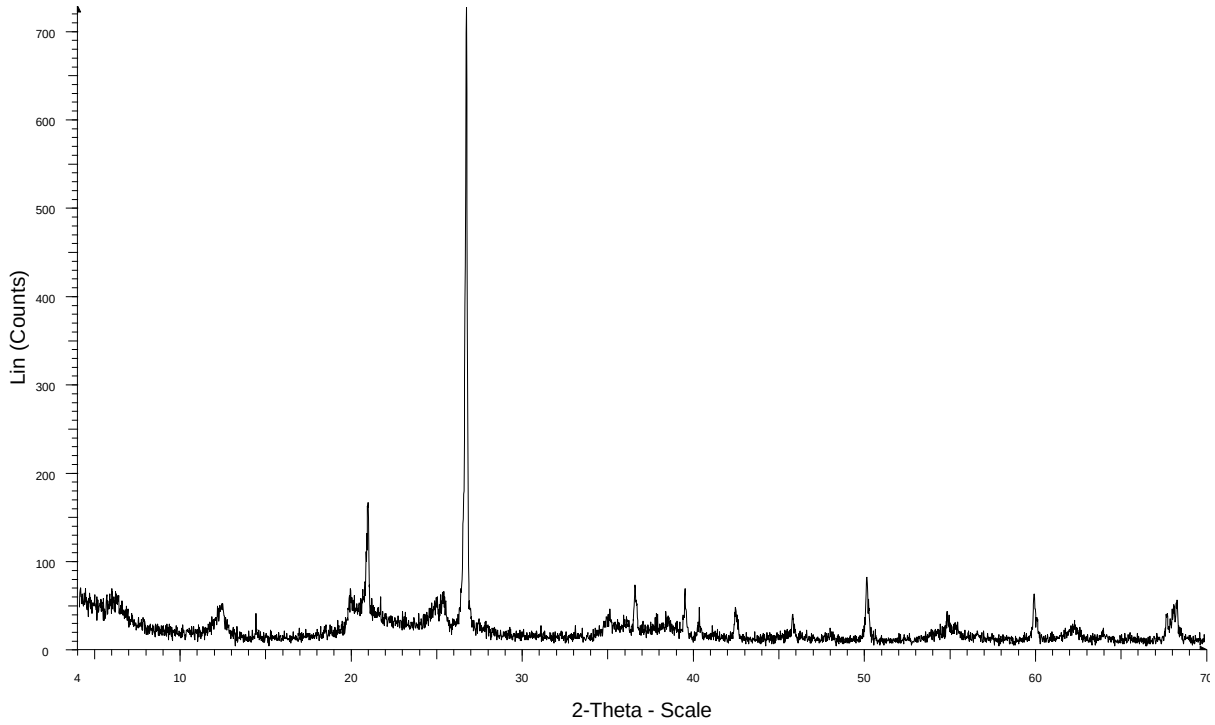

Figure B 9. X-ray diffractogram of the A_1 horizon in Algarrobo profile B.

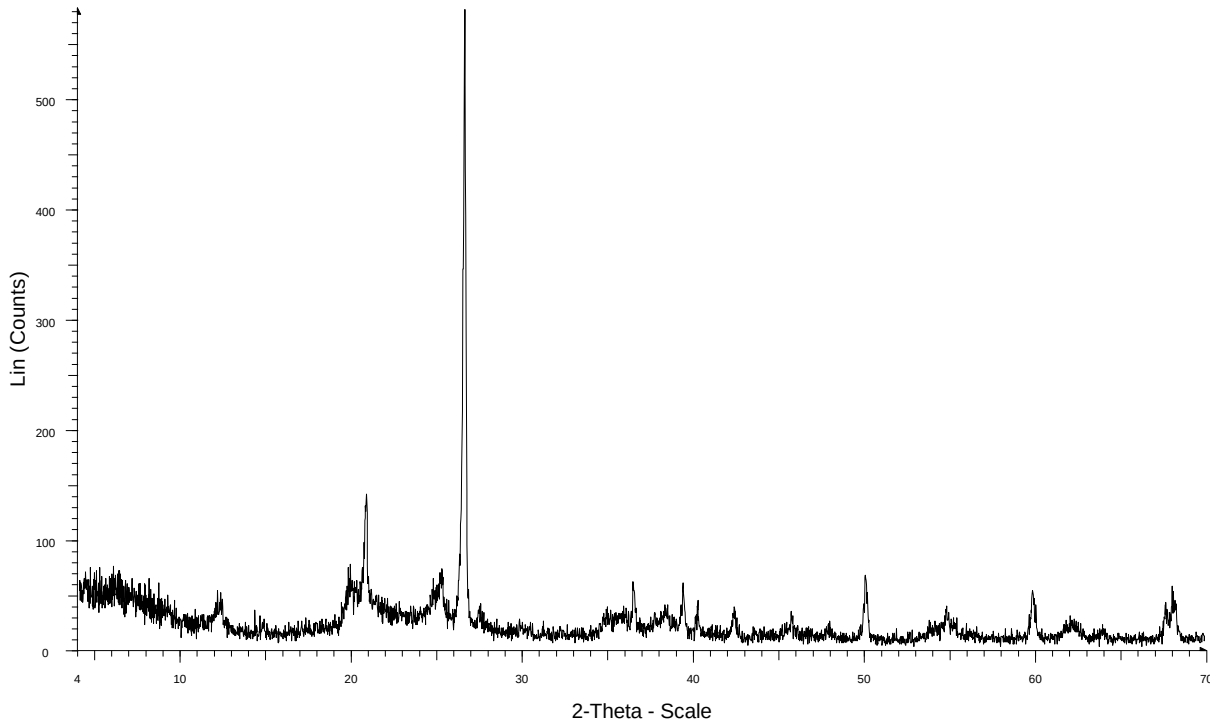

Figure B 10. X-ray diffractogram of the A_2 horizon in Algarrobo profile B.

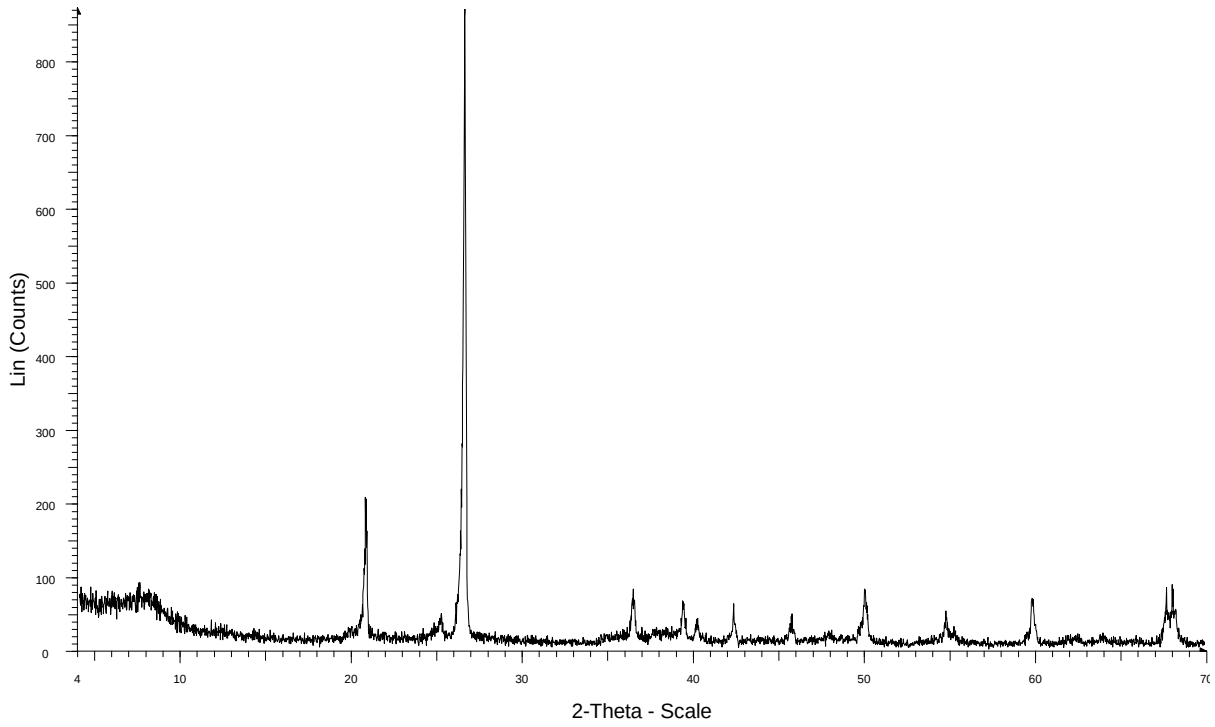

Figure B 11. X-ray diffractogram of the E horizon in Algarrobo profile B.

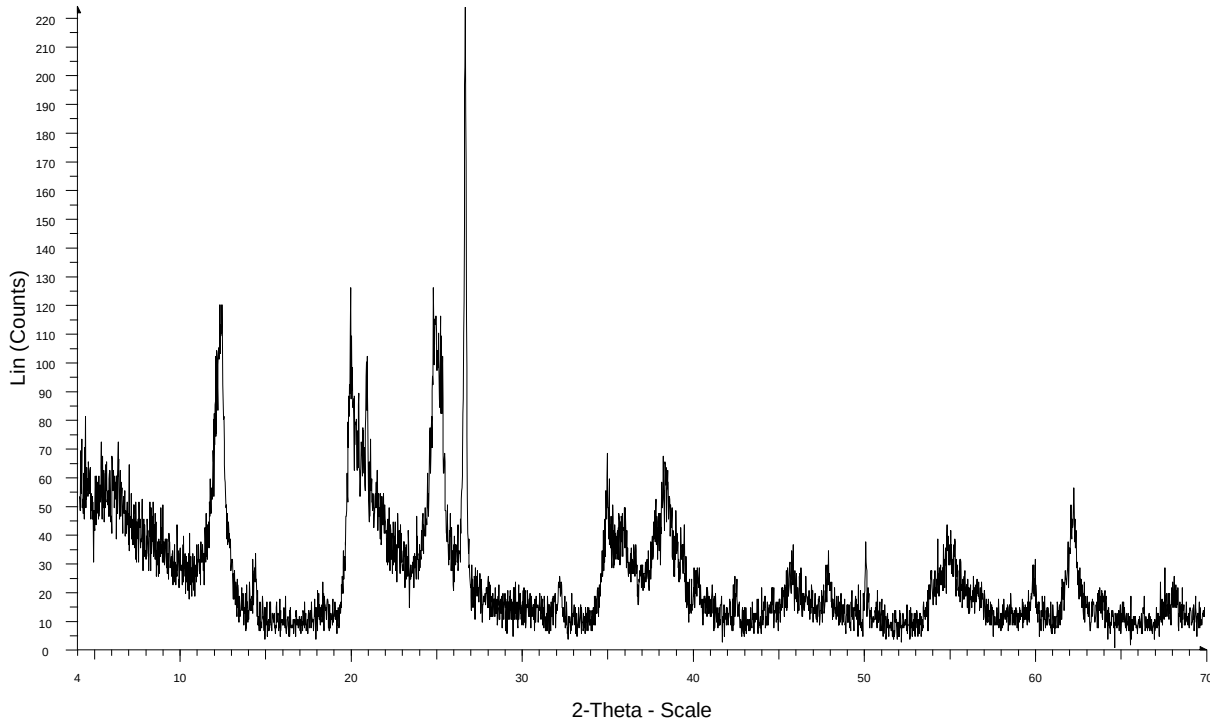

Figure B 12. X-ray diffractogram of the B_{hs1} horizon in Algarrobo profile B.

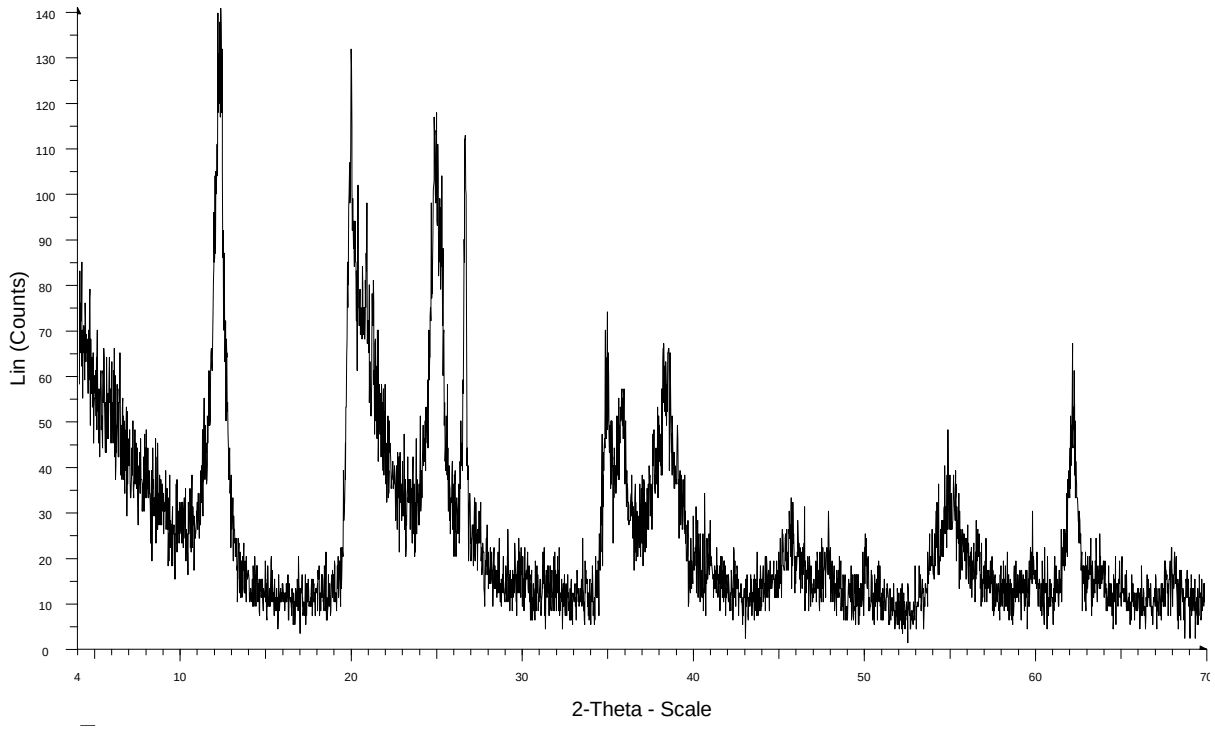

Figure B 13. X-ray diffractogram of the B_{hs2} horizon in Algarrobo profile B.

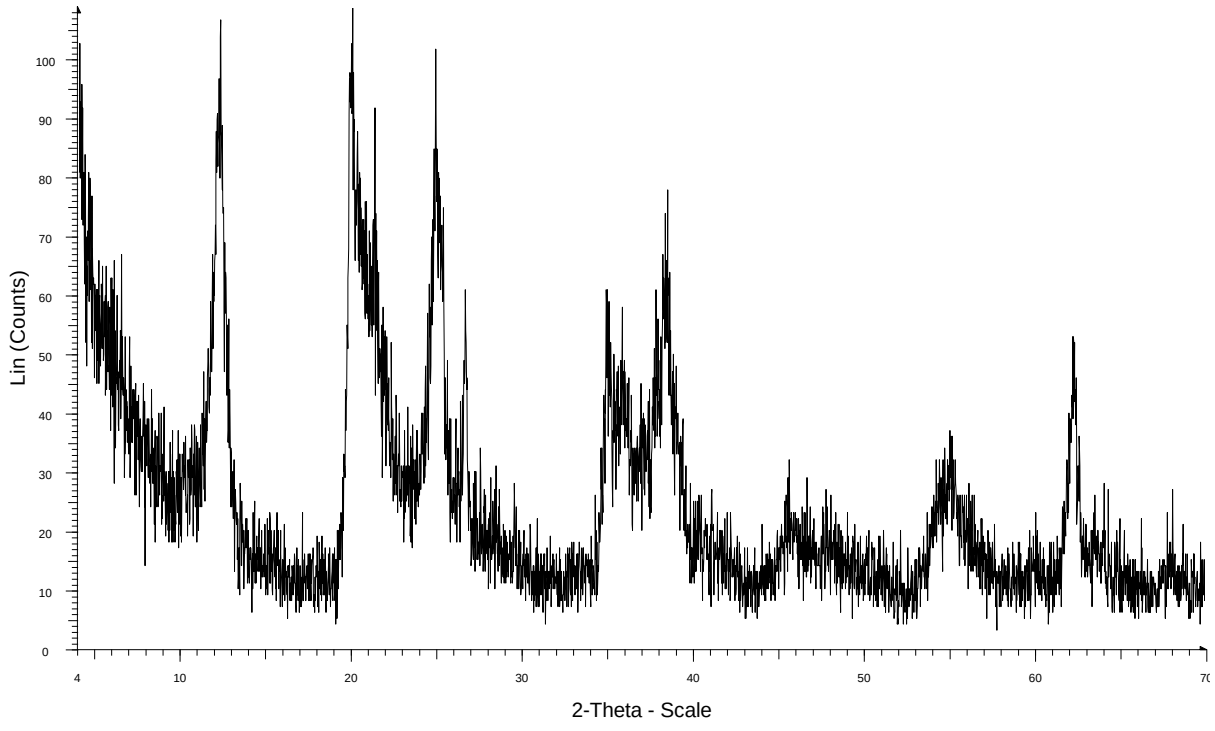

Figure B 14. X-ray diffractogram of the B_{s1} horizon in Algarrobo profile B.

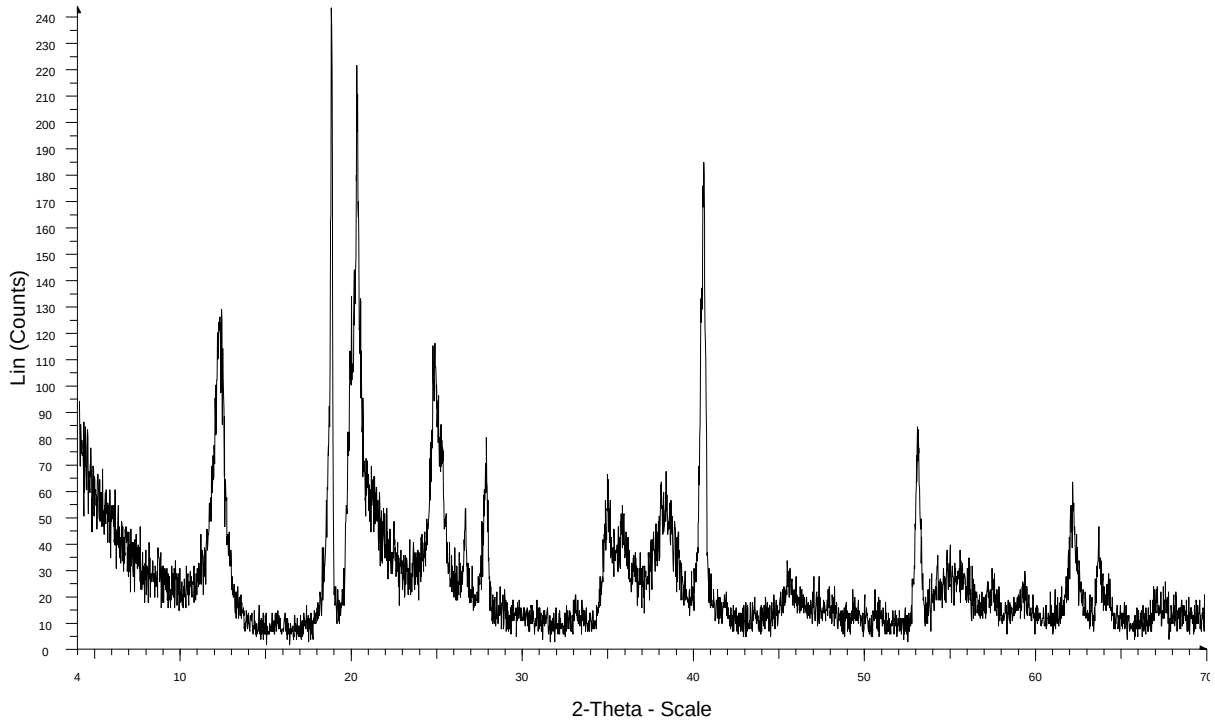

Figure B 15. X-ray diffractogram of the 2BC horizon in Algarrobo profile B.

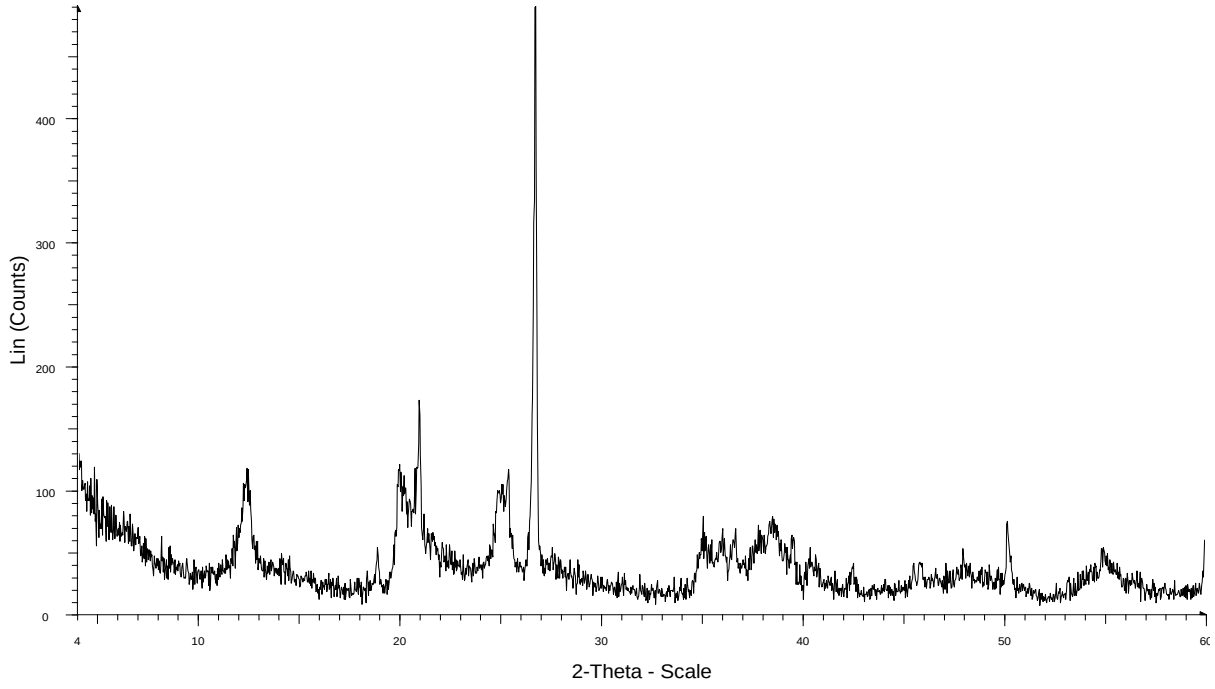

Figure B 16. X-ray diffractogram of the A horizon in Algarrobo profile D.

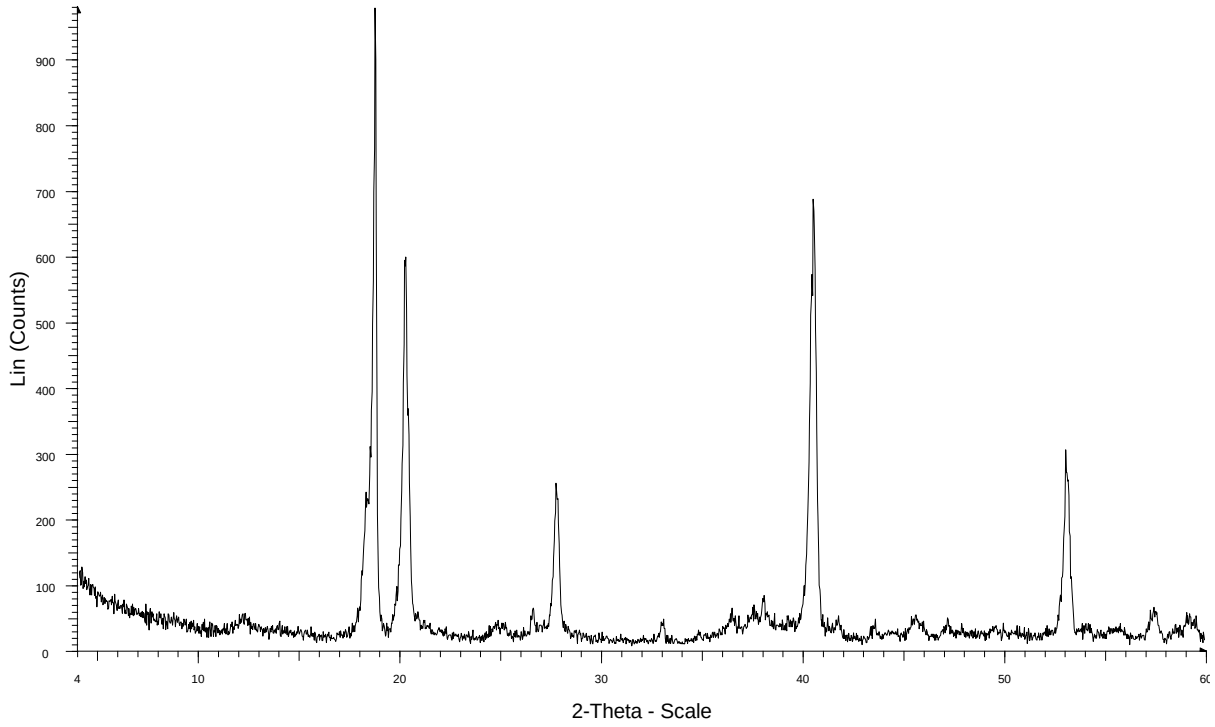

Figure B 17. X-ray diffractogram of the E horizon in Algarrobo profile D.

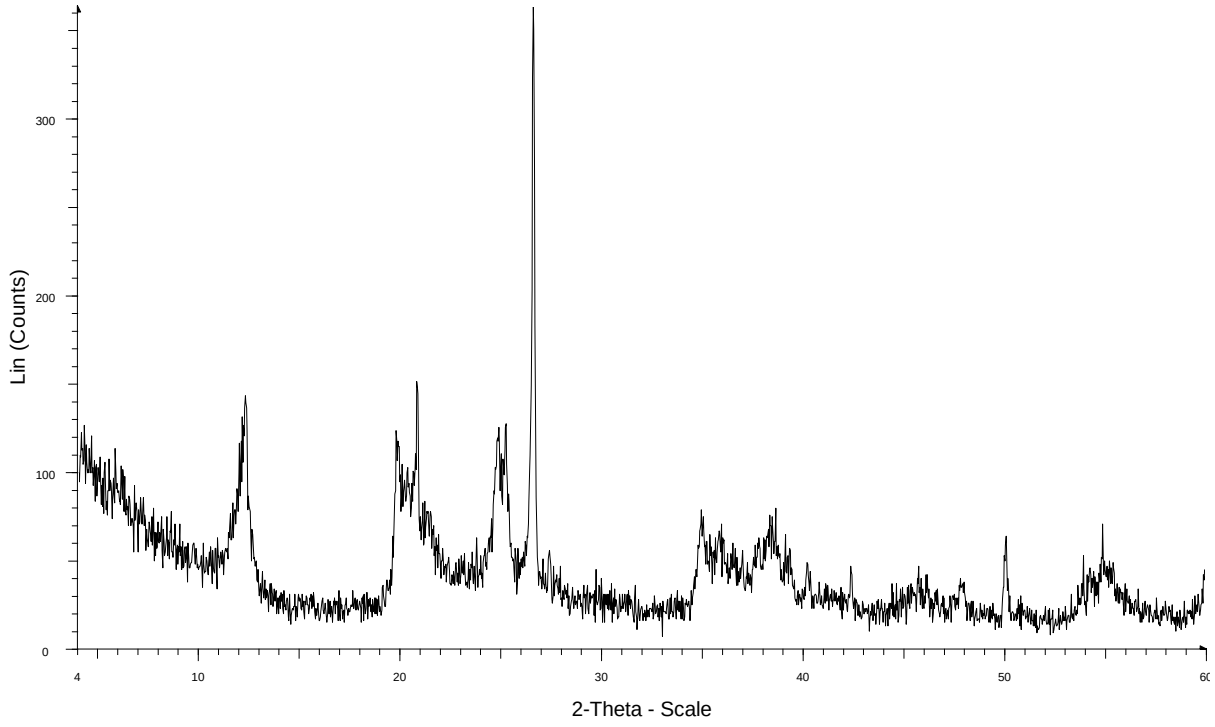

Figure B 18. X-ray diffractogram of the B_{hs} horizon in Algarrobo profile D.

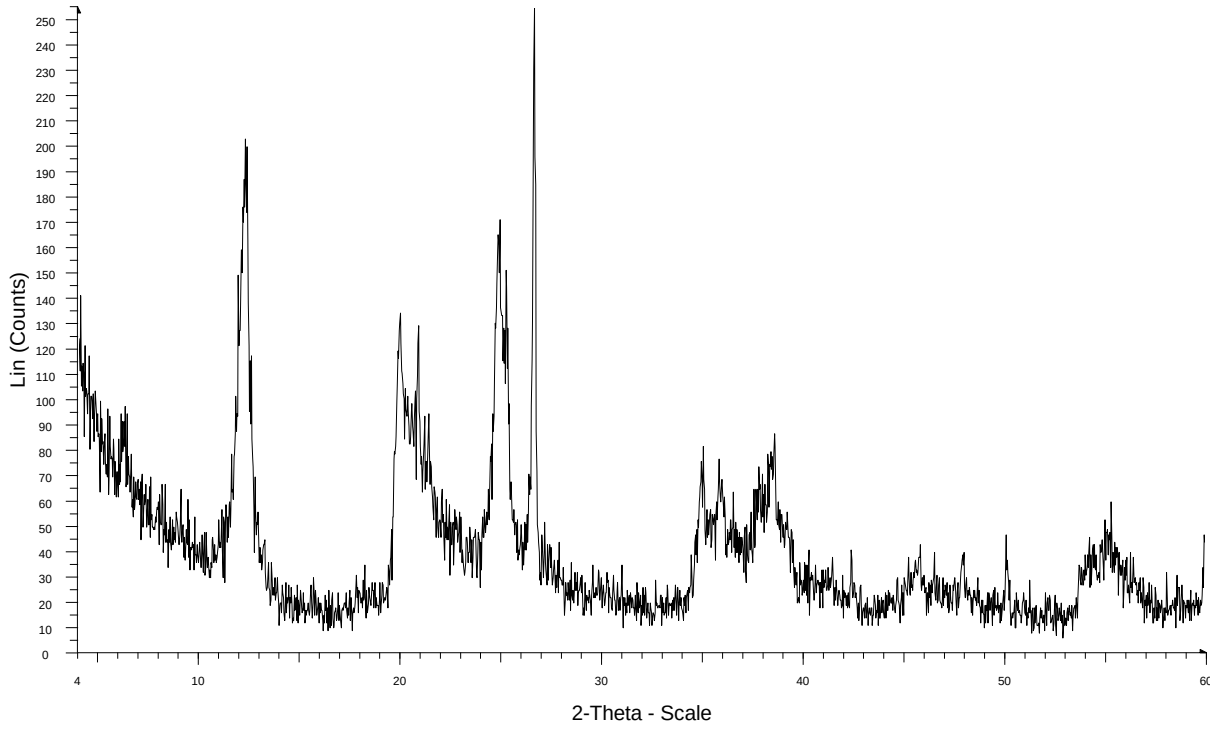

Figure B 19. X-ray diffractogram of the B_s horizon in Algarrobo profile D.

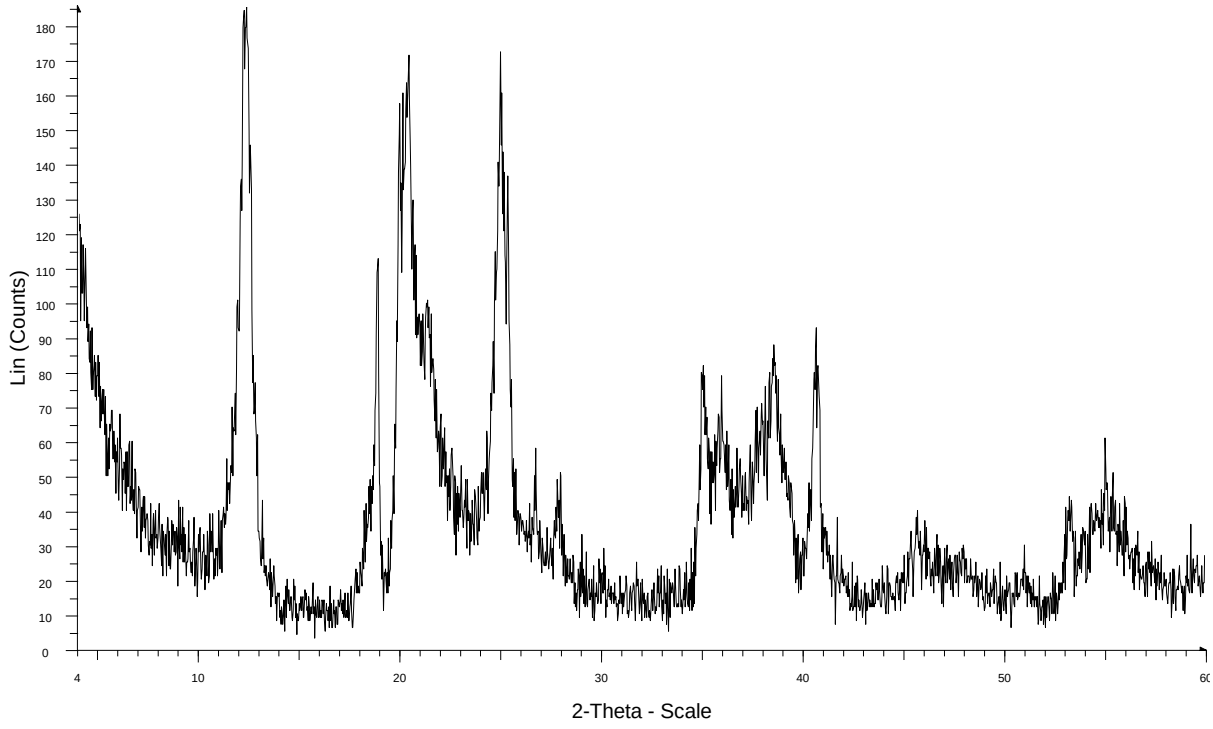

Figure B 20. X-ray diffractogram of the A horizon in Algarrobo profile D.

Appendix C. Site photographs from the Carmen Regadera Farm, Vega Alta, Puerto Rico and photographs of laboratory procedures.

Figure C 1. Dense vegetation of Cupey tree (Clusia rosea) over Spodosol profile A.

Figure C 2. Vegetation cover surrounding over Spodosol profile C.

Figure C 3. Limestone outcrop formation southeast of the sampling sites.

Figure C 4. Seepage from the backside of the profile pit of Algarrobo profile B.

Figure C 5. Flooded condition of Spodosols profile C during the first evaluation.

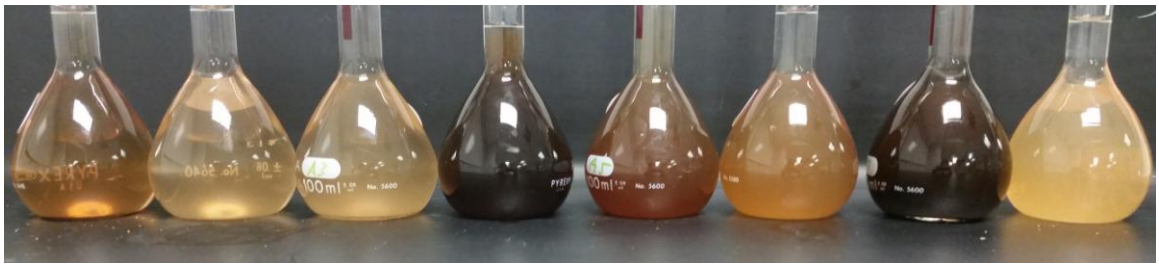

Figure C 6. Shade of the aluminum and iron oxide extract of Algarrobo profile A from the surface (left) to deepest horizon (right).

Figure C 7. Shade of the aluminum and iron oxide extract of Algarrobo profile B from the surface (left) to deepest horizon (right).

Figure C 8. Shade of the aluminum and iron oxide extract of Algarrobo profile C from the surface (left) to deepest horizon (right).

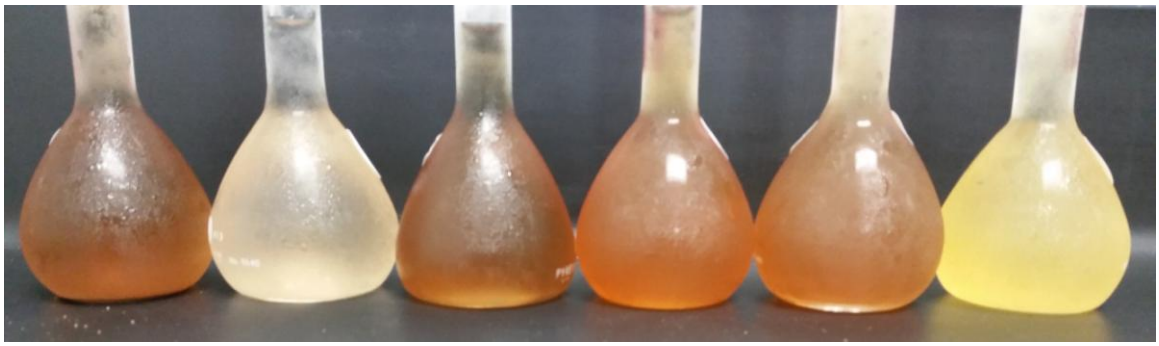

Figure C 9. Shade of the aluminum and iron oxide extract of Algarrobo profile D from the surface (left) to deepest horizon (right).

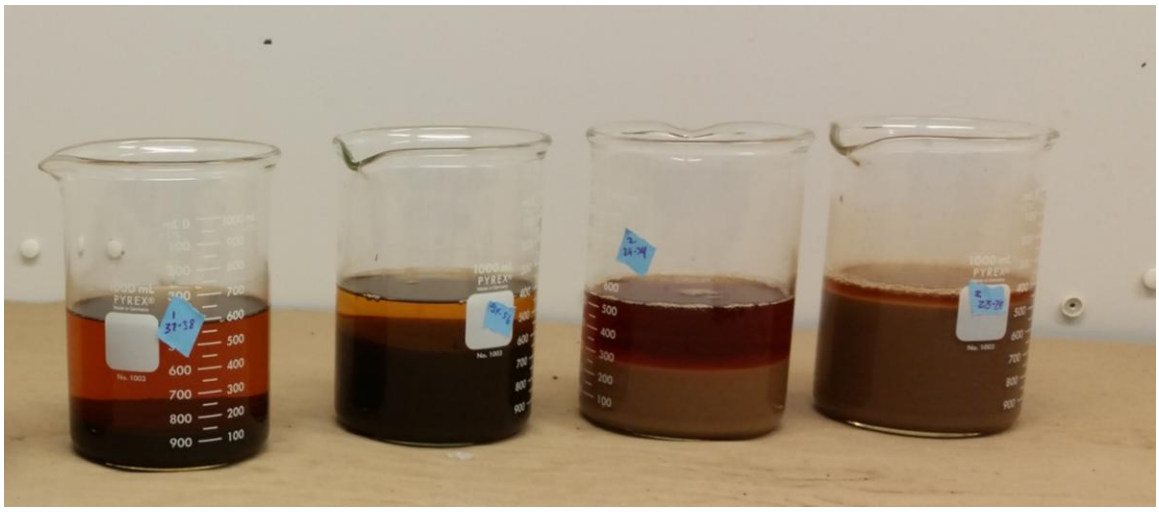

Figure C 10. Humic acid precipitate and fulvic acid supernatant separates in aqueous solution.